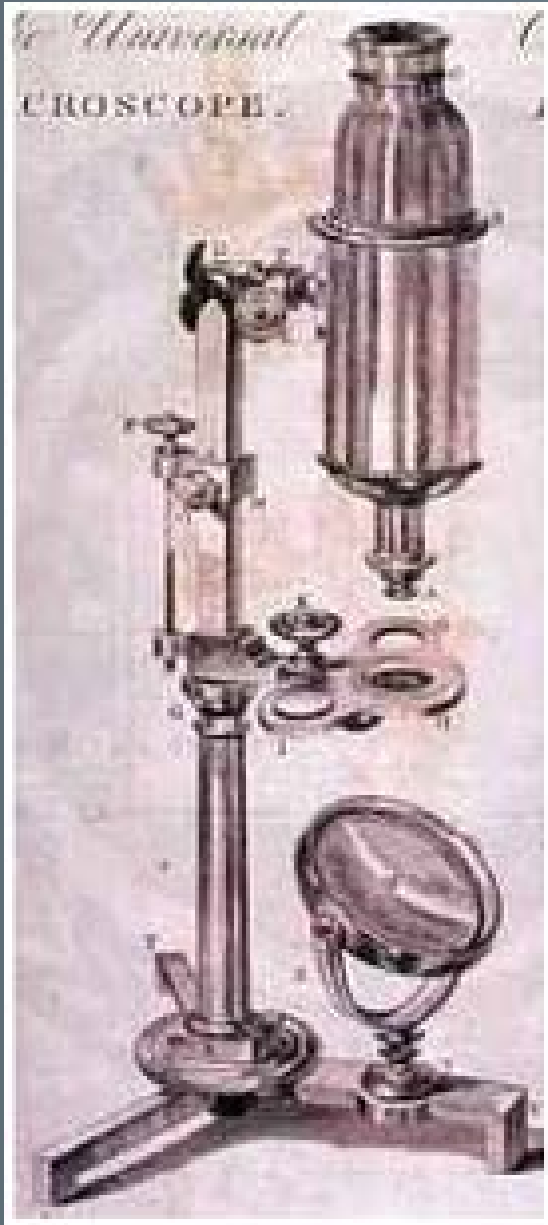


Confocal Microscopy and Living Cell Studies

Eva Bártoová

*Institute of Biophysics
Academy of Sciences of the Czech
Republic*



History of microscopy:

the light microscope (discovered by Robert Hook, 1665): an instrument that enables the human eye, by means of a lens or combinations of lenses, to observe enlarged images of tiny objects. It made visible the fascinating details of naked eye invisible worlds.

1957: Marvin Minsky patented the first confocal microscope

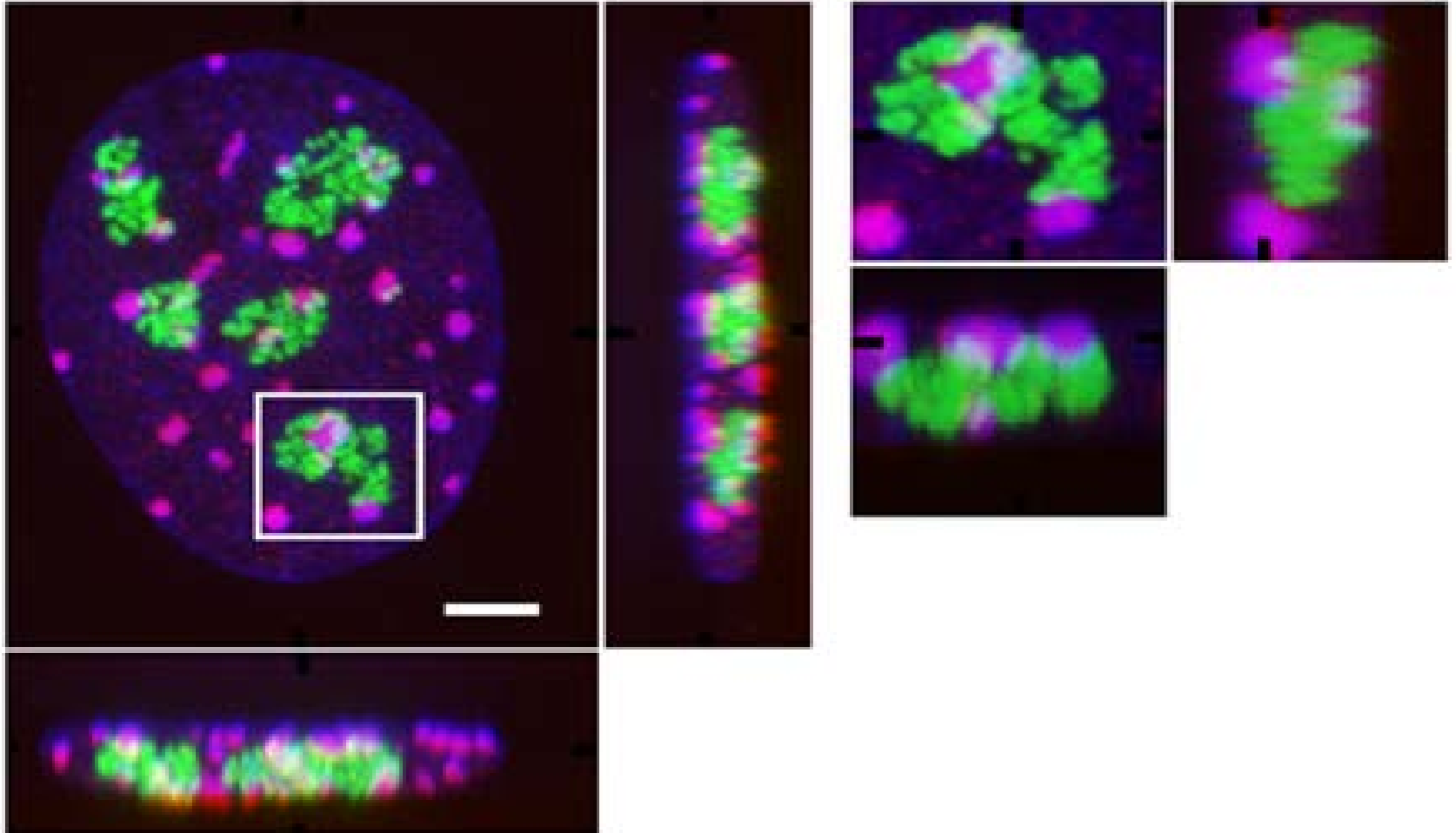


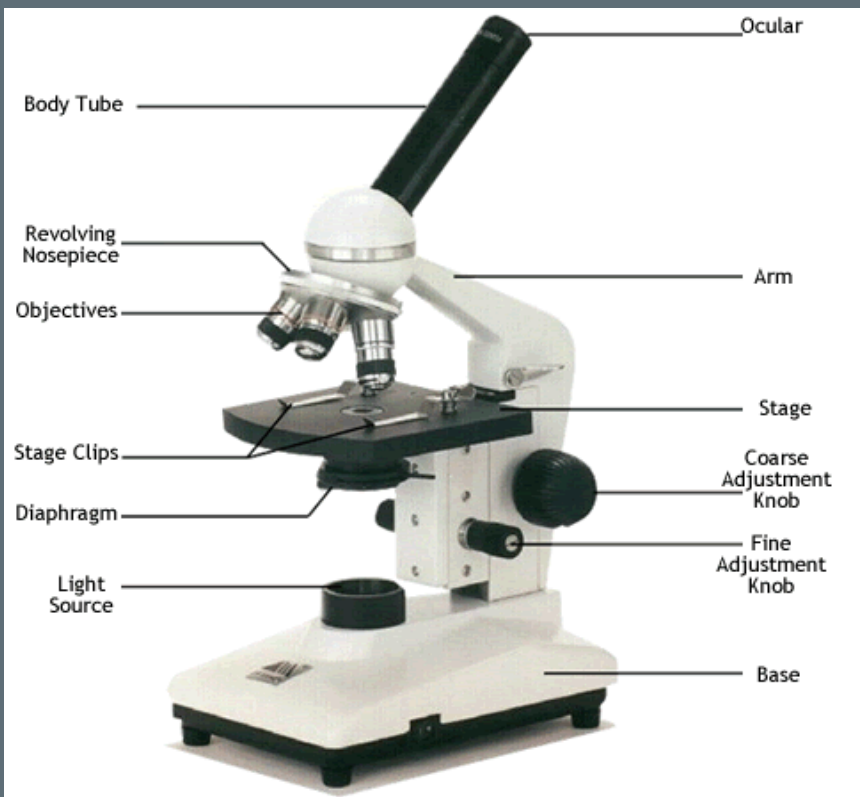
Fibrilarin / HP1 α / DNA

nucleus

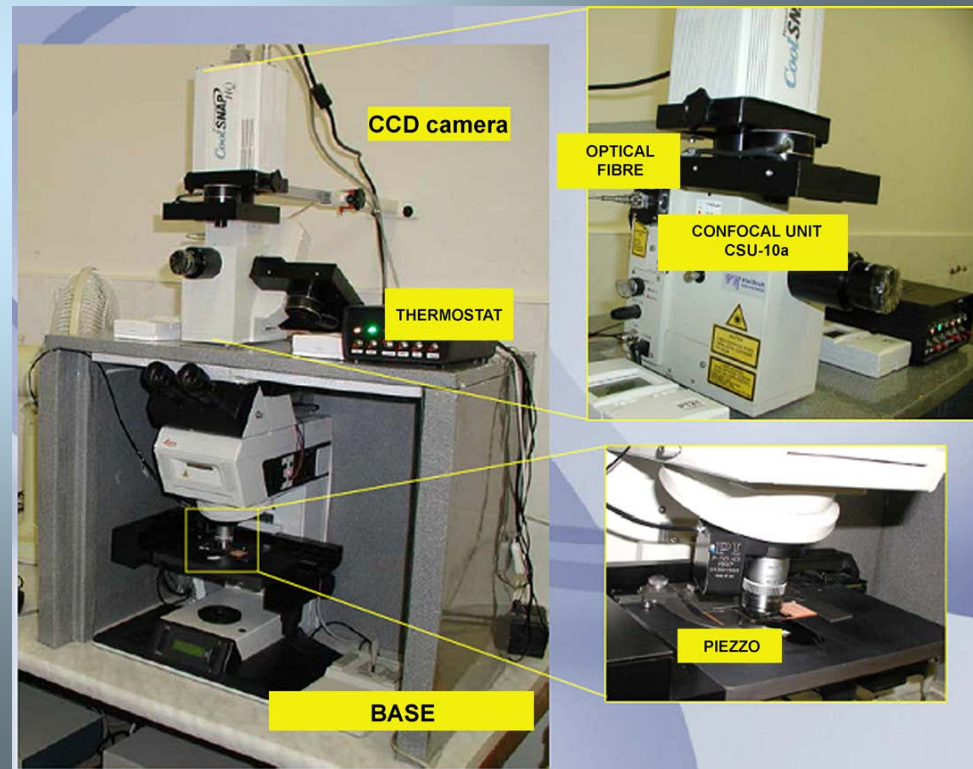
nucleolus

SUV39h1 +/+





<http://www.google.cz/imgres?imgurl=http://www.microscopehelp.com/>



Brno laboratory at IBP

Visible Light Microscopy:

Objectives: numerical aperture

- NA=ability of lens to gather light and resolve detail at a fixed distance from object.
 - Dependent on ability of lens to capture diffracted light rays.
- n =Refractive index is limiting (air=1.0, oil=1.51)
 - Do not mix mediums when using a lens
- Theoretical resolution depends on NA and the wavelength of light. $NA=n \cdot \sin(\mu)$
 - Shorter wavelengths=higher resolution.
 - Resolution limit for green light ($NA=1.4$, 100X) is $0.2 \mu\text{m}$.
 - $R=0.61\lambda/NA$

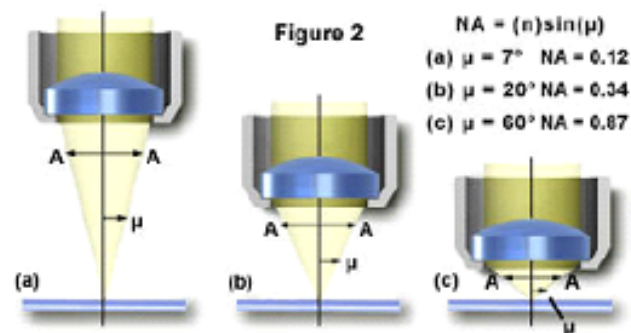
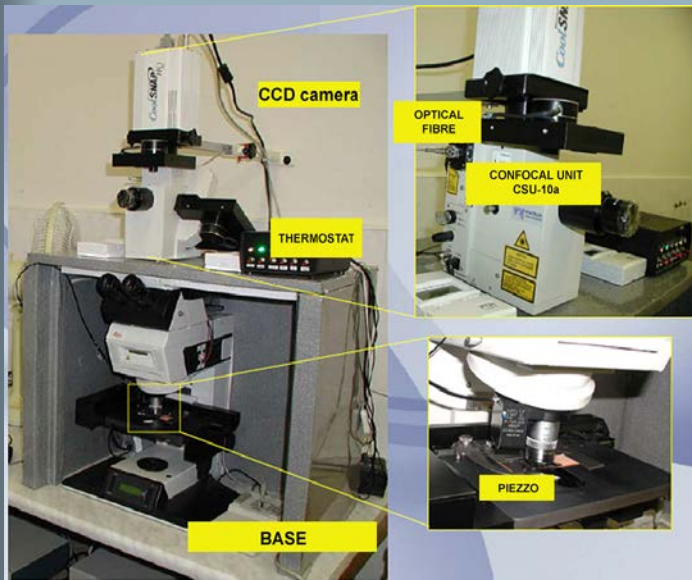
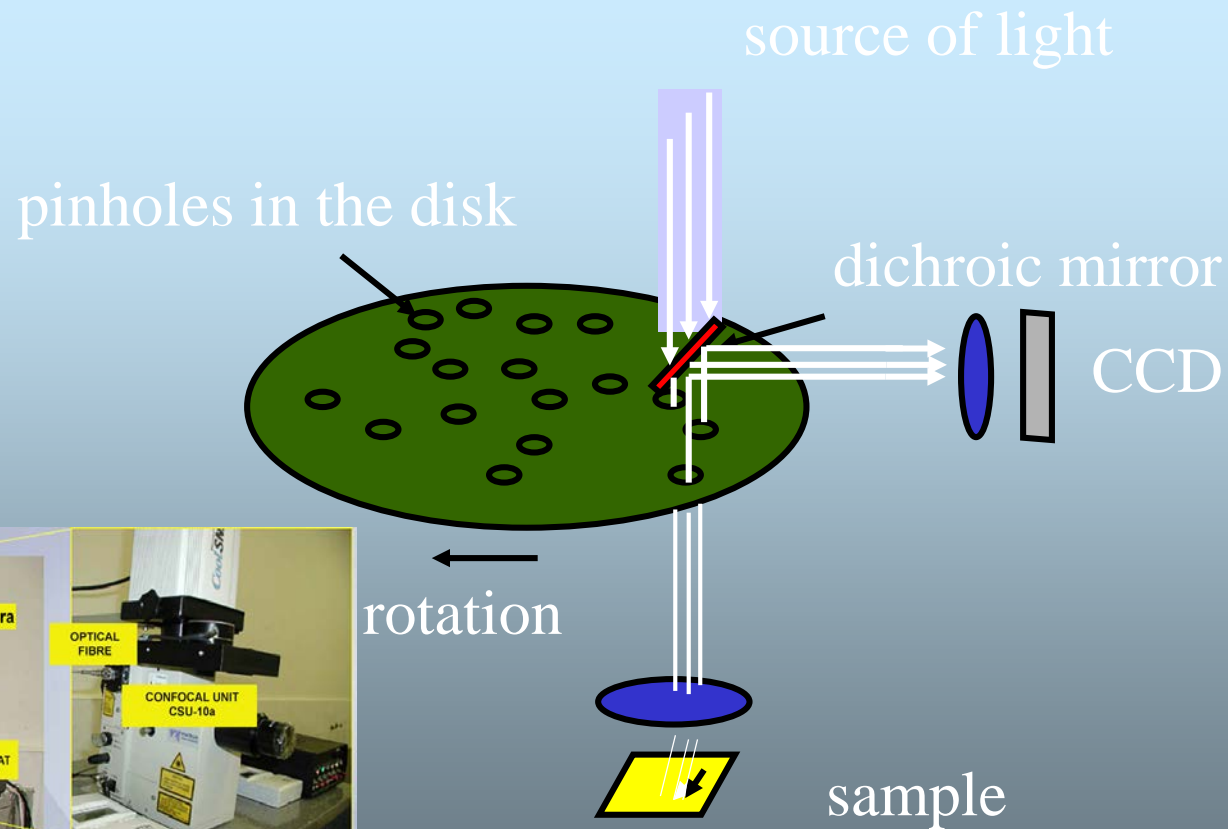
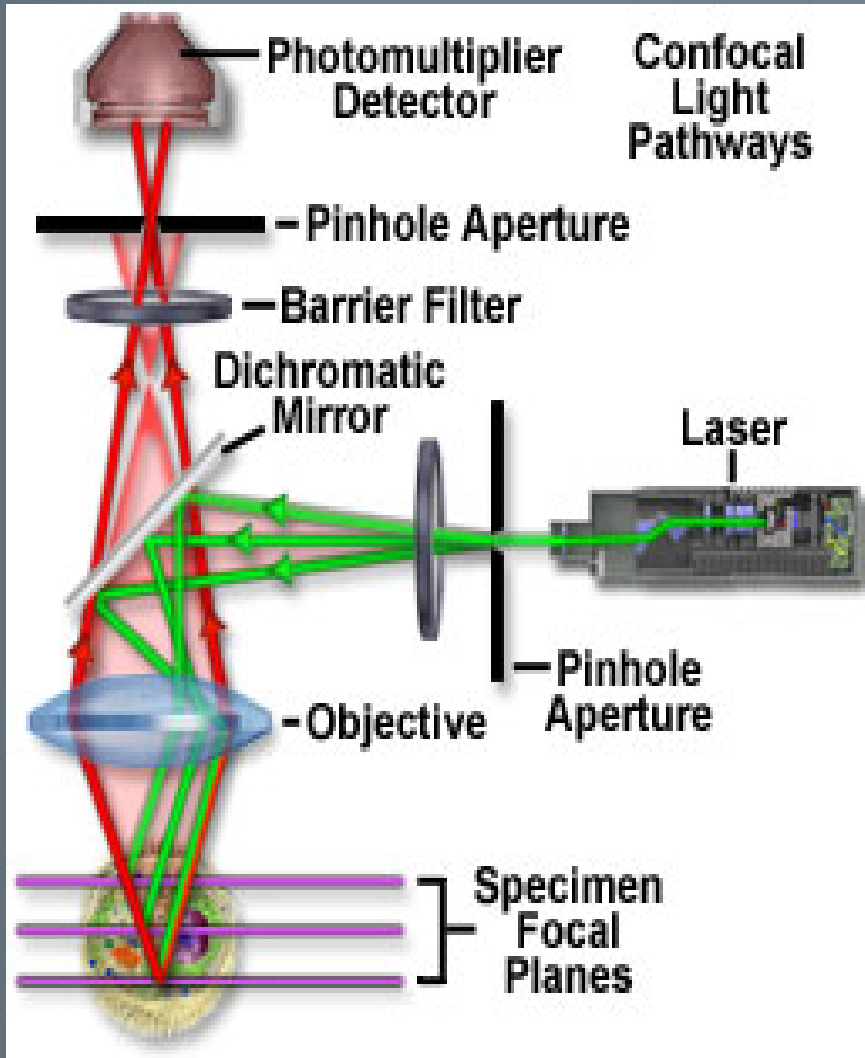


Figure 1

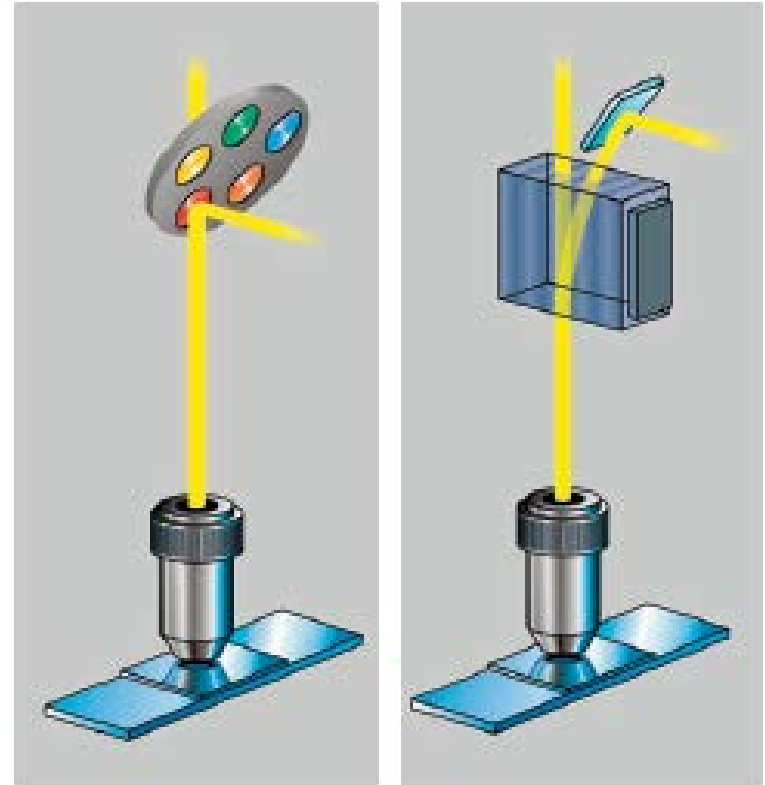
Tandem scanning microscopes based on Nipkow disk



Confocal microscopy - principles



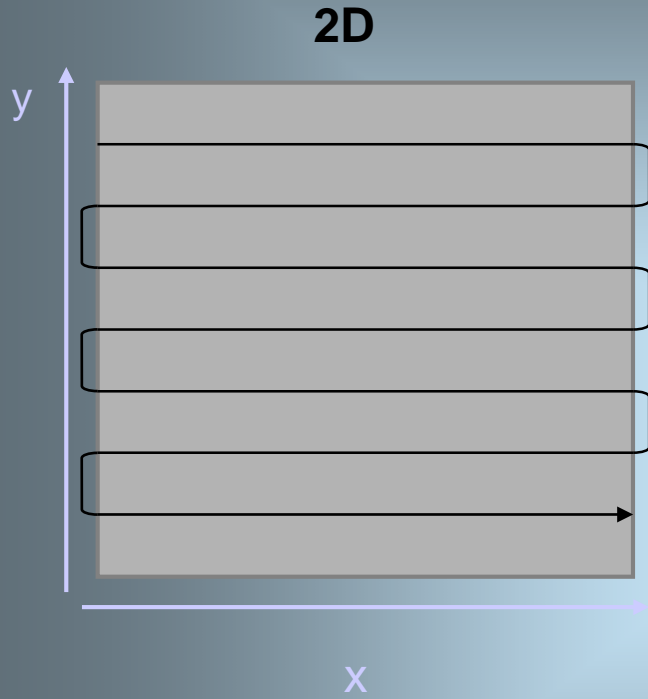
AOTF and AOBS



Left: conventional beam splitting by dichroic mirrors requires many optical elements with fixed properties.

Right: the AOBS* is electronically adaptable to all tasks.

Scanning in 2D and 3D by confocal microscope



Laser beam moves firstly along x axis and then starts with new line in y axis.

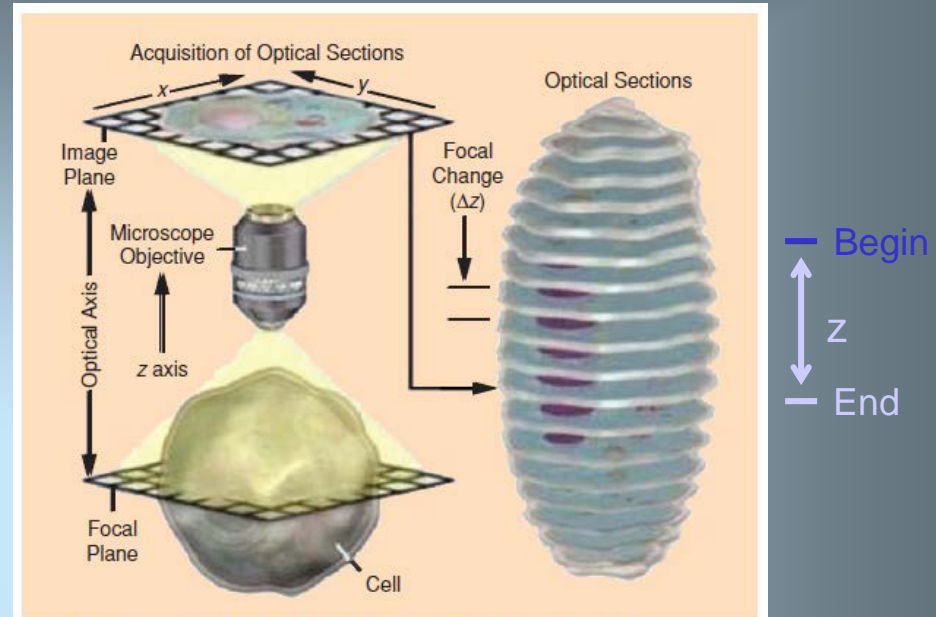


[FIG1] An example of the acquired 3-D Image of a cell, captured by a fluorescence microscope.

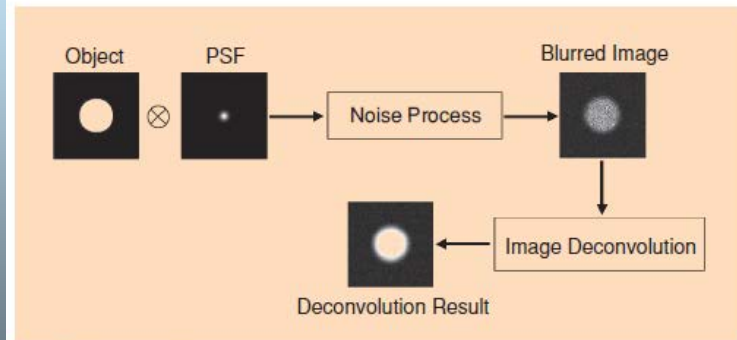
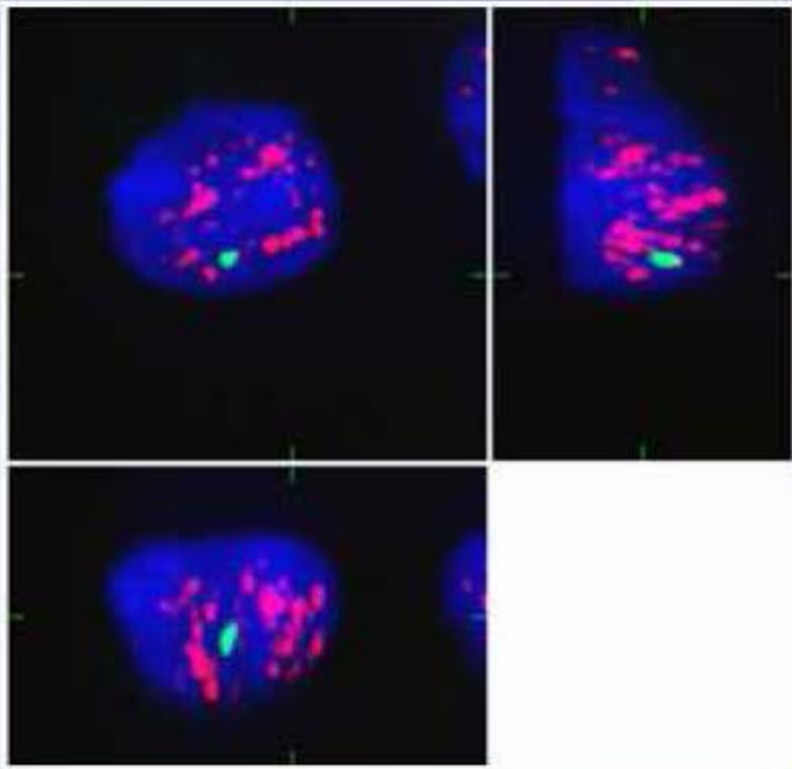
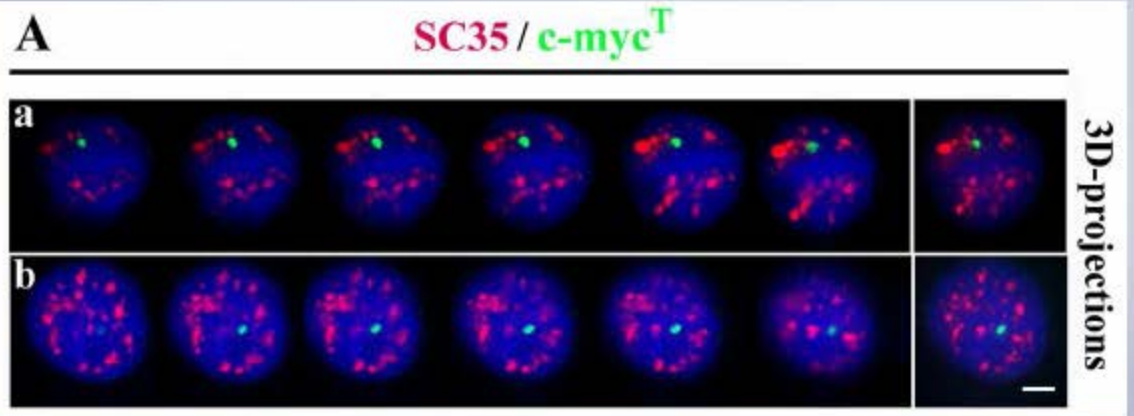


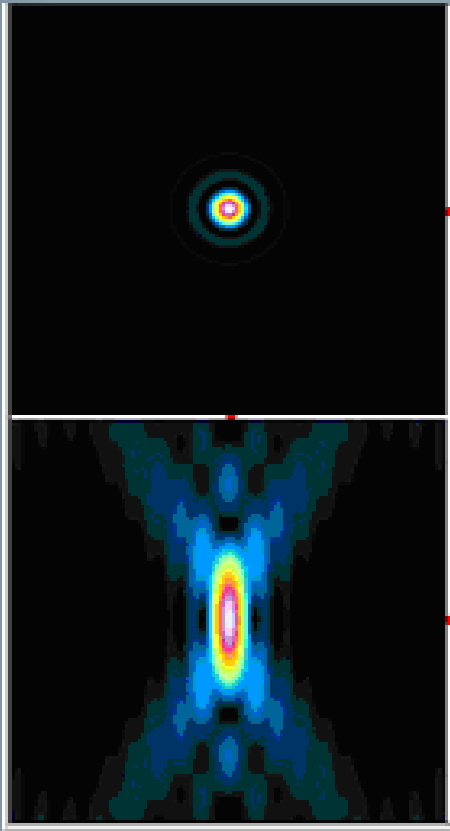
[FIG2] Schematic of a general deconvolution procedure.

3D-projection



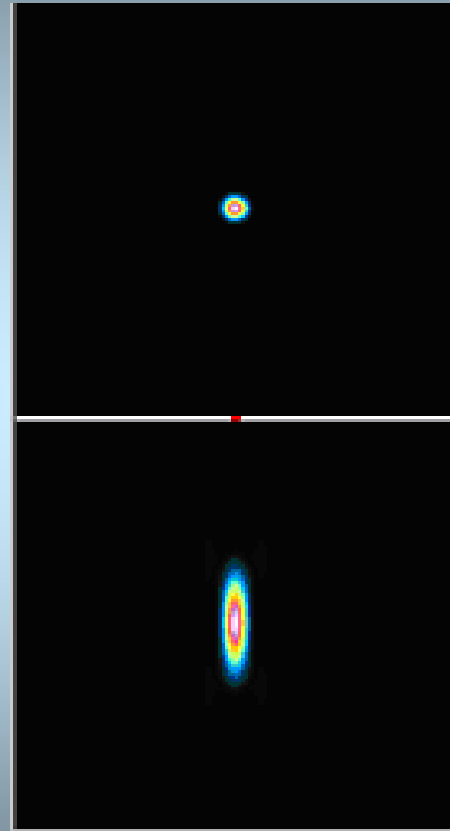
Optical resolution: conventional versus confocal

Conventional



$$\text{Res} = 0.61 \cdot \lambda / \text{NA}$$

Confocal



$$\text{Res}(xy) = 0.4 \cdot \lambda / \text{NA}$$

$$\text{Res}(xz) = 0.45 \cdot \lambda / n(1 - \cos\alpha)$$

Formulas by Kino

4PI and STED resolution are much higher...

Deconvolution

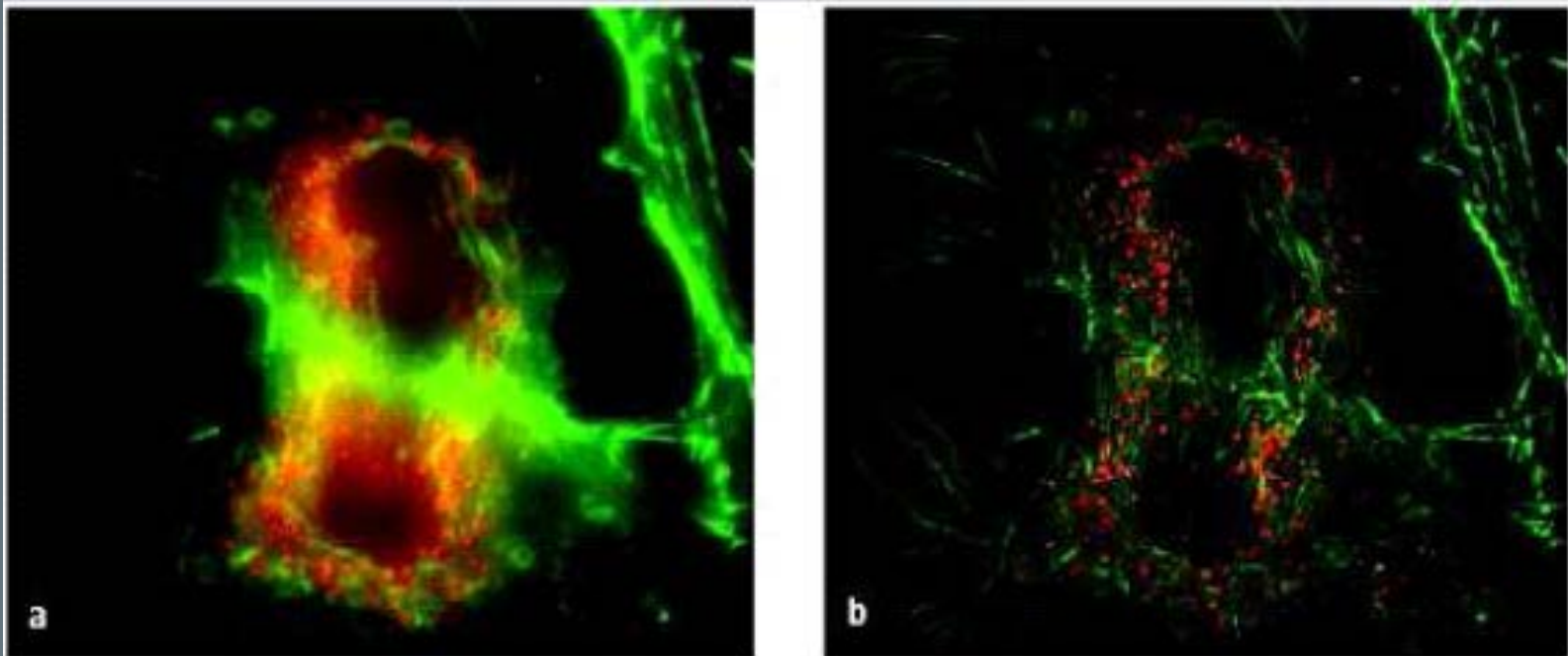


Fig. 3: Via deconvolution, artefacts can be computed out of fluorescence images. a). These artefacts are caused by the stray light from non-focused areas above and below the focus level. These phenomena, referred to as convolution, result in glare, distortion and blurriness. b). Deconvolution is a recognised mathematical procedure for eliminating such artefacts. The resulting image displayed is sharper with less noise and thus at higher resolution. This is also advantageous for more extensive analyses.

Assuming linearity, convolution of the object and the imaging system PSF is affected by noise and produces a blurred image. Deconvolution restores the original object to an improved resolution and higher signal-to-noise ratio (SNR) level.

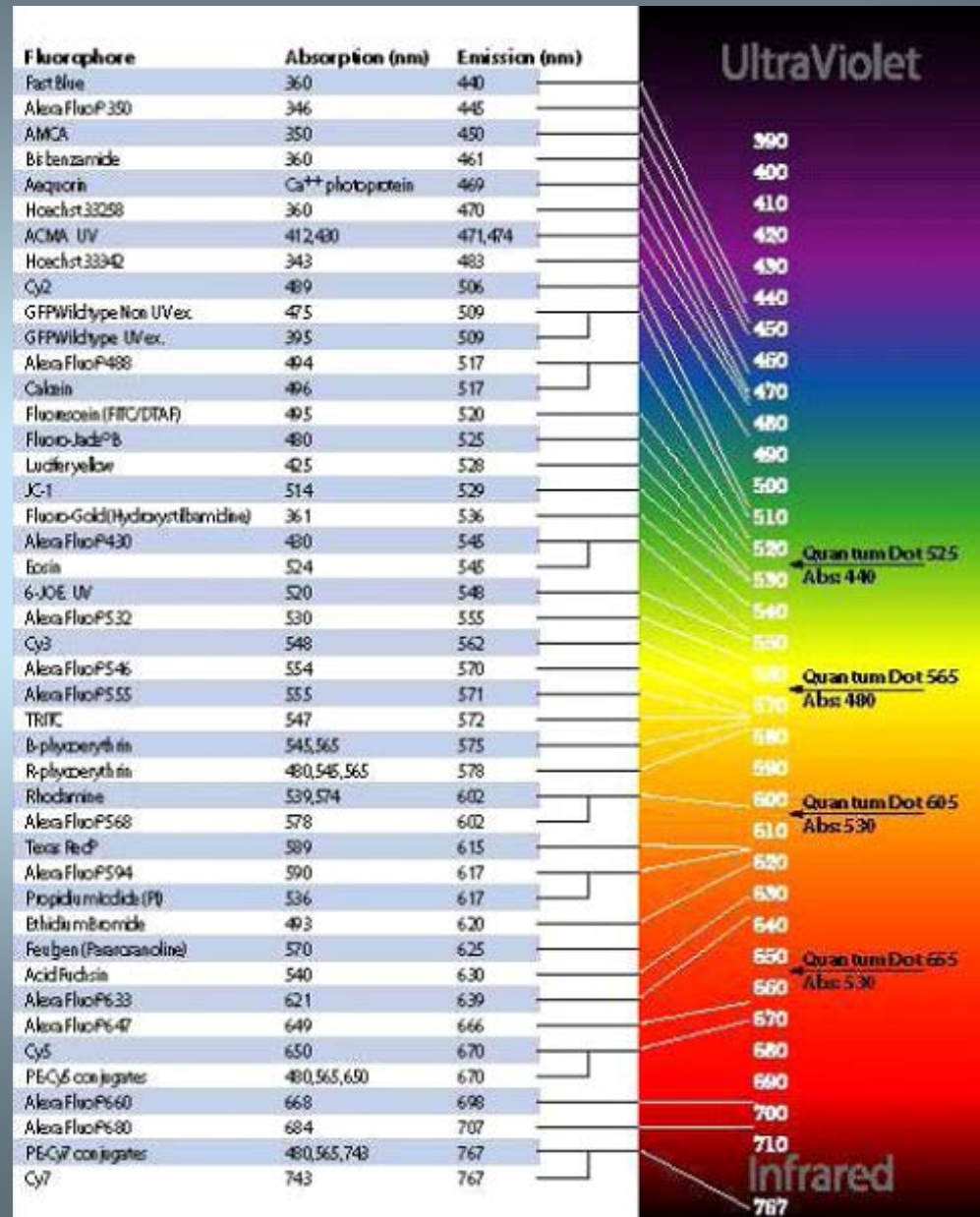
Types of fluorochromes

Fluorochromes are essentially dyes, which accept light energy (e.g. from a laser) at a given wavelength and re-emit it at a longer wavelength. These two processes are called excitation and emission.

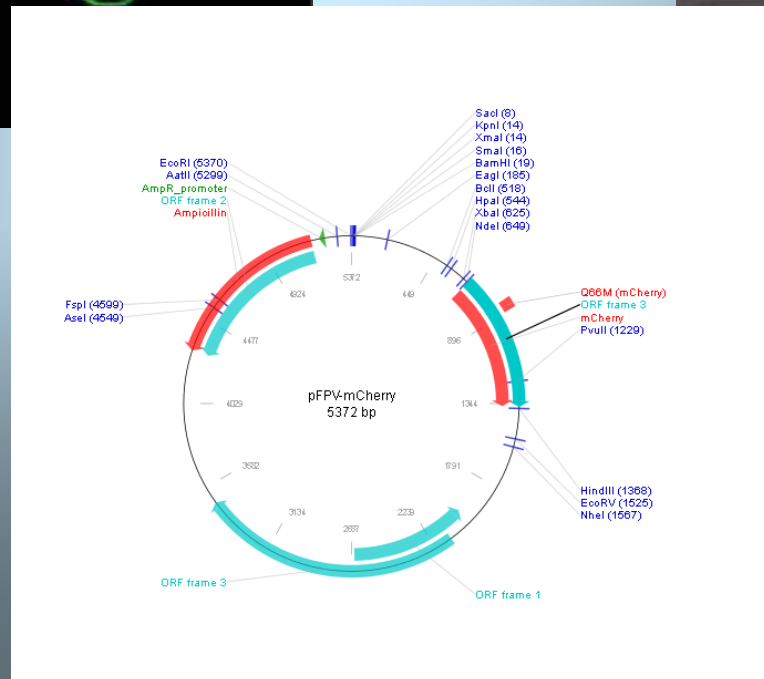
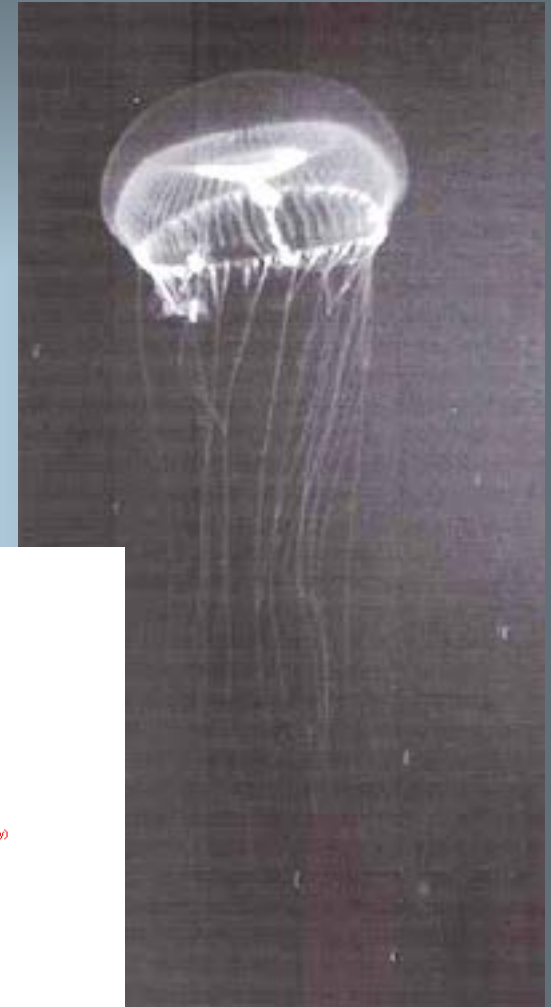
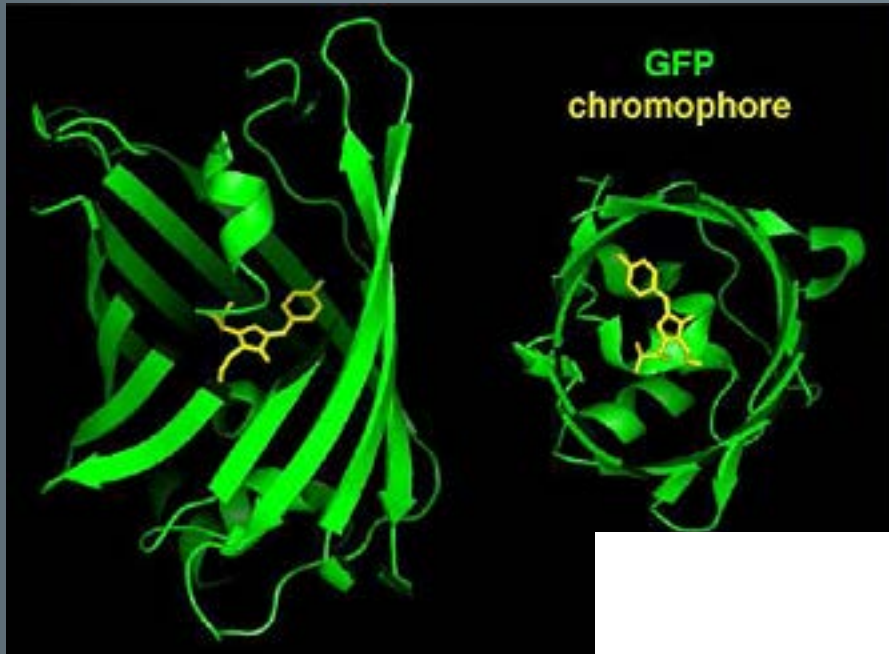
1. Fluorochromes conjugated with other molecule. Example represents quantum dots, used for ultra-sensitive nonisotopic detection.

2. Fluorochromes that binds directly to some structure. For example, DAPI or PI binds to DNA

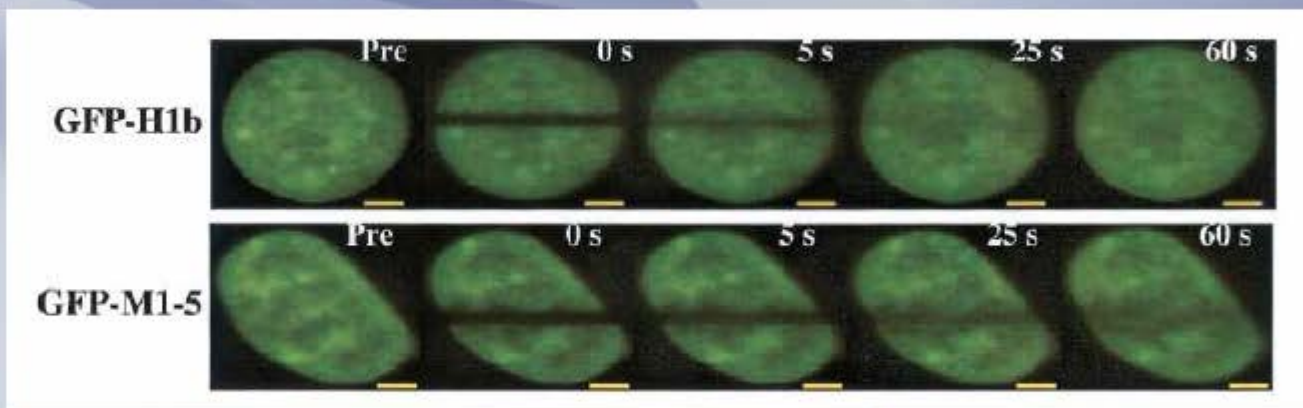
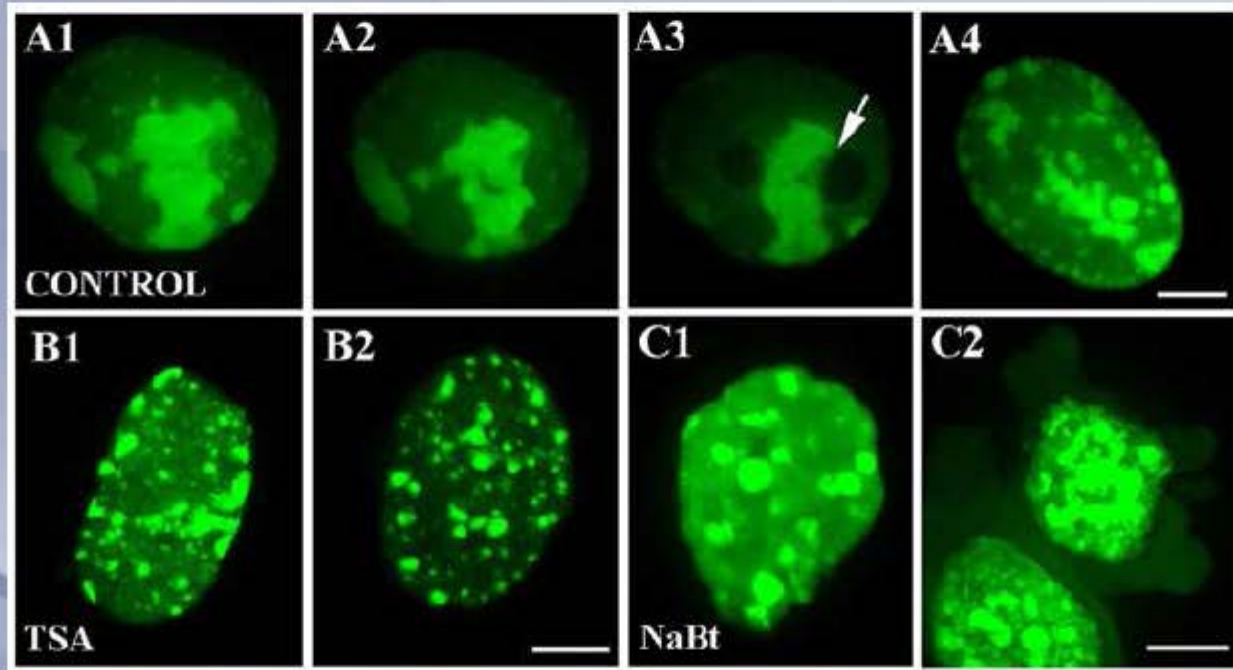
3. Fluorochromes produced by organism like *Aequorea victoria* (GFP) or octocoral *Dendronephthya sp.* (Dendra2)

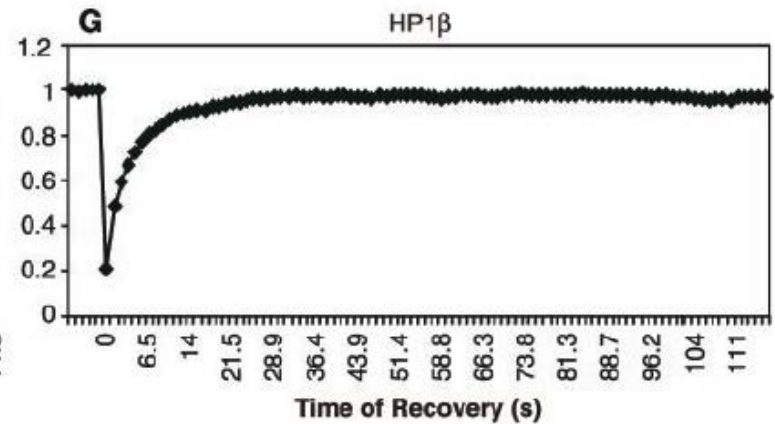
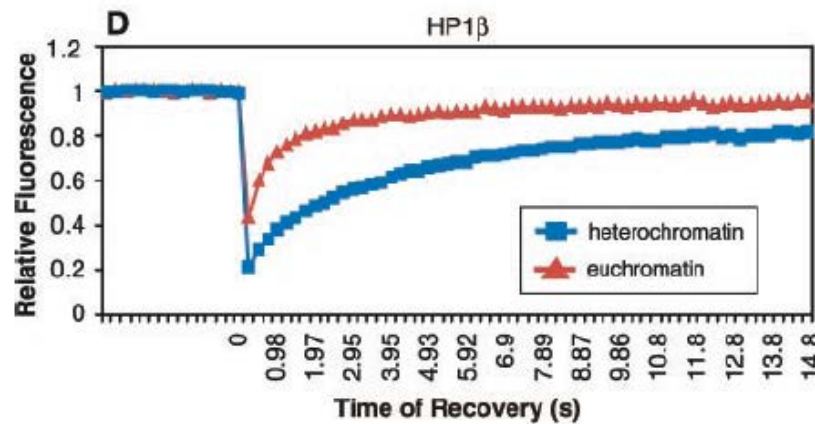
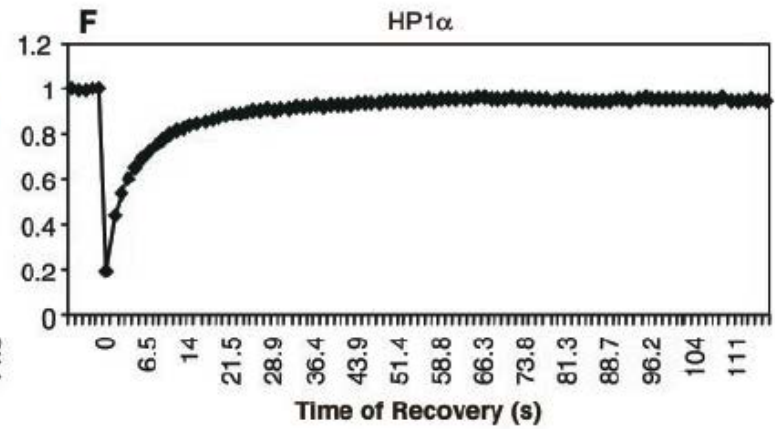
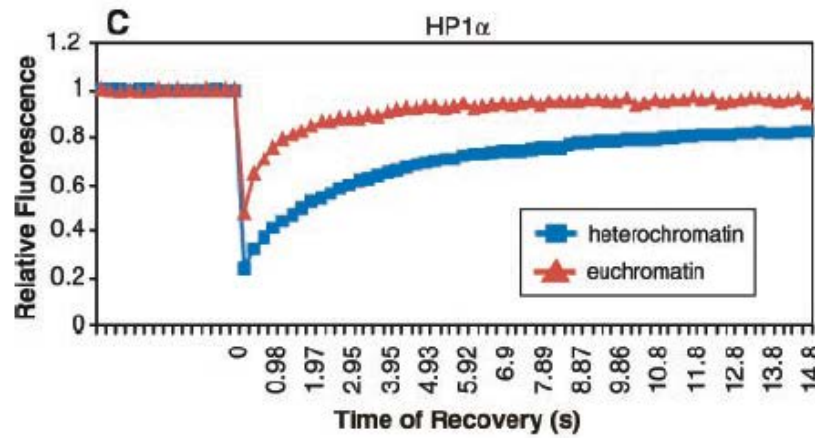
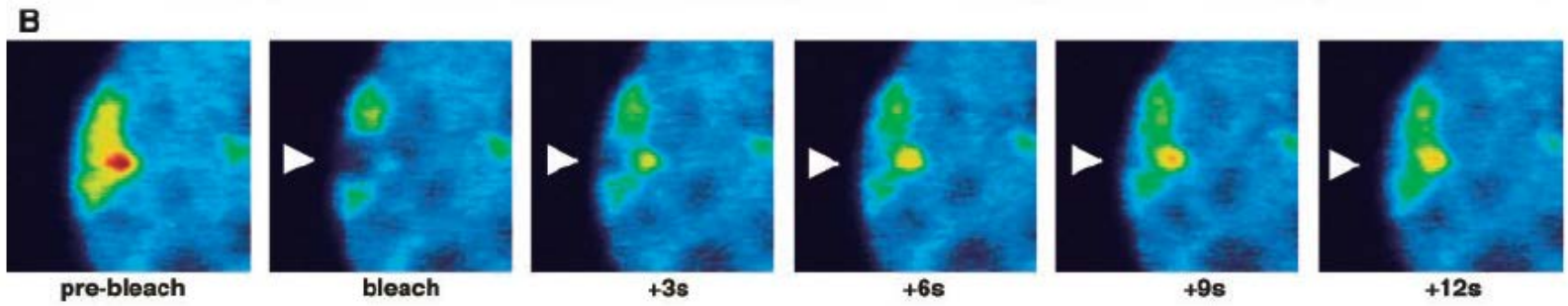


Living Cell Studies - GFP technology

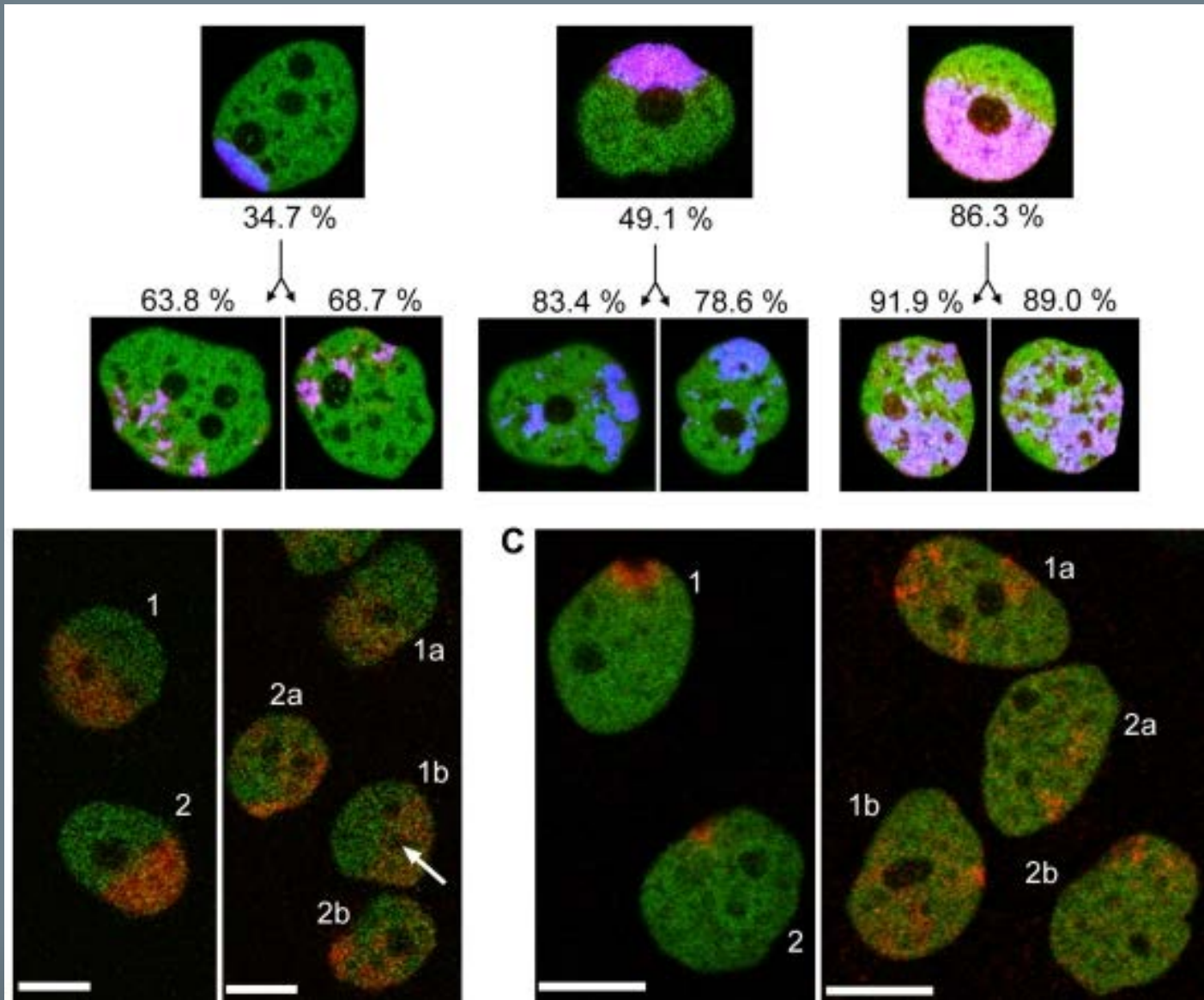


GFP-HP1 β

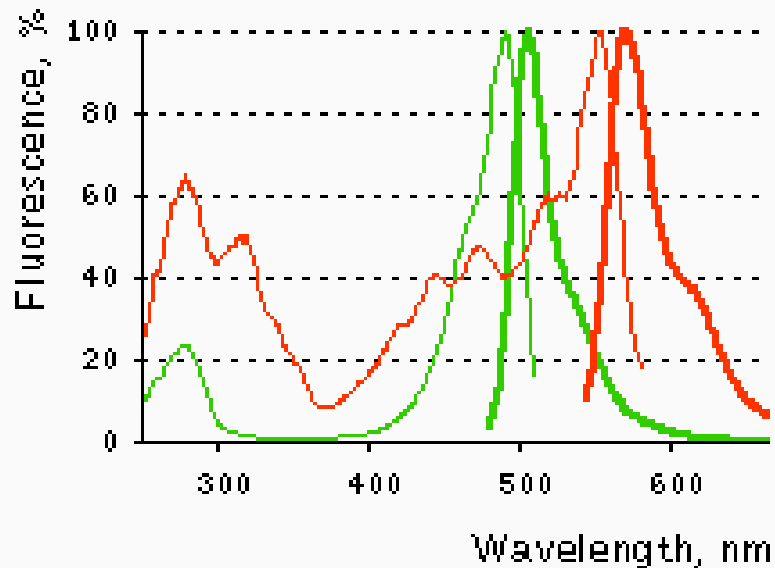




Dendra2 photo-conversion



Dendra2 is an improved version of a green-to-red photoswitchable fluorescent protein Dendra, derived from octocoral *Dendronephthya* sp. (Gurskaya *et al.*, 2006).

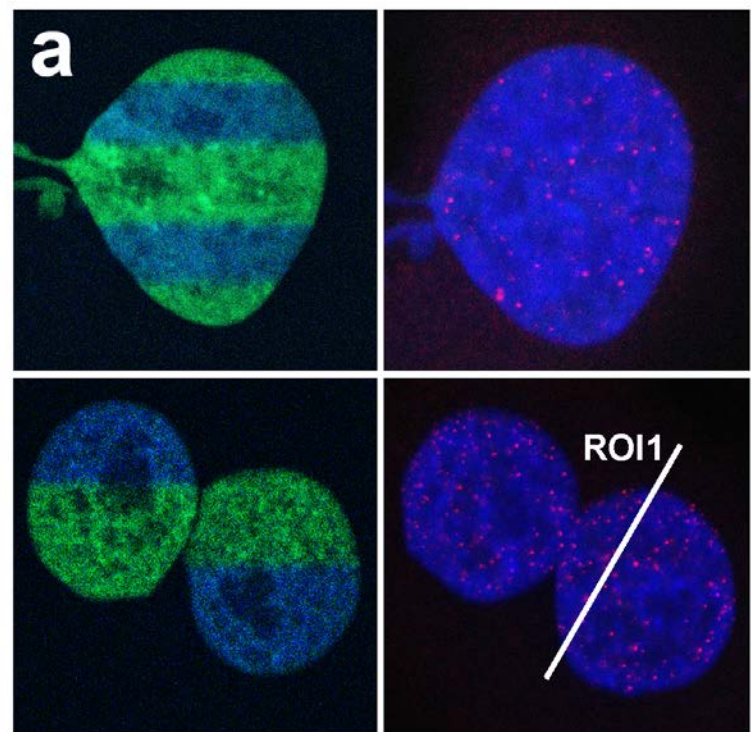


Normalized excitation (thin line) and emission (thick line) for non-activated (green) and activated (red) spectra.

Photoconversion by UV laser

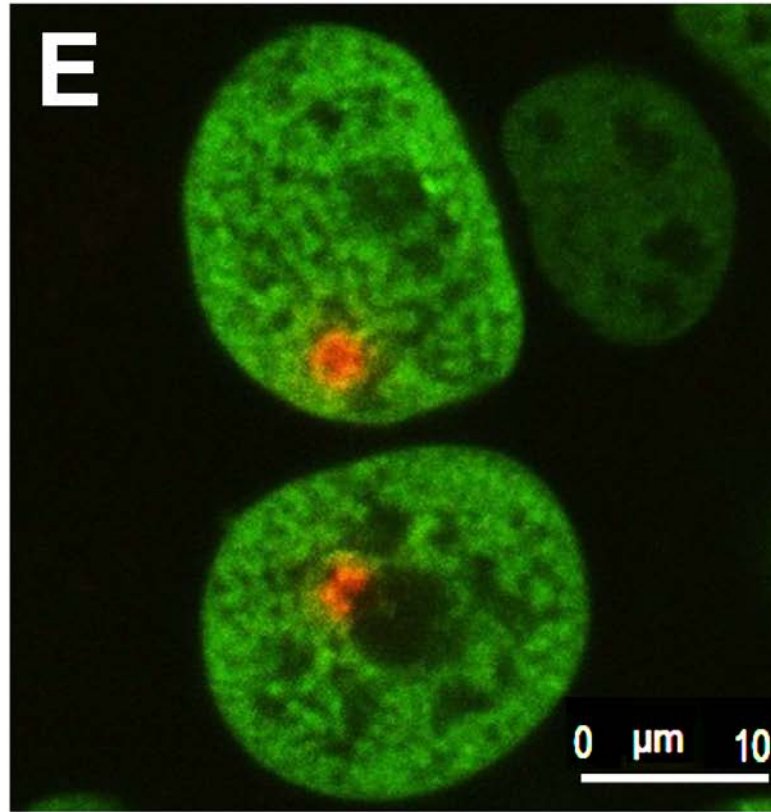
H4-Dendra2

CPDs / Nucleus

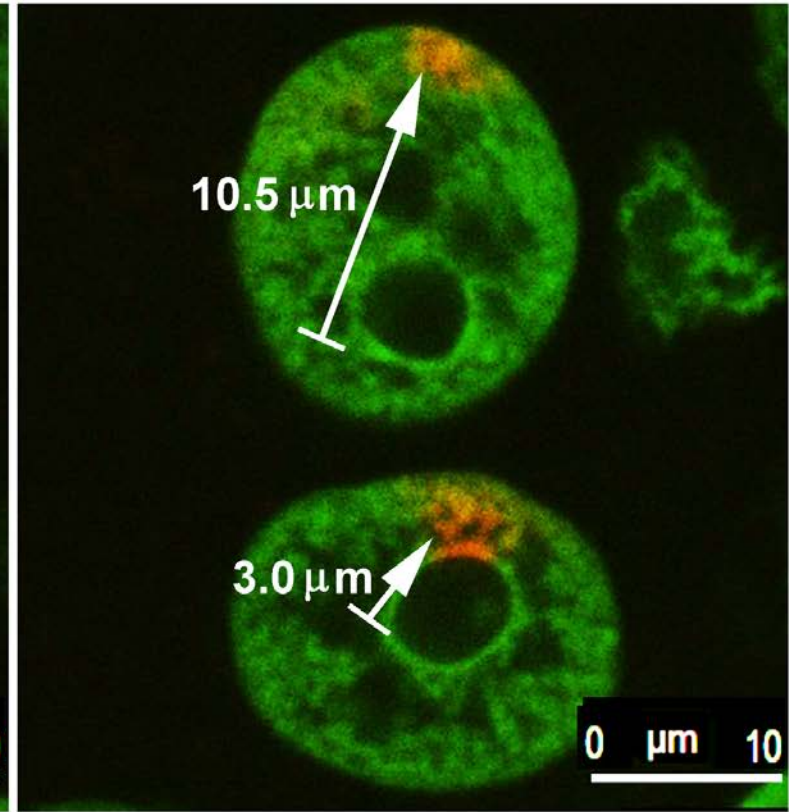


H4-Dendra2 / H4-Dendra2

Actinomycin-D
(0 min. after photoconversion)



Actinomycin-D (90 min.)



Leica TCS SP-5 X



Incubation chambers for living cell studies

Part I – cells can be grown on both upper and lower sides of the chamber; this part is filled fully with medium

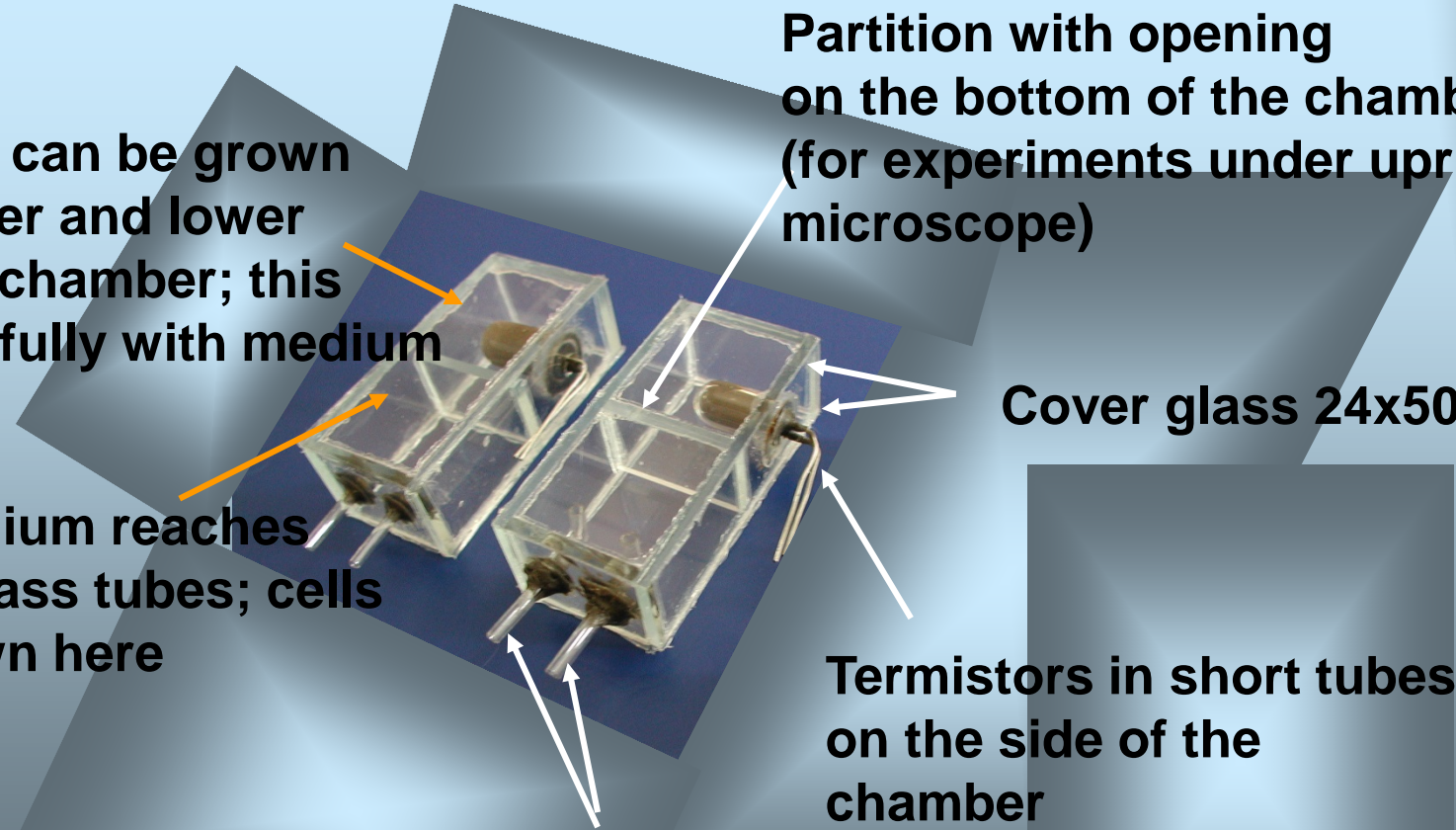
Part II – medium reaches under the glass tubes; cells are not grown here

Partition with opening on the bottom of the chamber (for experiments under upright microscope)

Cover glass 24x50 mm

Termistors in short tubes on the side of the chamber

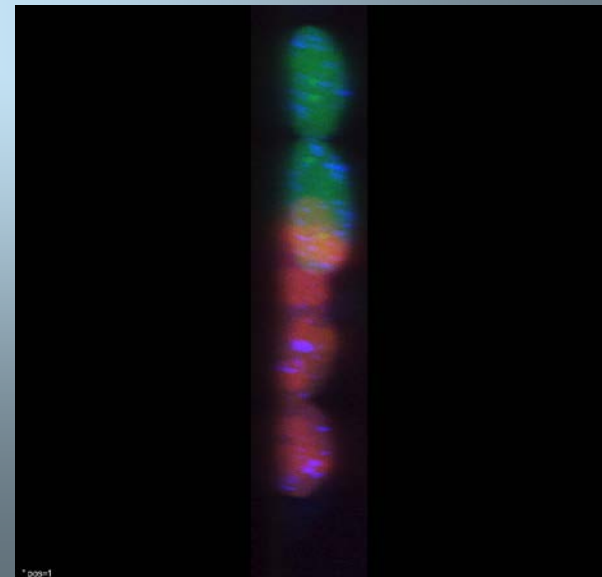
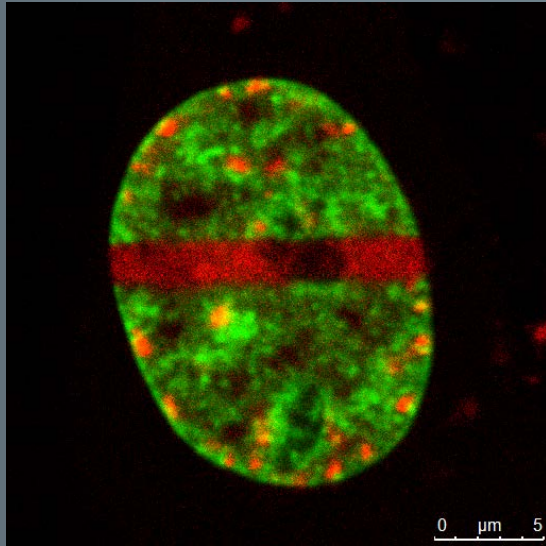
Glass tubes bent under the upper glass (to enable CO₂ to flow above medium in the part II of the chamber)



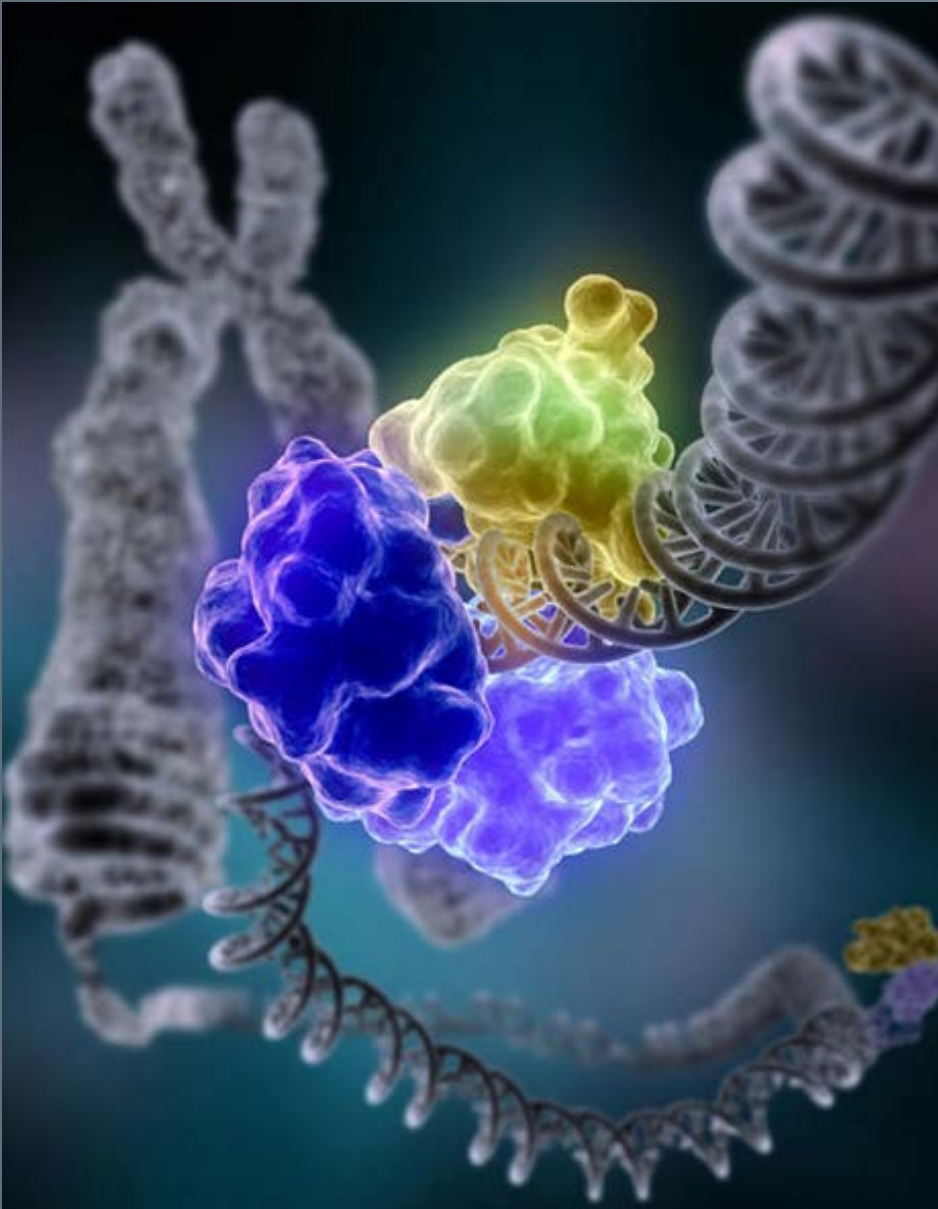
Application of UV-laser (355 nm) in experimental studies on DNA repair



Advanced confocal microscopy



DNA repair



Single-strand damage

❖ Base excision repair (**BER**), which repairs damage to a single base caused by oxidation, alkylation, hydrolysis, or deamination.

❖ Nucleotide excision repair (**NER**), which recognizes bulky, helix-distorting lesions such as pyrimidine dimers and 6,4 photoproducts.

❖ Mismatch repair (**MMR**), which corrects errors of DNA replication and recombination that result in mispaired (but undamaged) nucleotides.

Double-strand breaks

❖ non-homologous end joining (**NHEJ**)

❖ microhomology-mediated end joining (**MMEJ**)

❖ homologous recombination (**HR**)

DNA repair

Box 1 | The two main types of double-stranded DNA-break repair

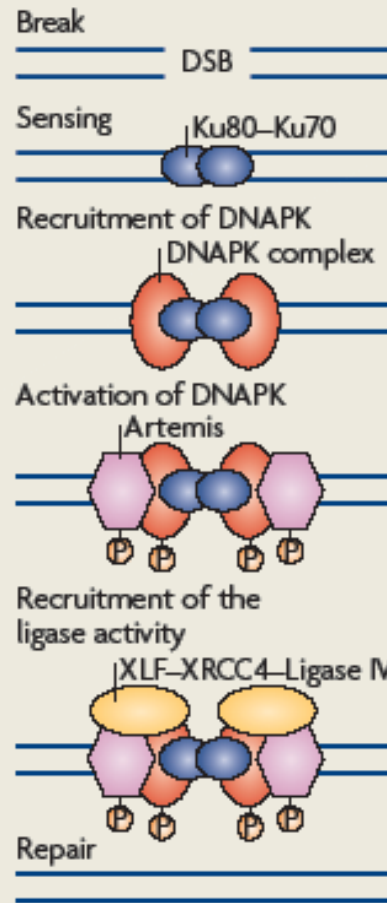
Non-homologous end joining

A DNA lesion (a double-stranded DNA break (DSB)) is sensed by the Ku80–Ku70 heterodimer, which in turn recruits the DNA-dependent protein kinase catalytic subunit DNAPKcs, resulting in assembly of the DNAPK complex and activation of its kinase activity (see the figure; left panel). Increasing evidence suggests that DNAPK functions as a regulatory component of non-homologous end joining (NHEJ), potentially facilitating and regulating the processing of DNA ends. DNAPK also increases the recruitment of XRCC4, DNA ligase IV, XLF and Artemis, which carry out the final rejoining reaction.

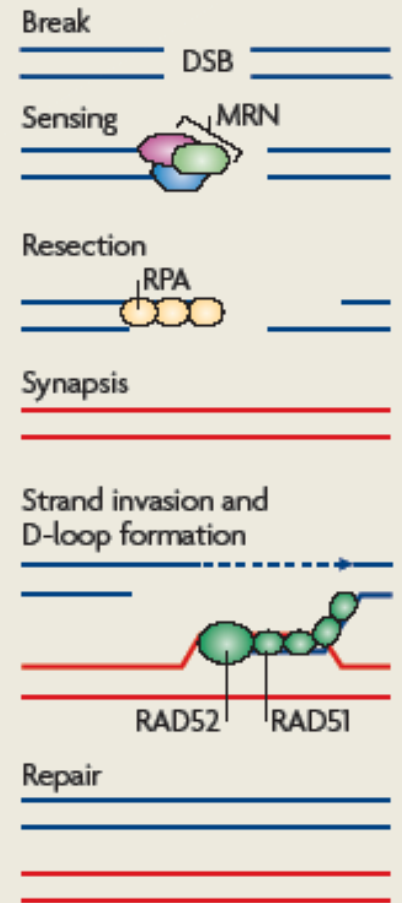
Homologous recombination repair

A DNA lesion is recognized by the MRN (MRE11–RAD50–NBS1) complex, which is recruited to the DSB to generate single-stranded DNA by resection (see the figure; right panel). The single-stranded ends are bound by replication protein A (RPA), RAD51 and RAD52 and can subsequently invade the homologous template, creating a D-loop and a Holliday junction, to prime DNA synthesis and to copy and ultimately restore genetic information that was disrupted by the DSB.

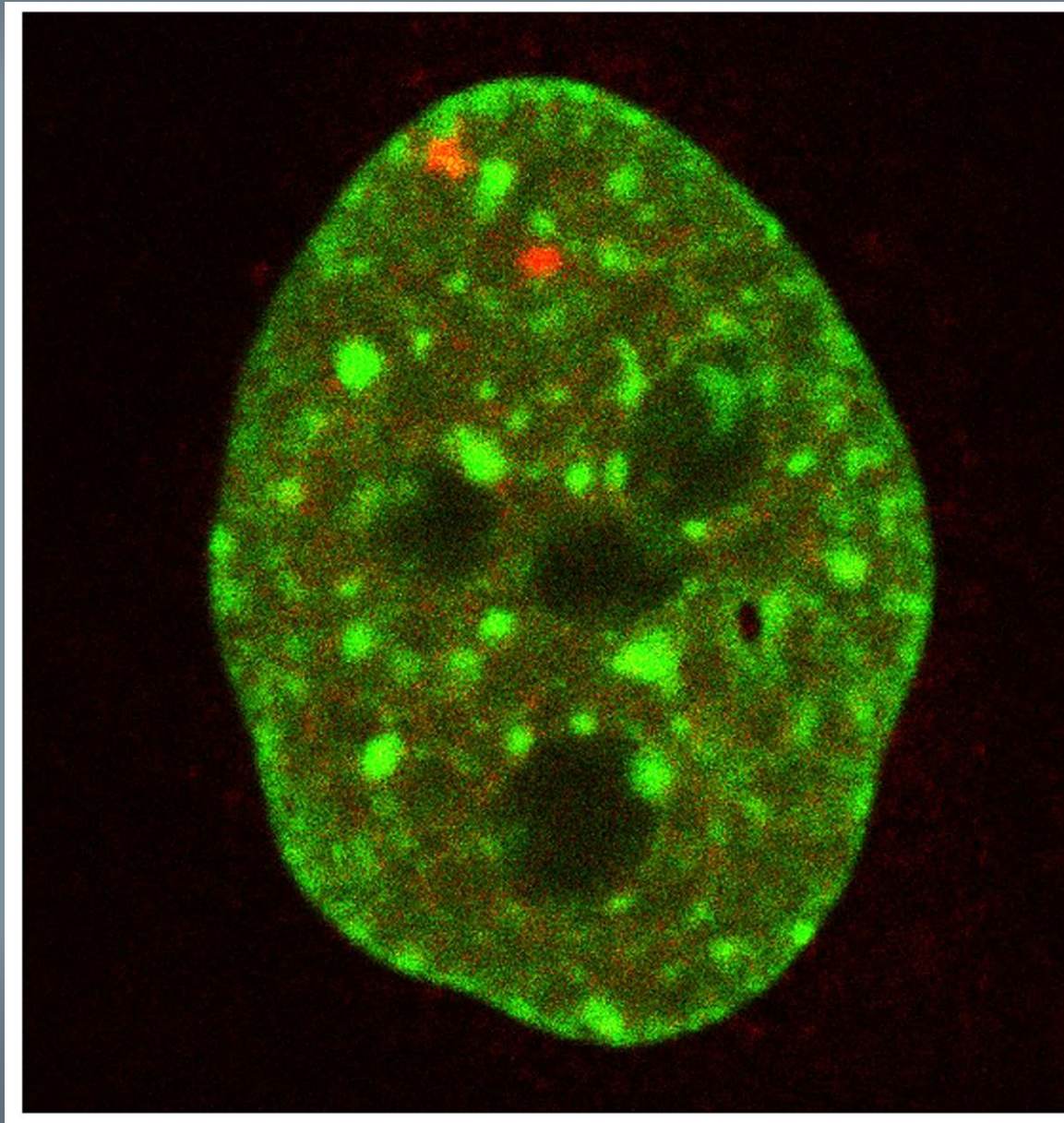
Non-homologous end joining



Homologous recombination

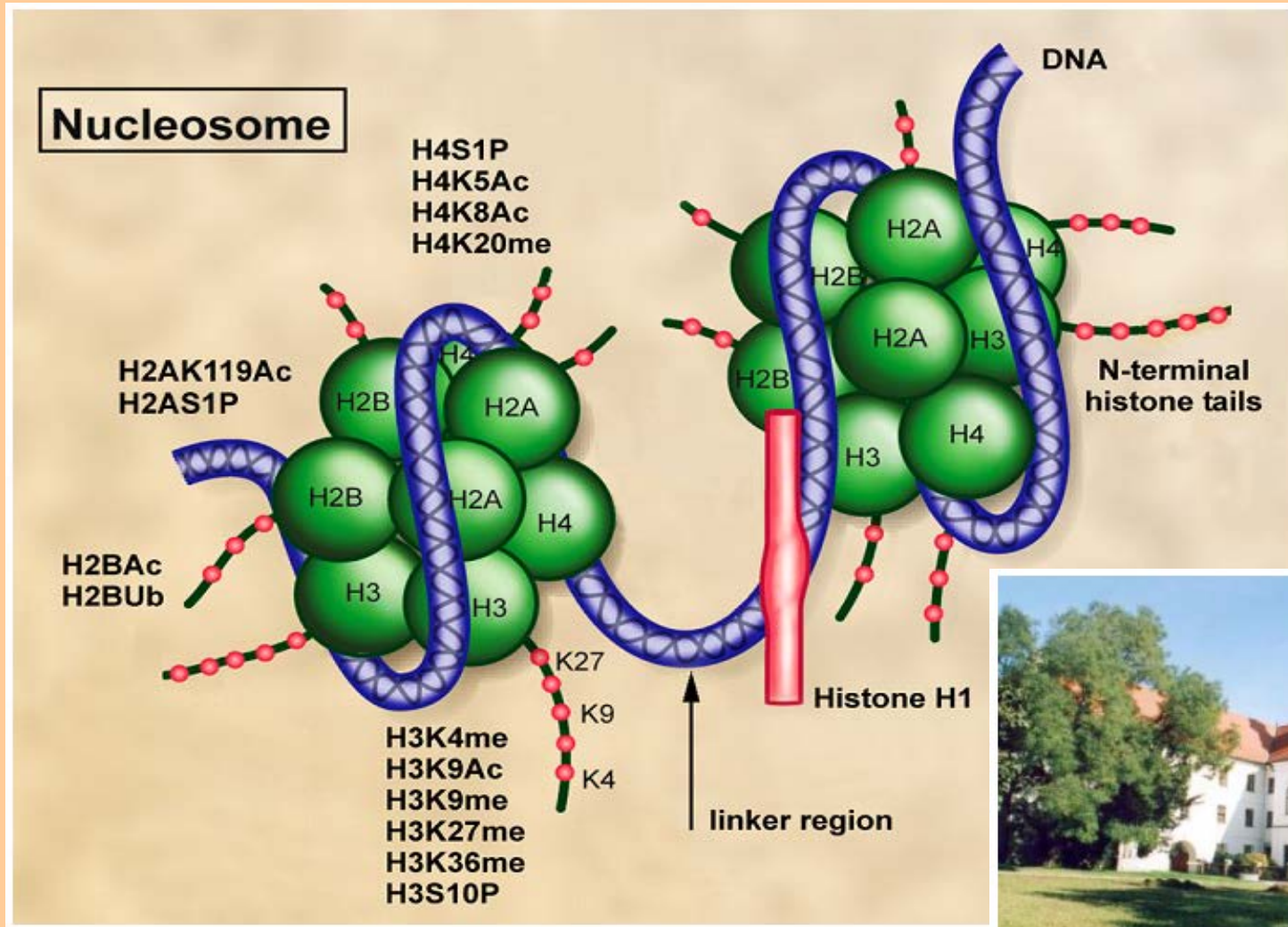


DNA repair foci

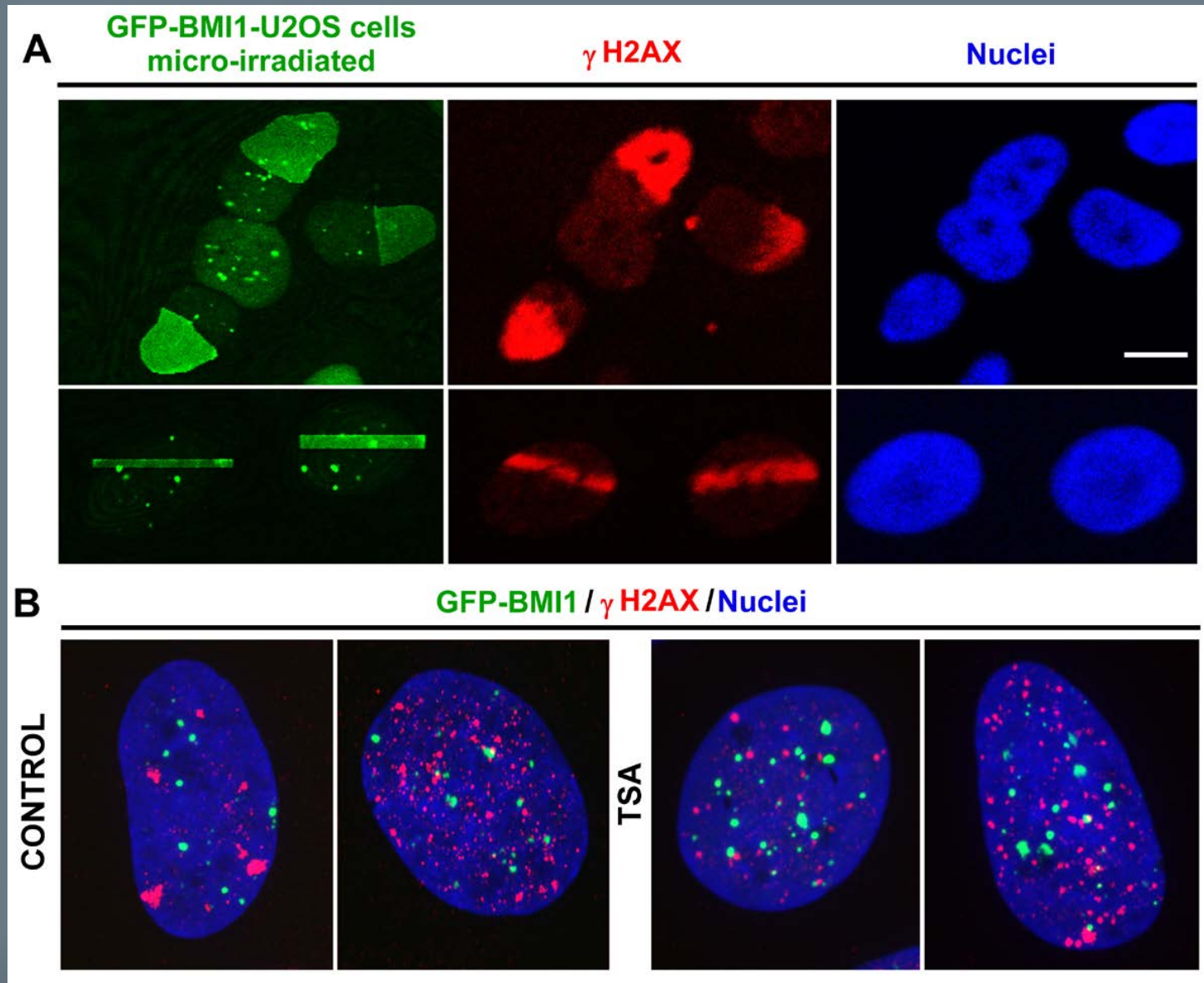


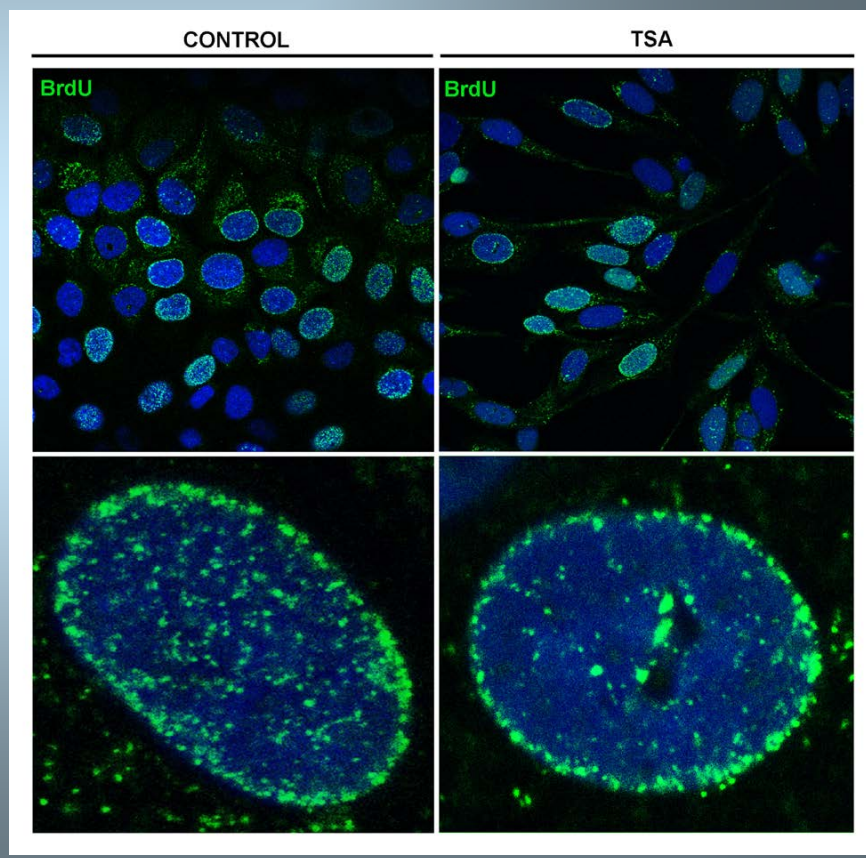
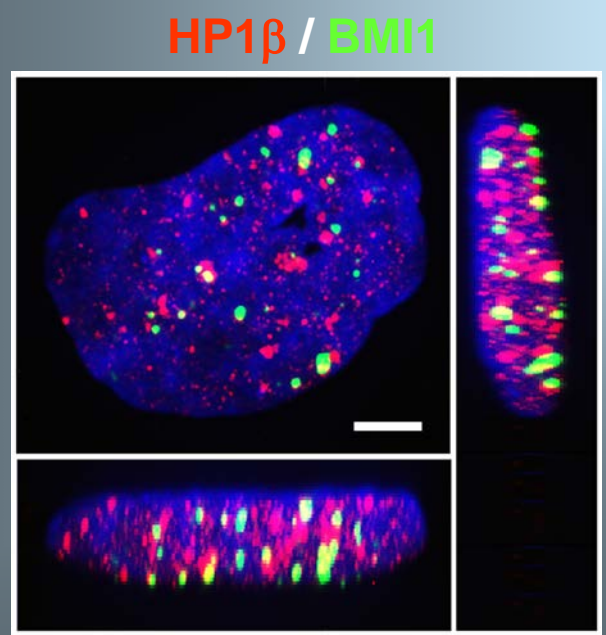
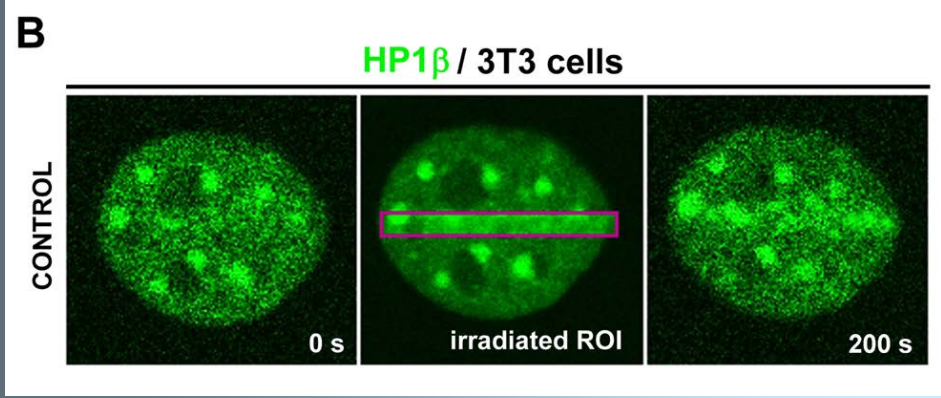
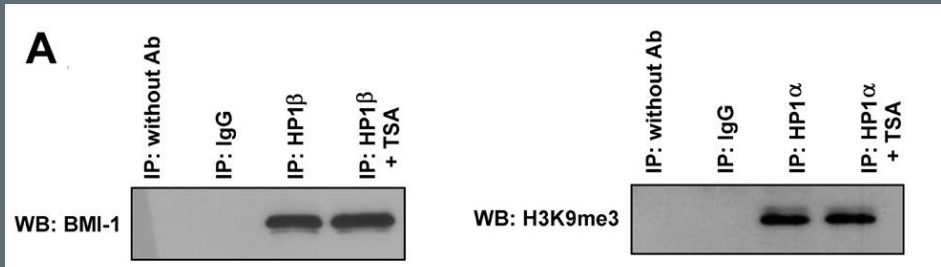
Histone signature

Brno nomenclature for histone modifications (Turner, 2005)



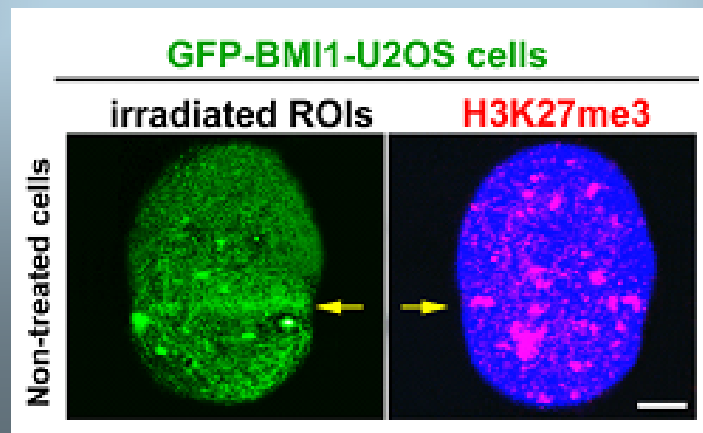
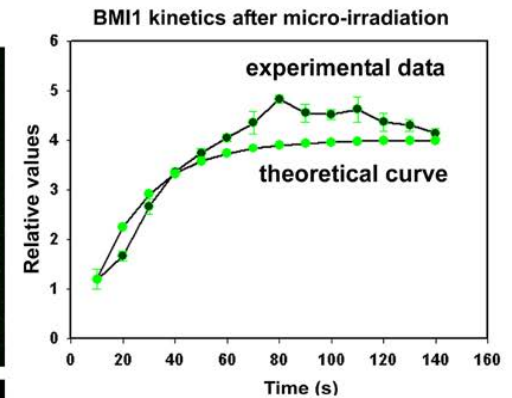
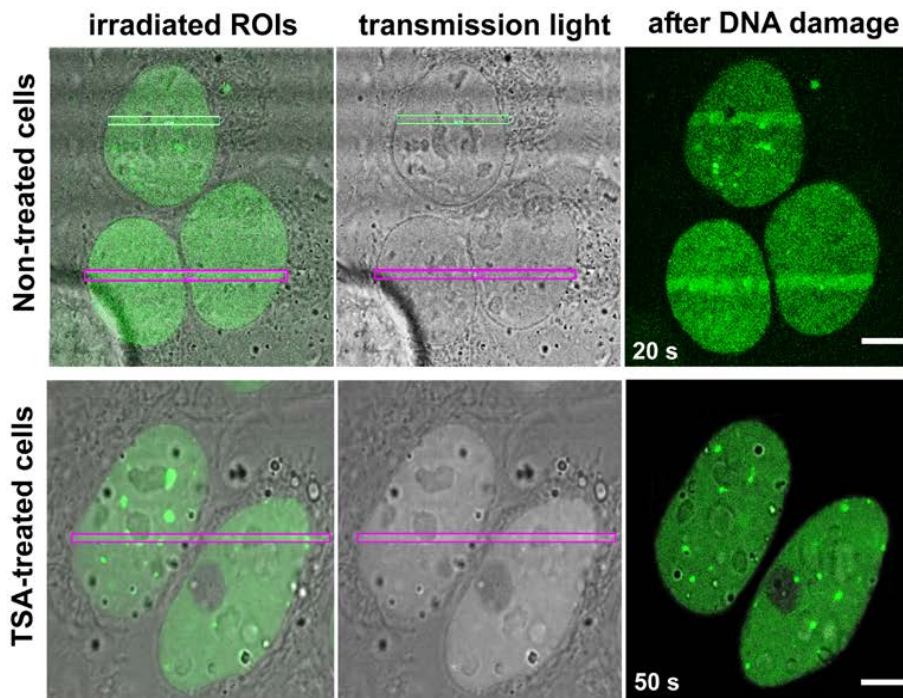
Využití UV laseru 355 nm ke studiu DNA reparace

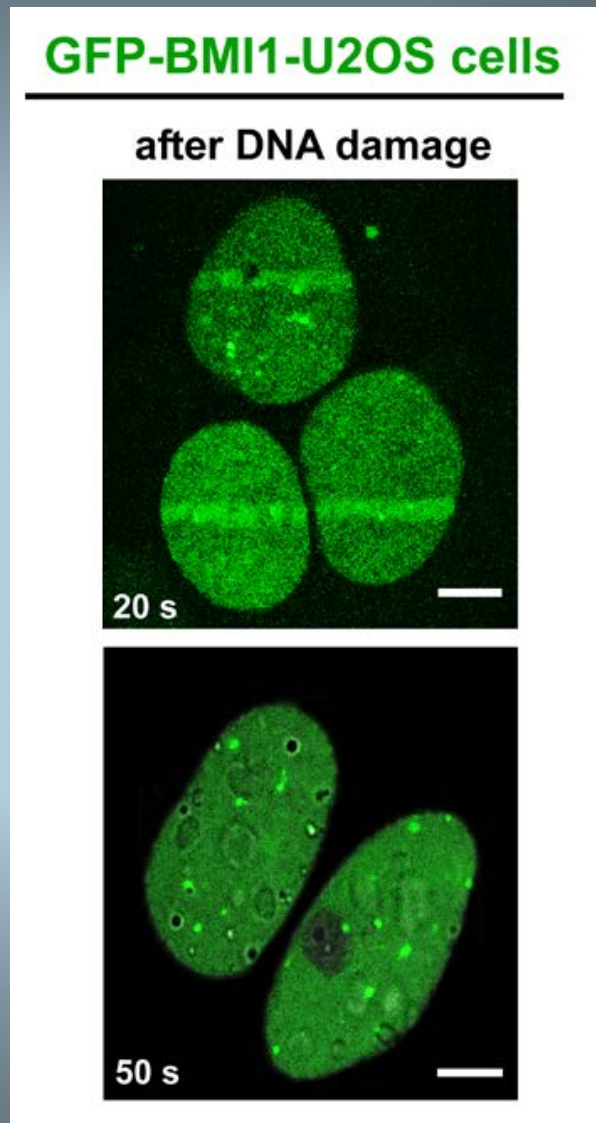
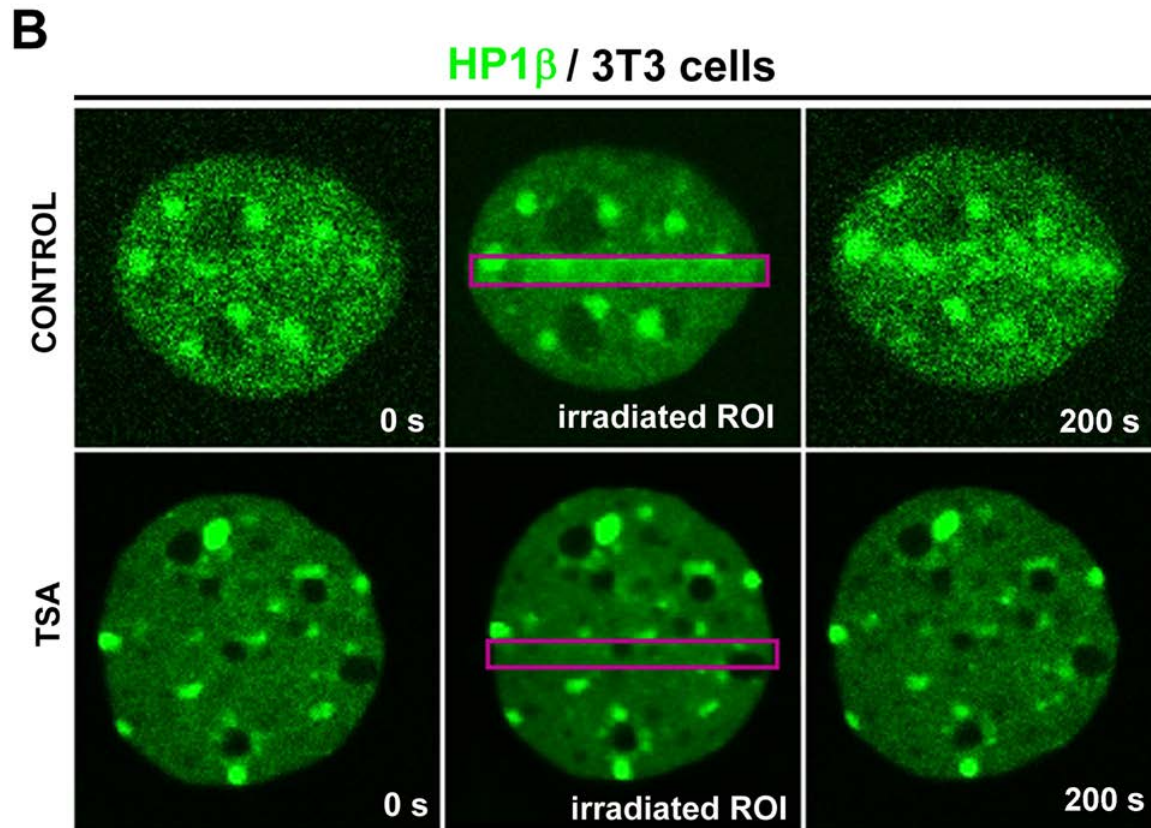
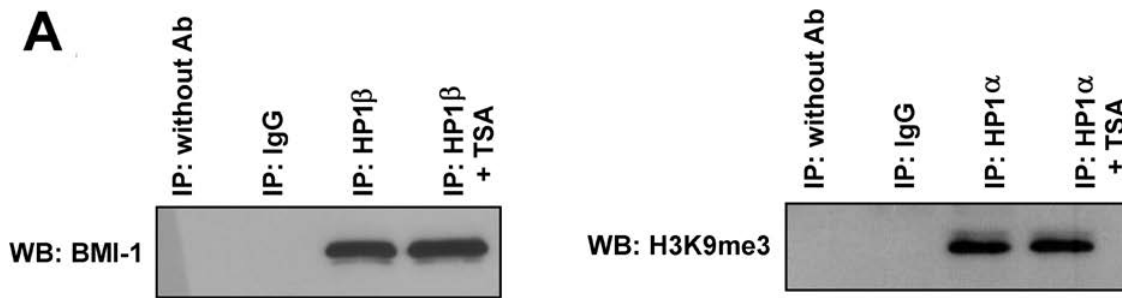




Experiments of Gabriela Šustáčková, Eva Bártová and Lenka Stixová

GFP-BMI1-U2OS cells

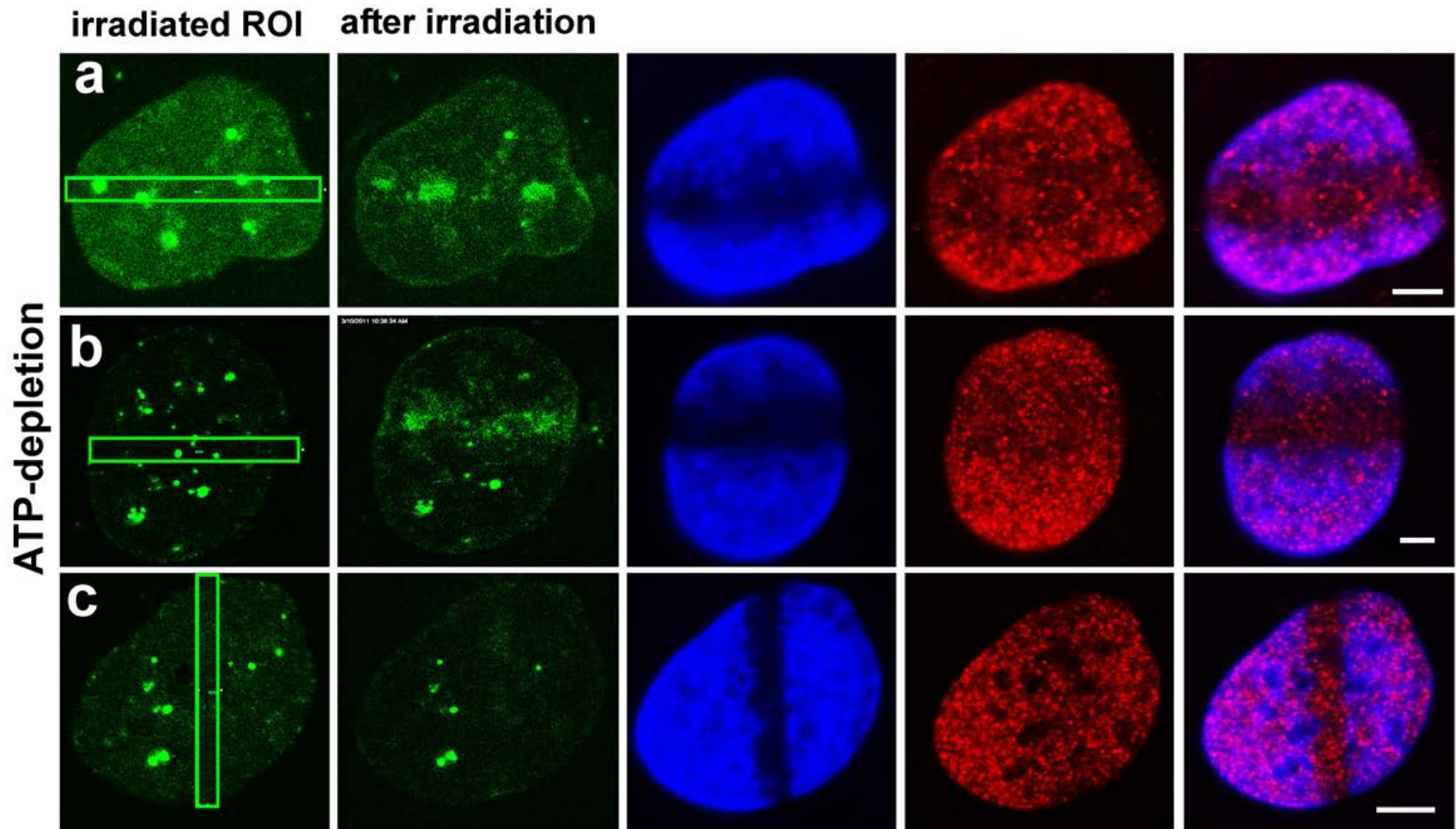




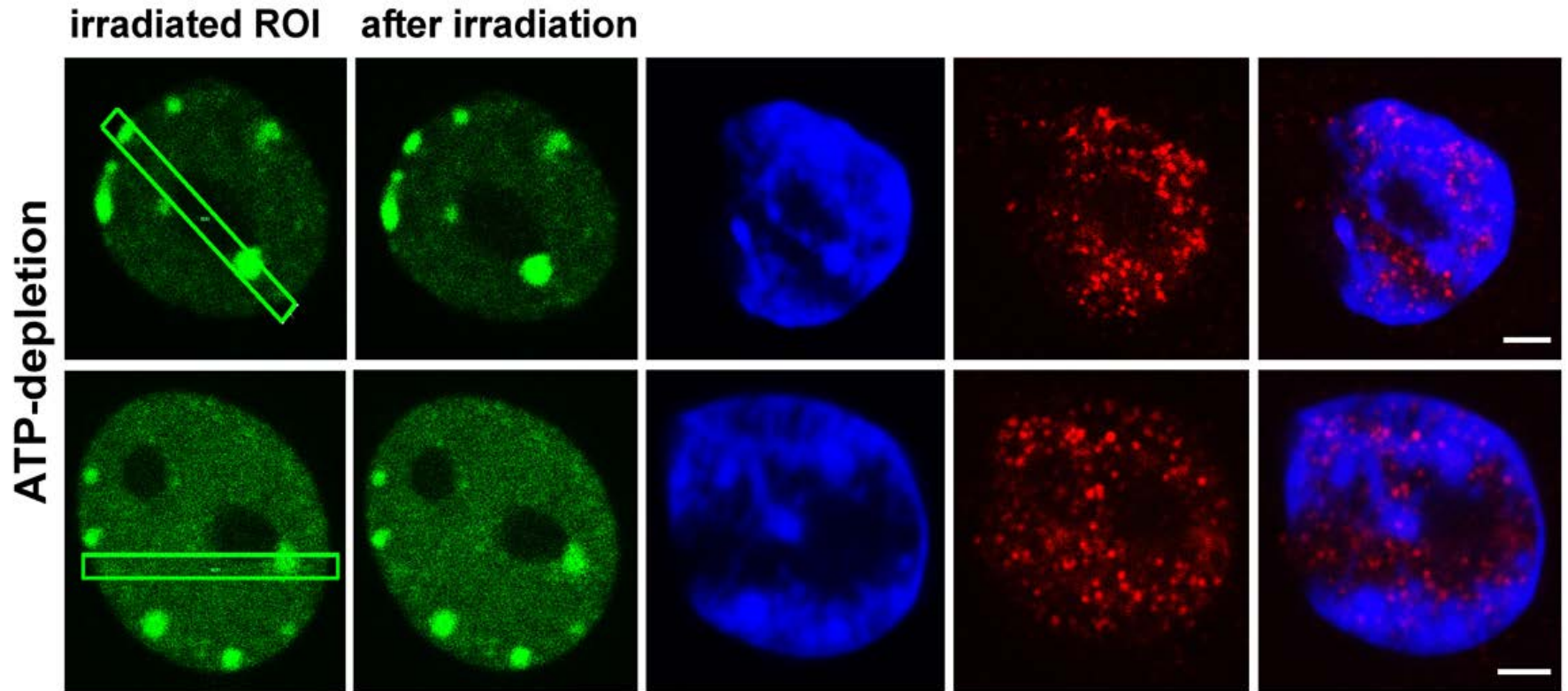
ATP depletion

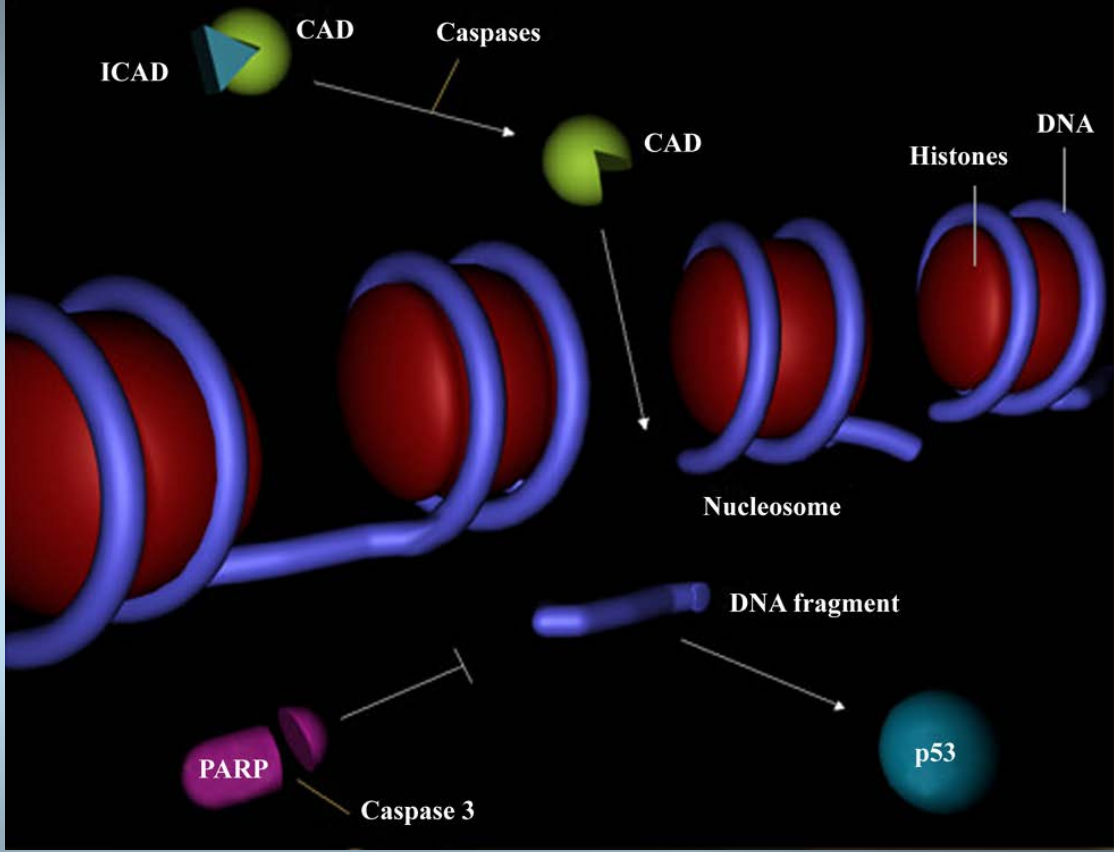
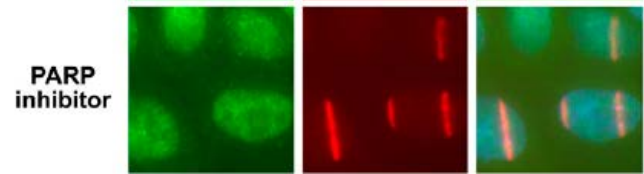
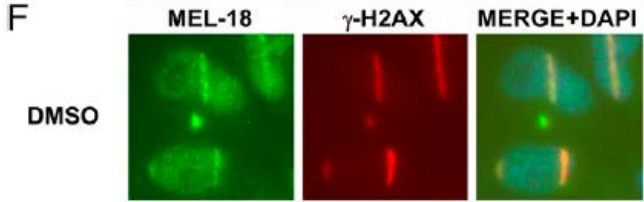
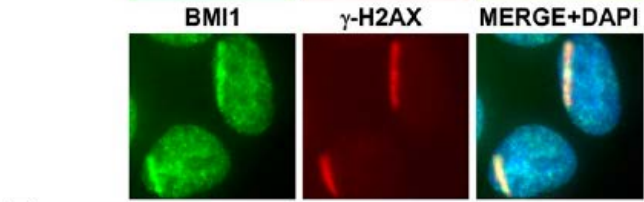
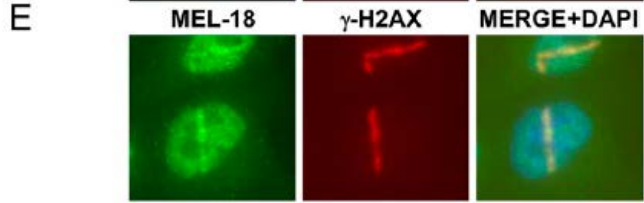
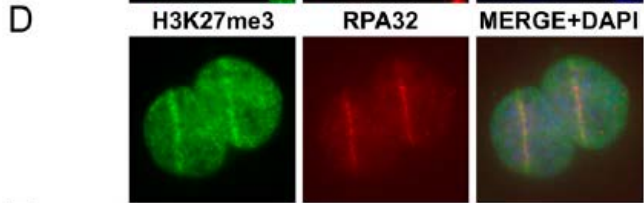
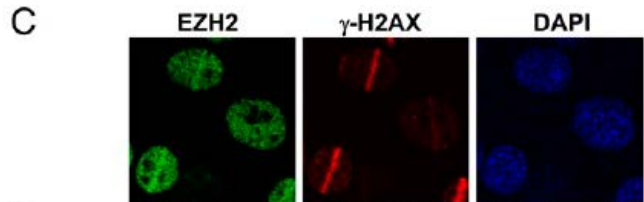
A

GFP-BMI1 / γ H2AX / Nucleus



GFP-HP1 β / γ H2AX / Nucleus





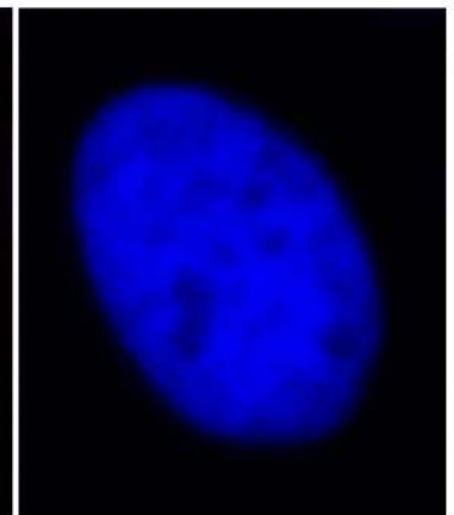
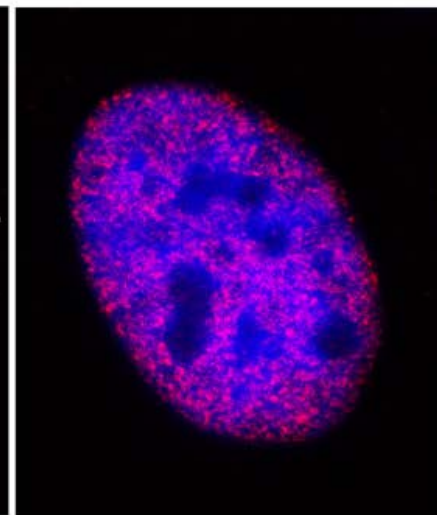
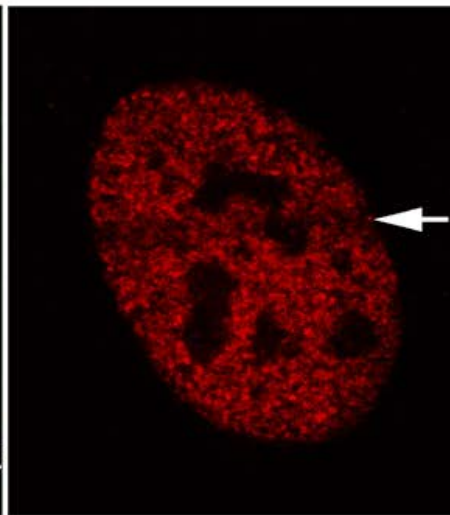
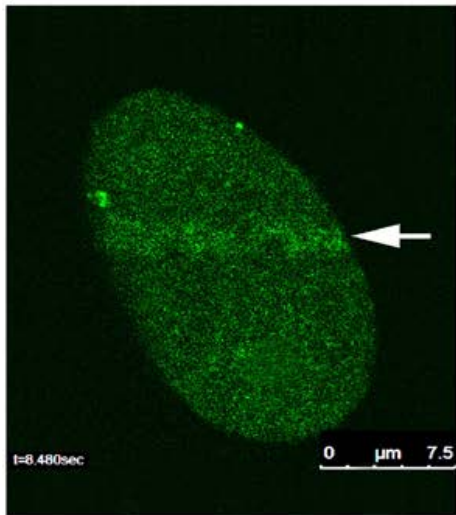
DNA repair

GFP-BMI1-U2OS cell

acetylated lysines

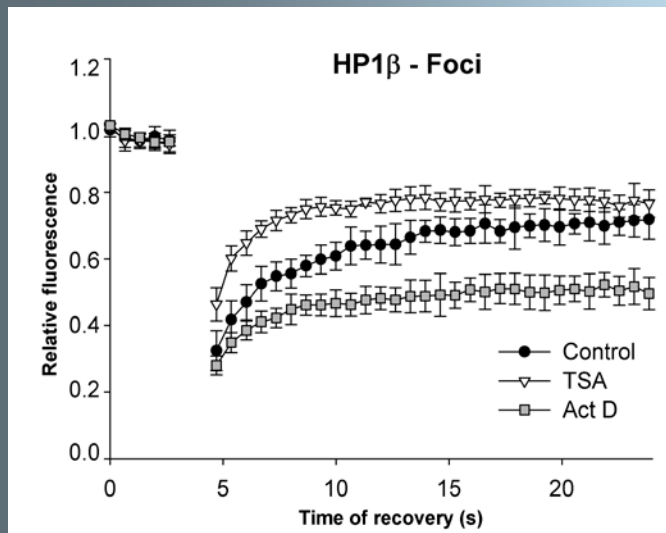
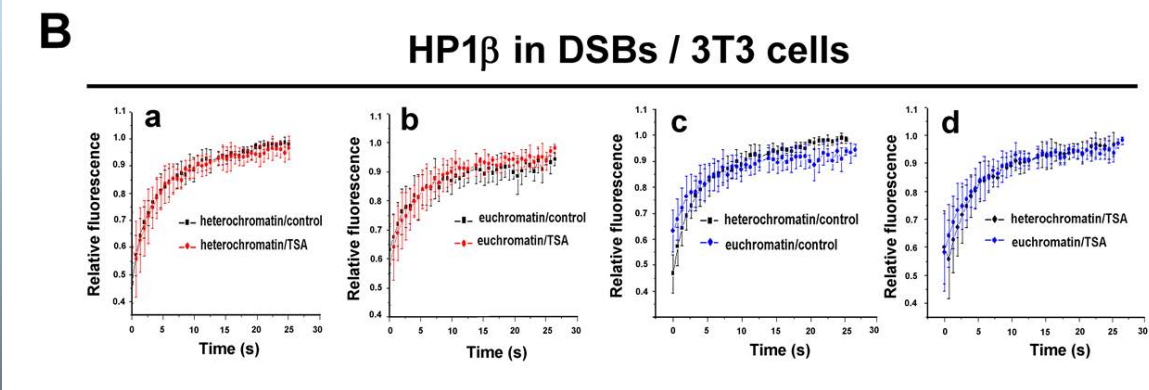
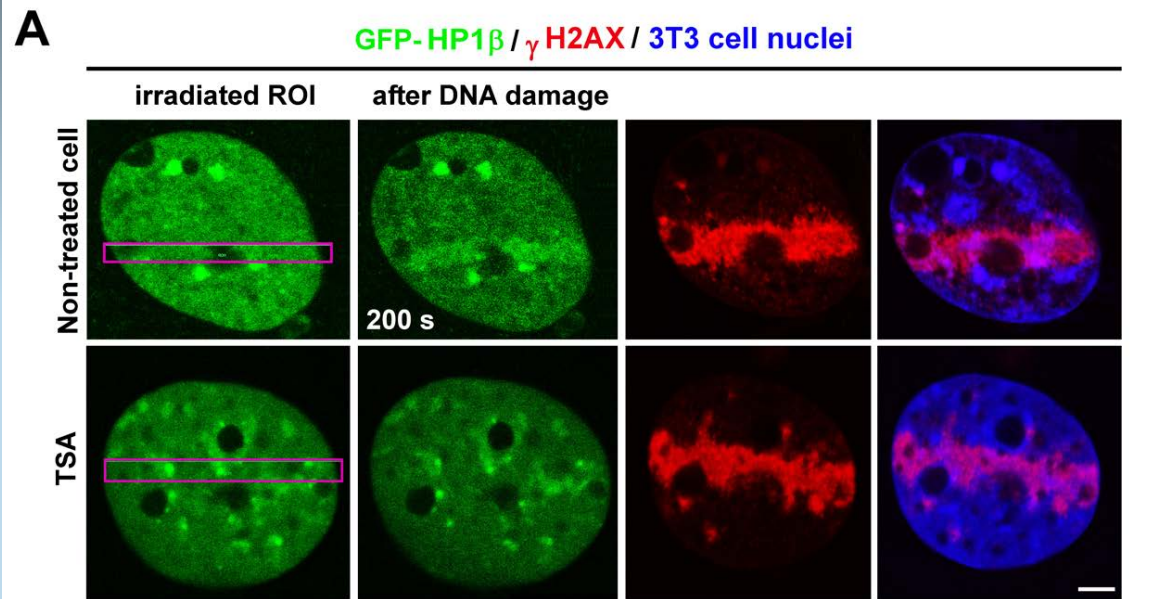
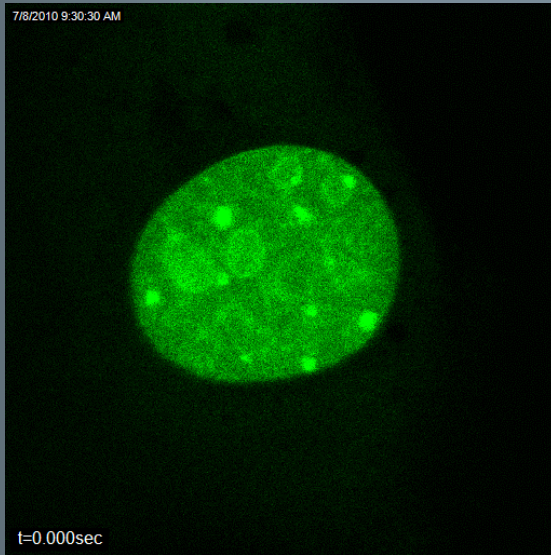
overlay

nucleus



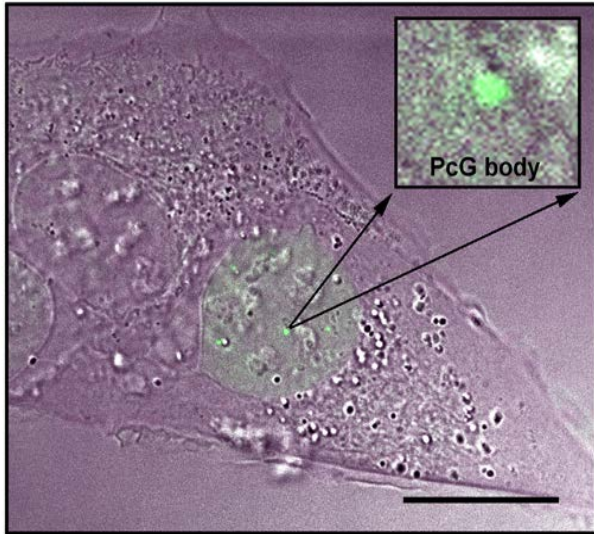
Experiments of Gabriela Šustáčková and Soňa Legartová

FRAP in UV-damaged chromatin with accumulated BMI1 and HP1 β

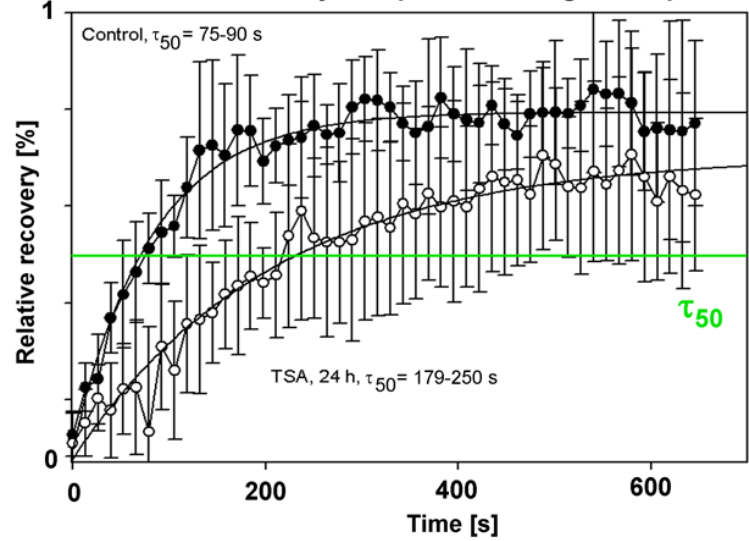


FRAP – BMI1

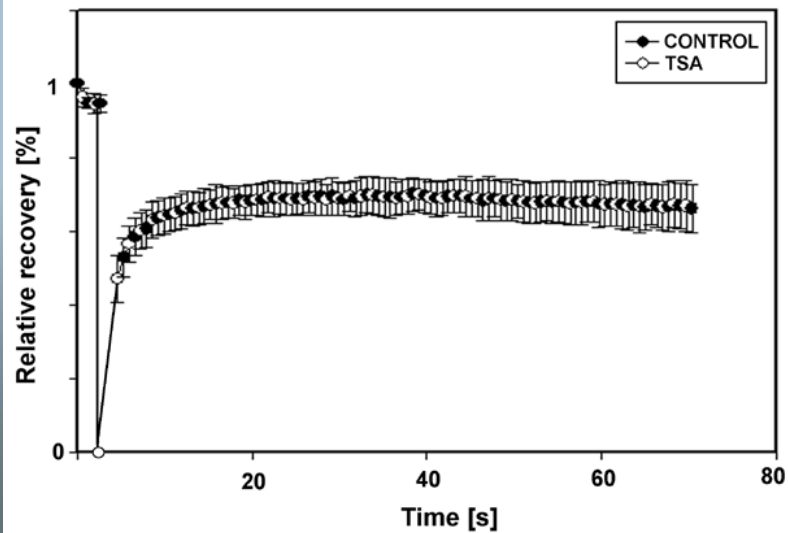
PcG bodies in living cell



Fluorescence recovery after photobleaching - BMI 1 protein

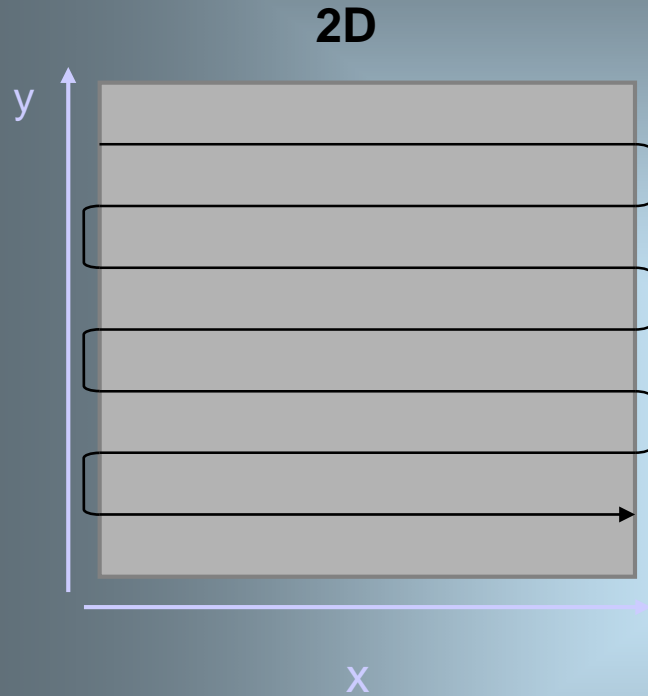


Fluorescence recovery after photobleaching in DSBs

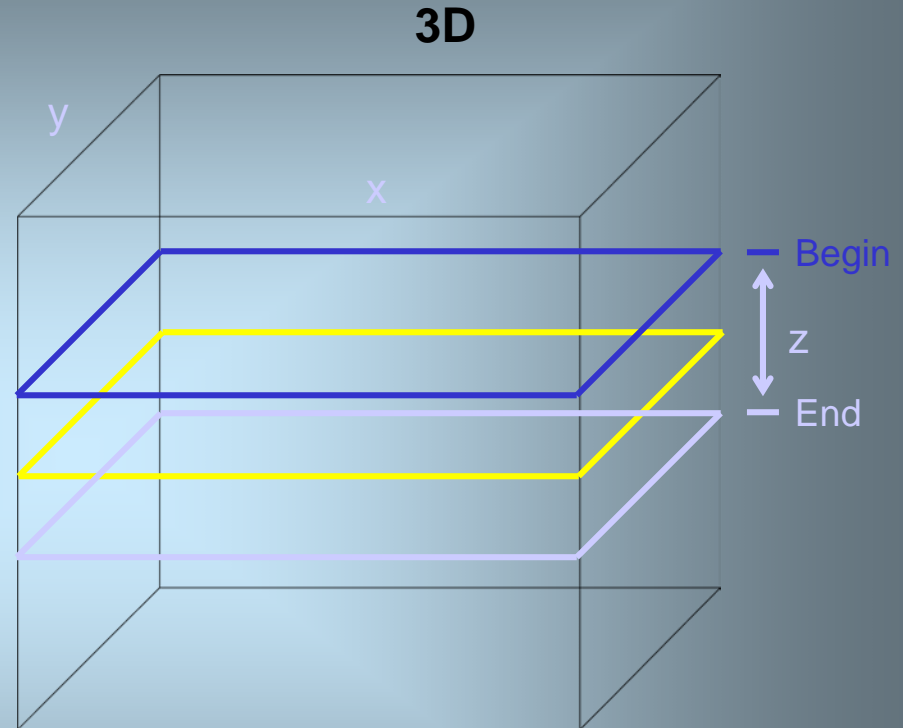


**Additional molecular-biology methods with
application for confocal microscopy**

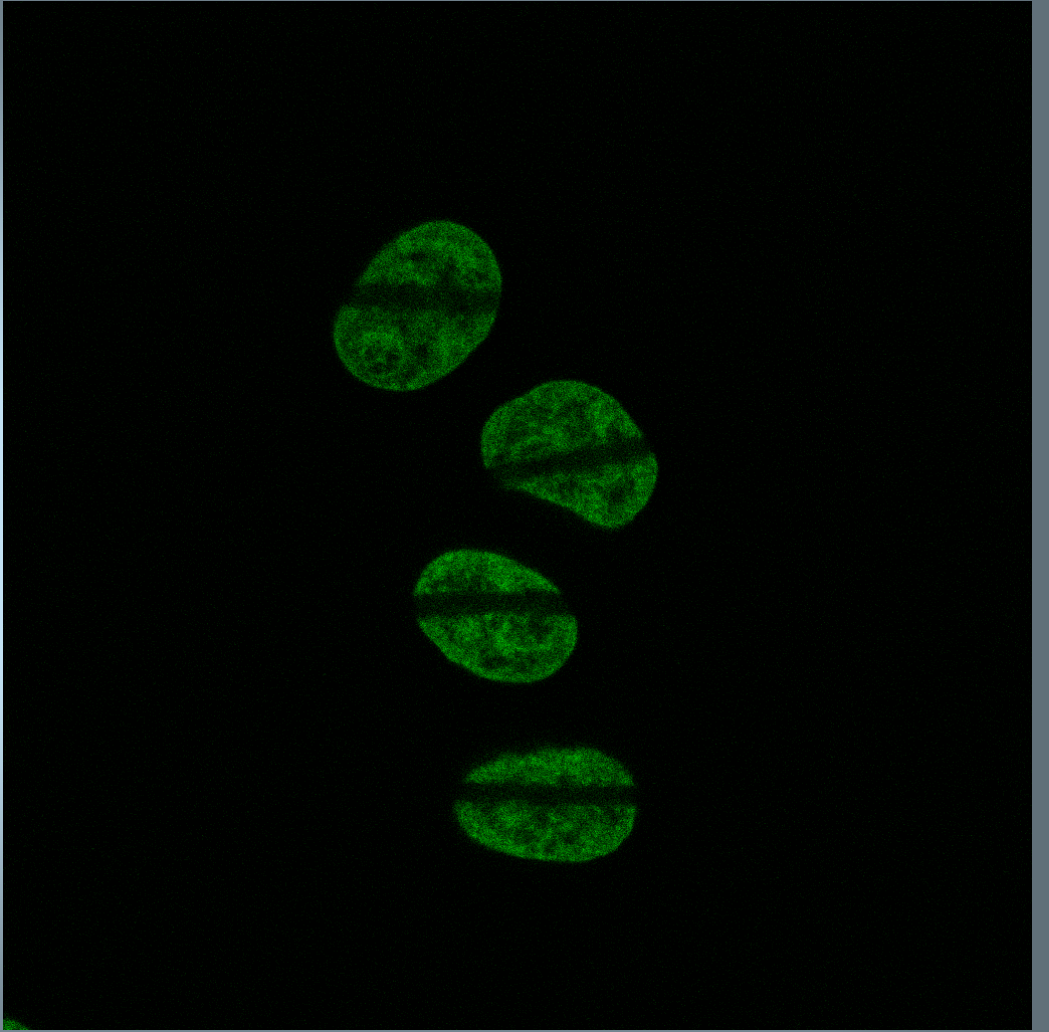
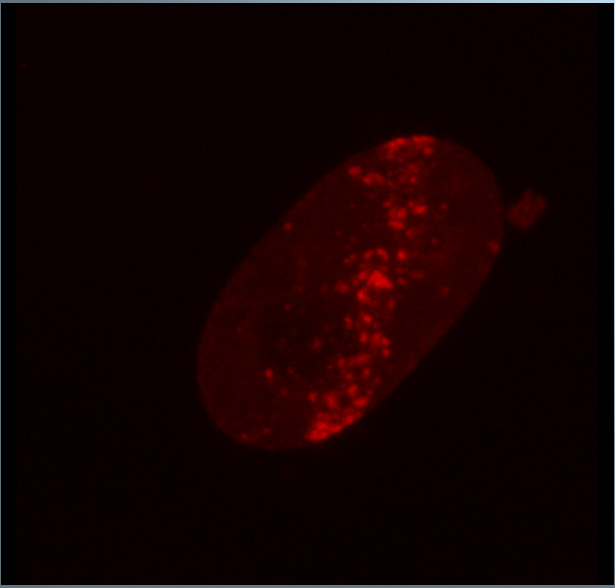
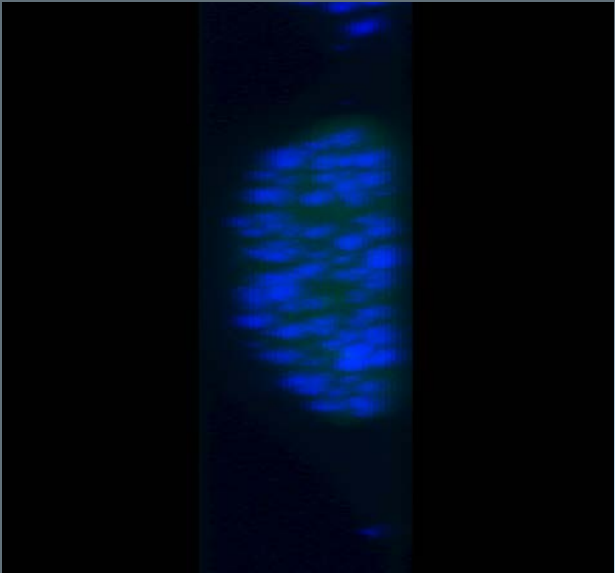
Scanning in 2D and 3D by confocal microscope



Laser beam moves firstly along x axis and then starts with new line in y axis.



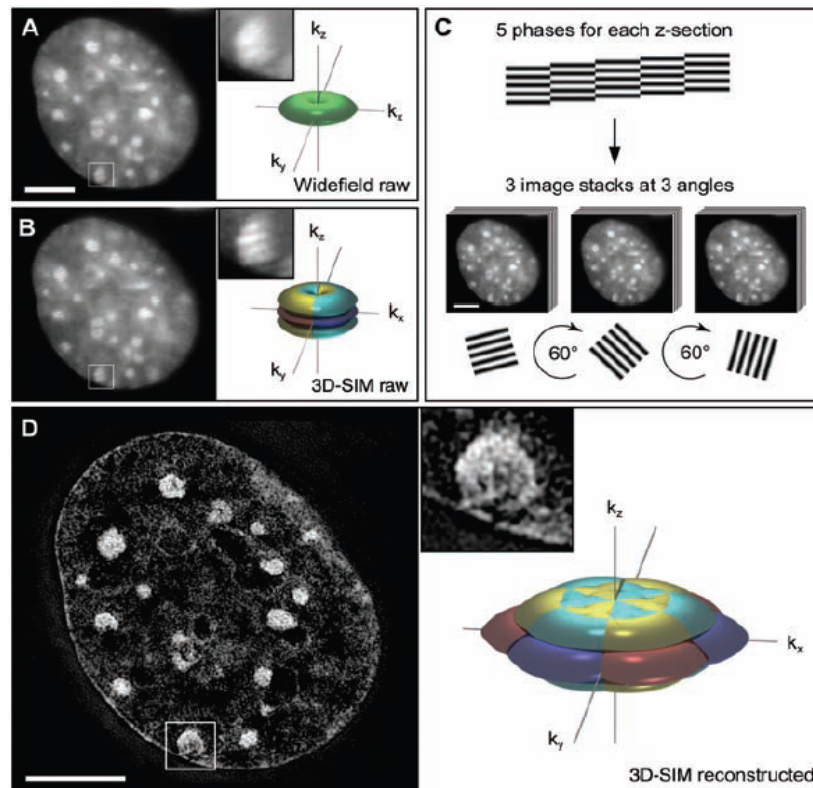
Finishing scanning of one thin optical slice in xy plane, the scanning plane is moved in z axis to other slice



Subdiffraction Multicolor Imaging of the Nuclear Periphery with 3D Structured Illumination Microscopy

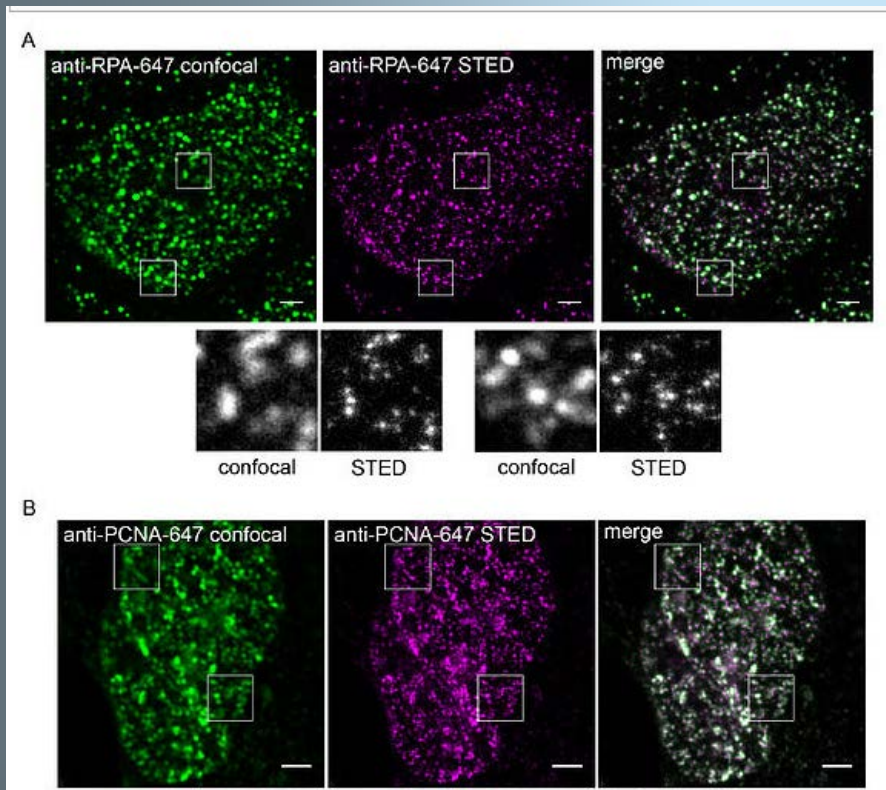
Lothar Schermelleh,^{1*} Peter M. Carlton,^{2*} Sebastian Haase,^{2,4} Lin Shao,²
Lukman Winoto,² Peter Kner,² Brian Burke,³ M. Cristina Cardoso,⁴ David A. Agard,²
Mats G. L. Gustafsson,⁵ Heinrich Leonhardt,^{1*†} John W. Sedat^{2*†}

Fig. 1. Subdiffraction resolution imaging with 3D-SIM. **(A and B)** Cross section through a DAPI-stained C2C12 cell nucleus acquired with conventional wide-field illumination (A) and with structured illumination (B), showing the striped interference pattern (inset). The renderings to the right illustrate the respective support of detection in frequency space. The axes k_x , k_y , and k_z indicate spatial frequencies along the x , y , and z directions. The surfaces of the renderings represent the corresponding resolution limit. The depression of the frequency support ("missing cone") in z direction in (A) indicates the restriction in axial resolution of conventional wide-field microscopy. With 3D-SIM, the axial support is extended but remains within the resolution limit. **(C)** Five phases of the sine wave pattern are recorded at each z position, allowing the shifted components to be separated and returned to their proper location in frequency space. Three image stacks are recorded with the diffraction grating sequentially rotated into three positions 60° apart, resulting in nearly rotationally symmetric support over a larger region of frequency space. **(D)** The same cross section of the reconstructed 3D-SIM image shows enhanced image details compared with the original image (insets). The increase in resolution is shown in frequency space on the right, with the coverage extending two times farther from the origin. Scale bars indicate $5 \mu\text{m}$.

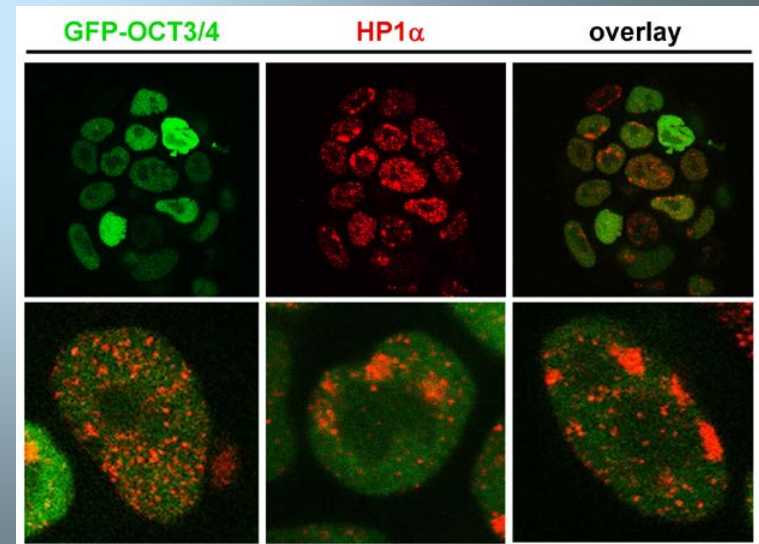


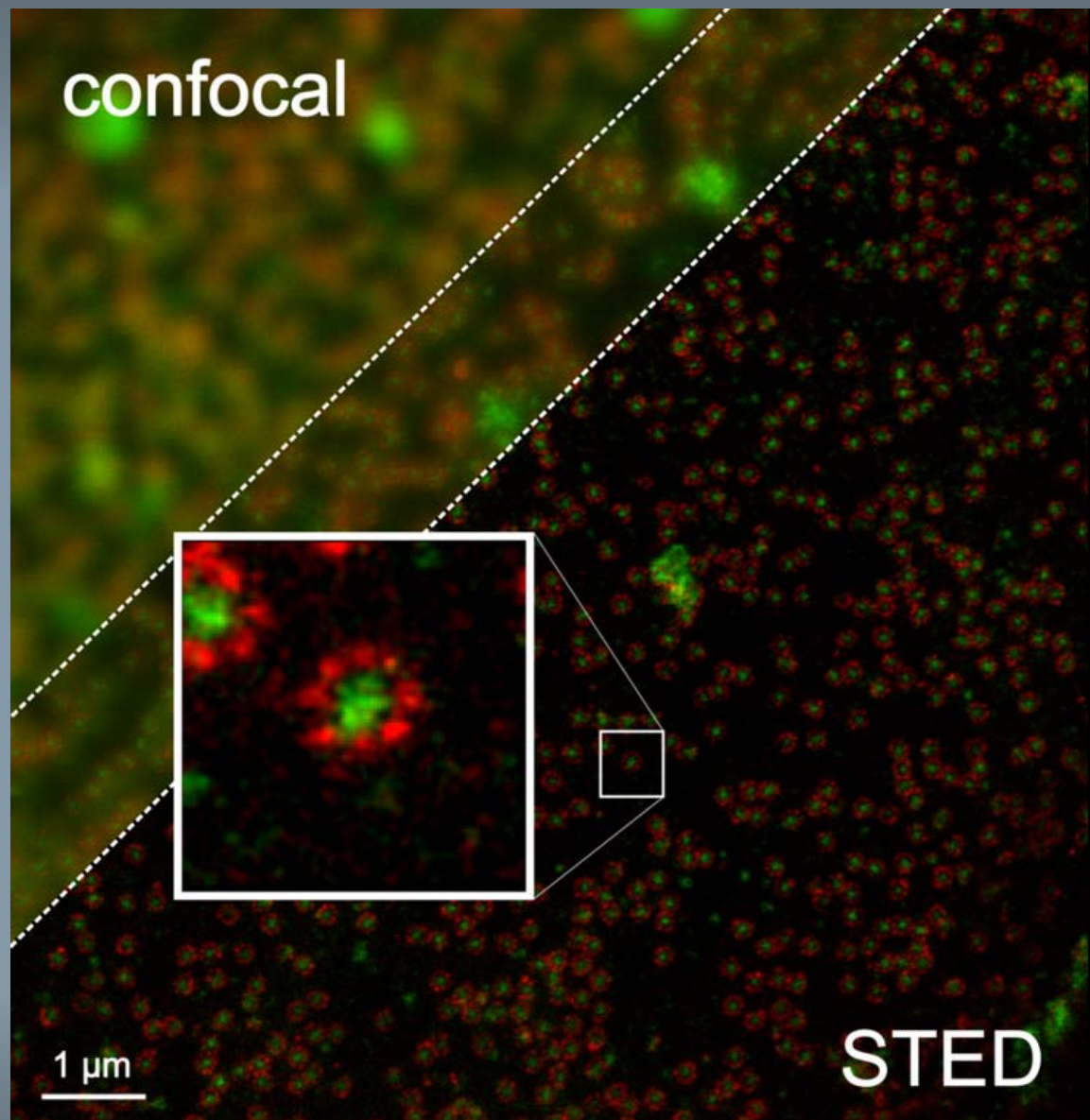
Stimulated Emission Depletion microscopy, or STED microscopy, is a fluorescence microscopy technique that uses the non-linear de-excitation of fluorescent dyes to overcome the resolution limit imposed by diffraction with standard confocal laser scanning microscopes and conventional far-field optical microscopes.

STED

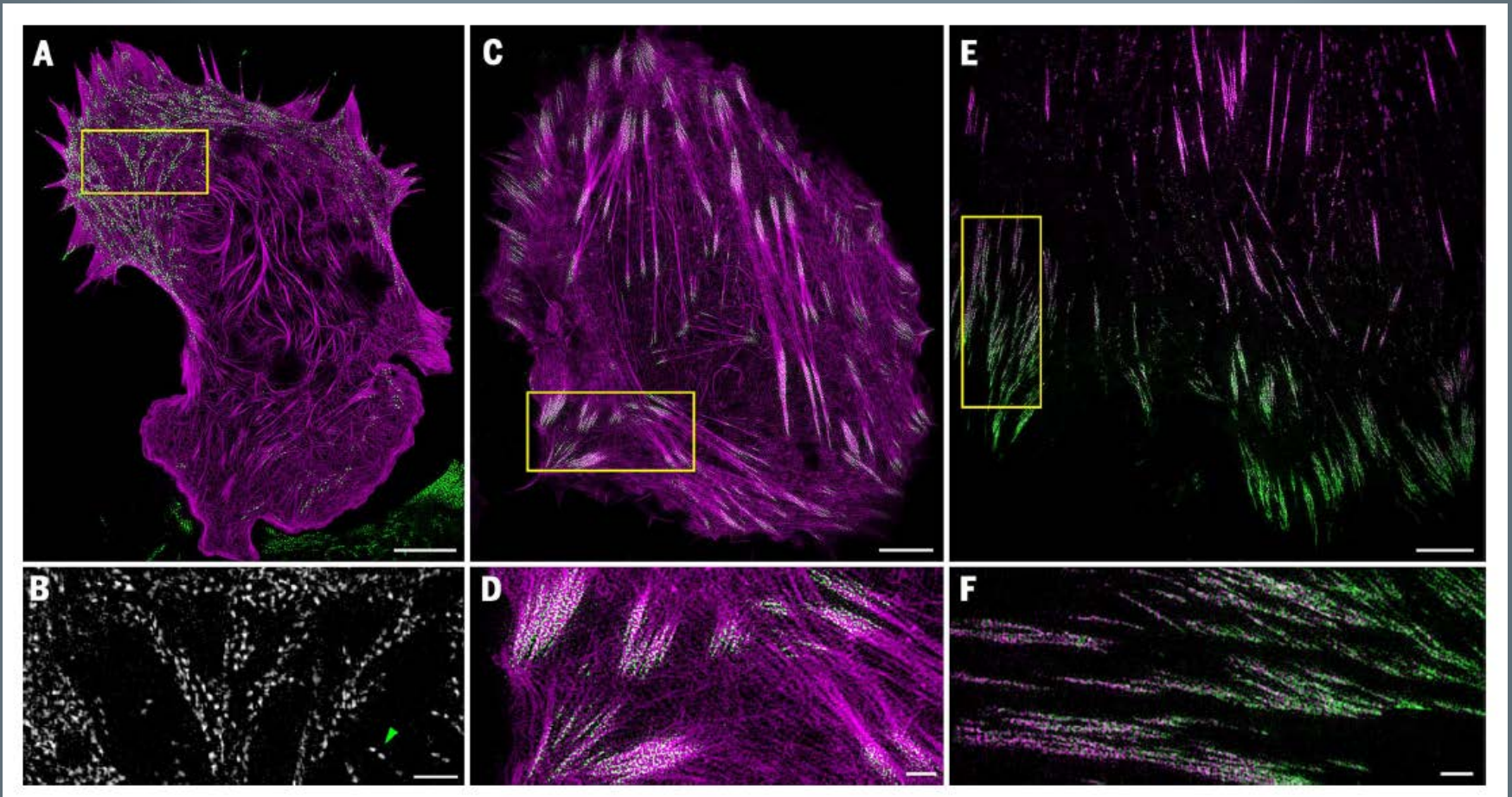


SP-5 LSCM





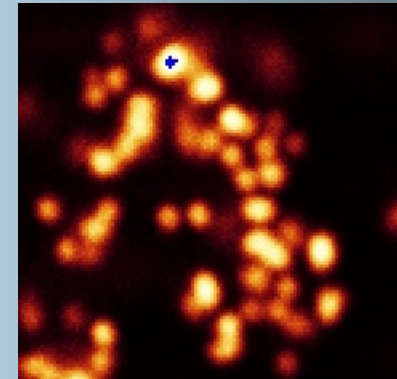
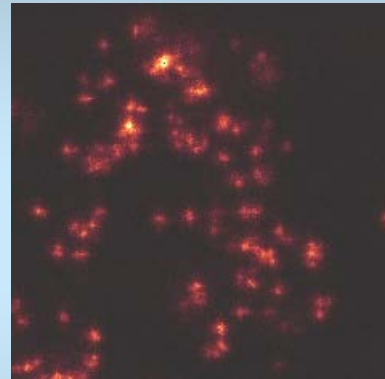
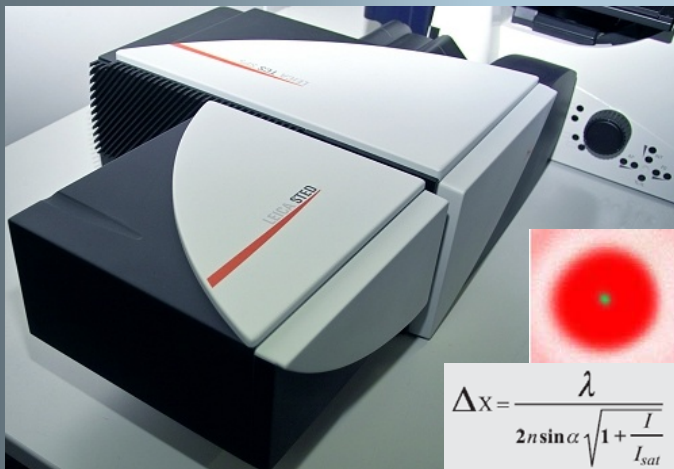
High-speed live-cell imaging



Li et al., Science (2015)

Leica STED – STimulated Emission Depletion SUPERRESOLUTION (subdiffraction) in xy plane

Hell, S. W. and J. Wichmann (1994). *Opt. Lett.*
"Breaking the diffraction resolution limit by stimulated emission"



neurobiology
membrane biology
membrane rafts
intracellular transport

Willig KI et al. *Nature* 2006

Sieber JJ et al. *Biophys J* 2006

Kittel RJ et al. *Science* 2006

Fitzner D et al. *EMBO J* 2006

Kellner RR et al. *Neuroscience* 2007

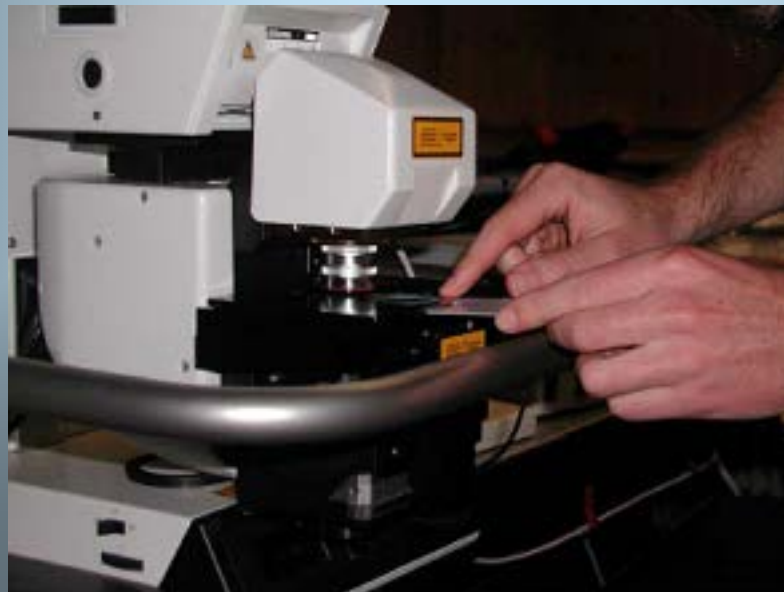
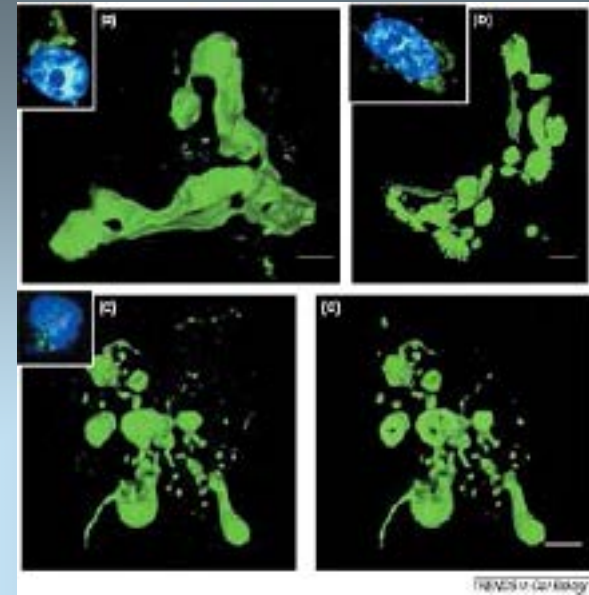
Lin W et al. *PNAS* 2007

Seebach J *Cardiovas. Res.* 2007

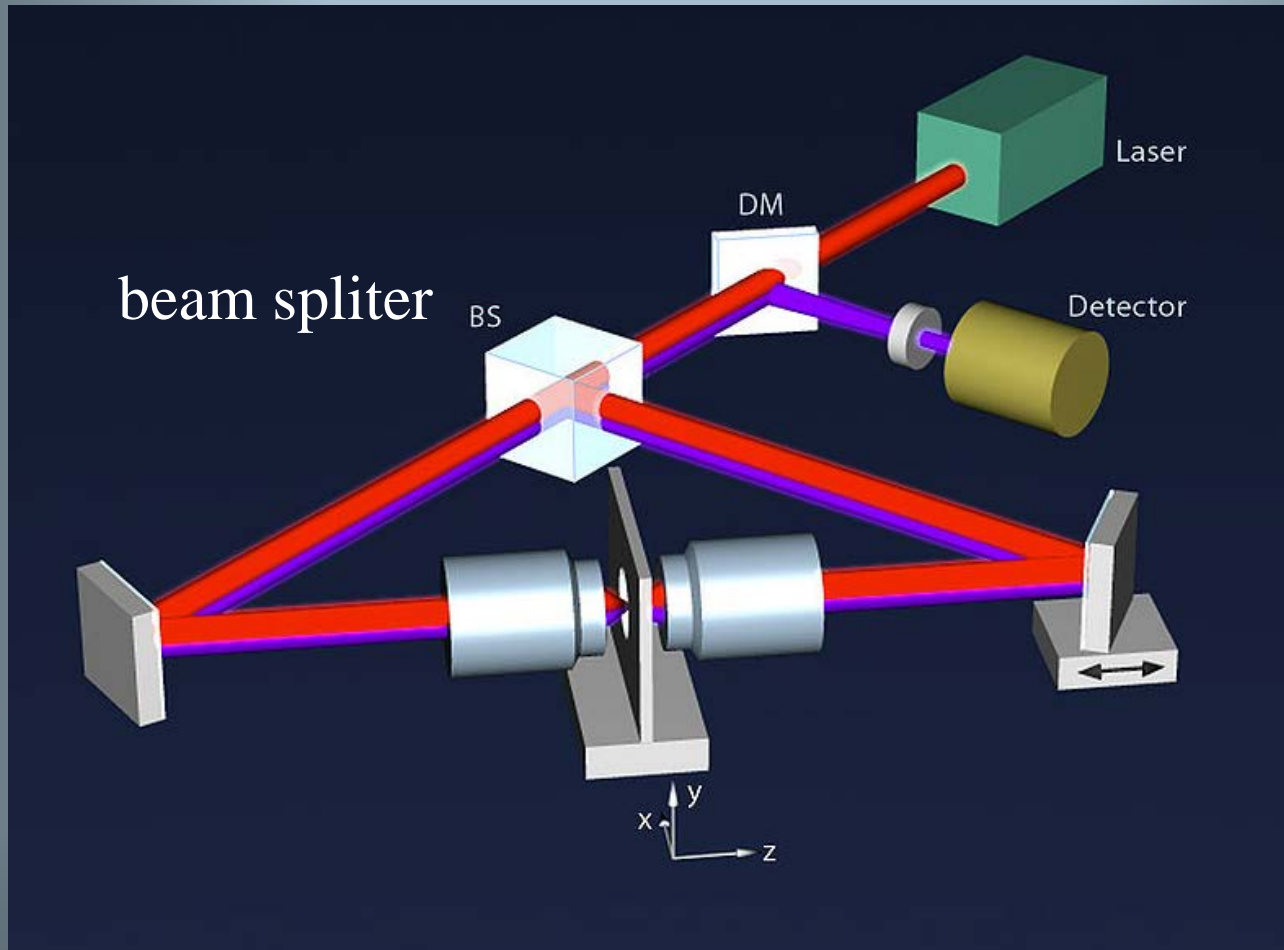
Sieber JJ *Science* 2007

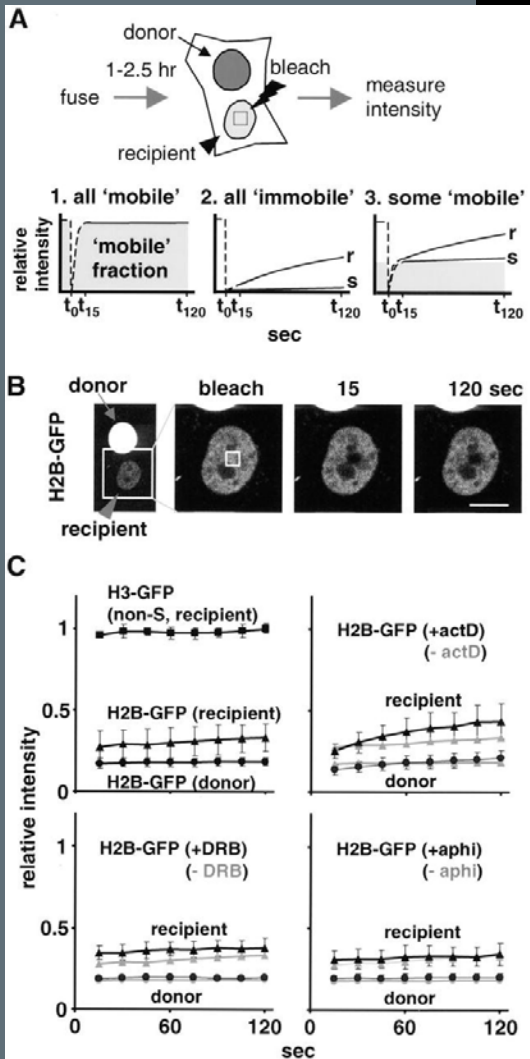
Unique

4-pi microscopy (CC lab in Heidelberg)



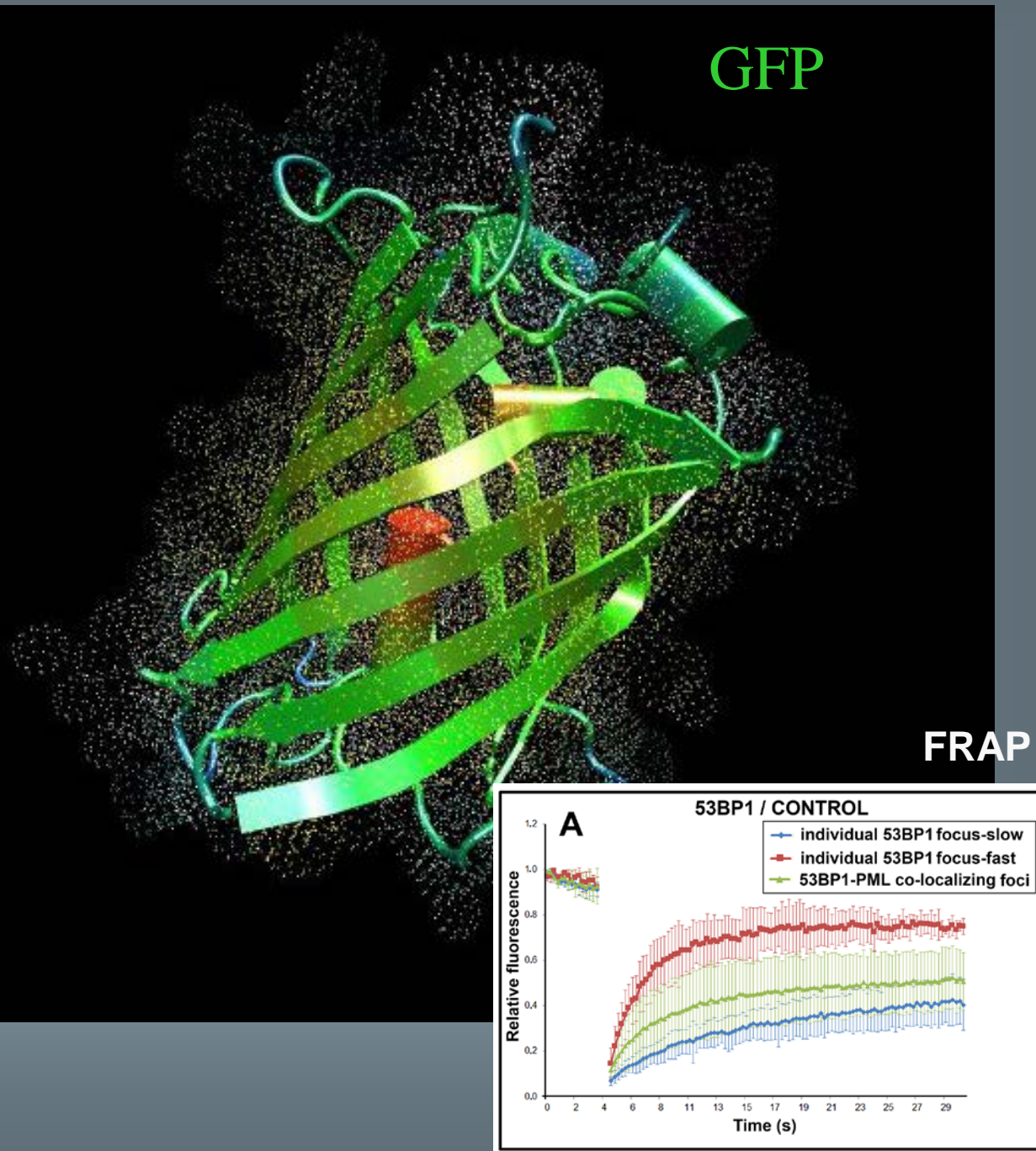
4pi: improved axial resolution. The typical value of 500-700 nm can be improved to 100-150 nm which corresponds to an almost spherical focal spot with 5-7 times less volume than that of standard confocal microscopy.



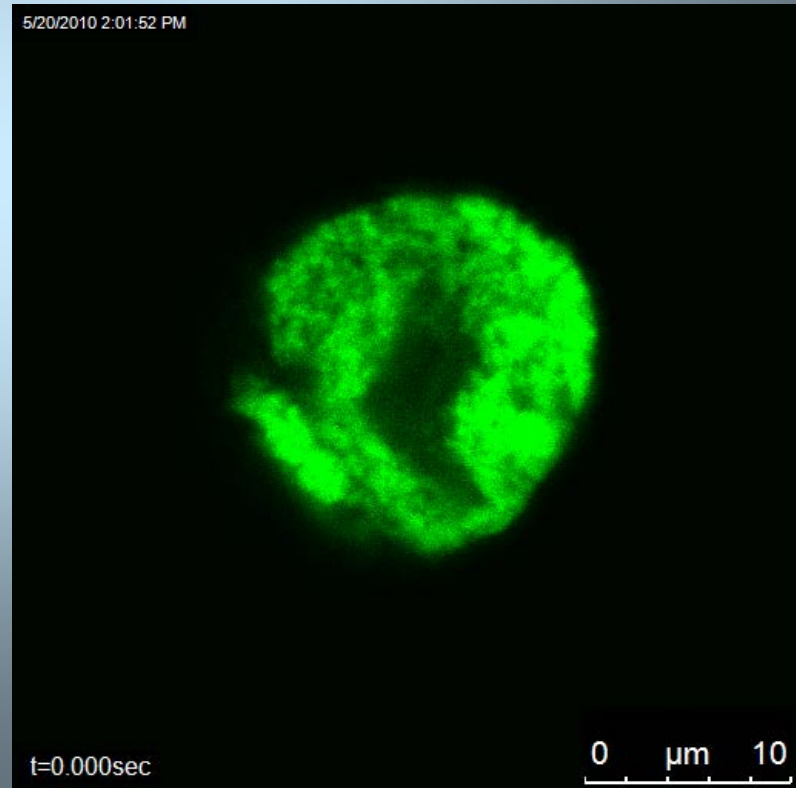
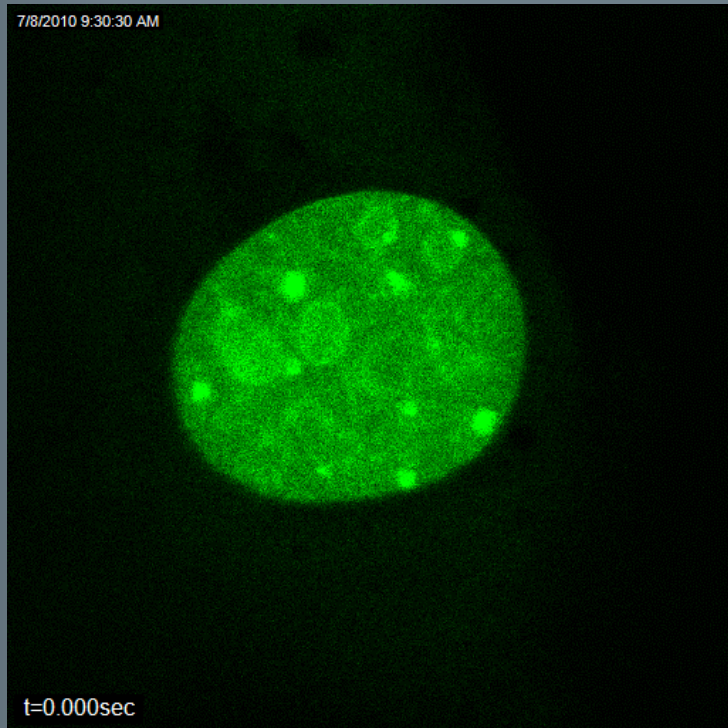


JCB

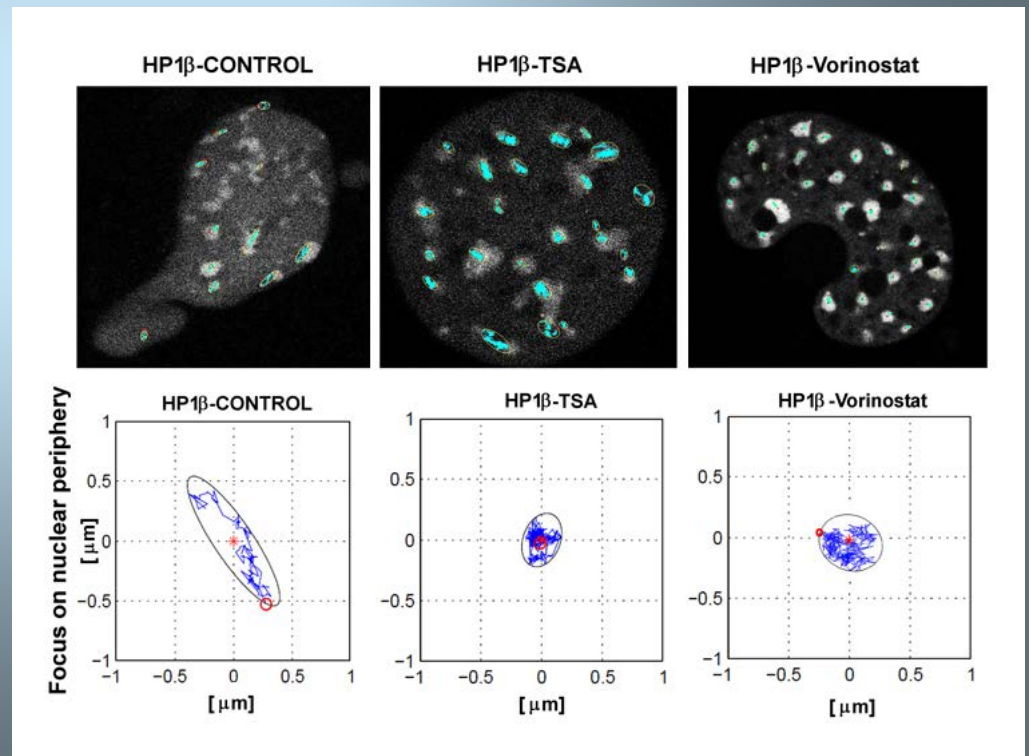
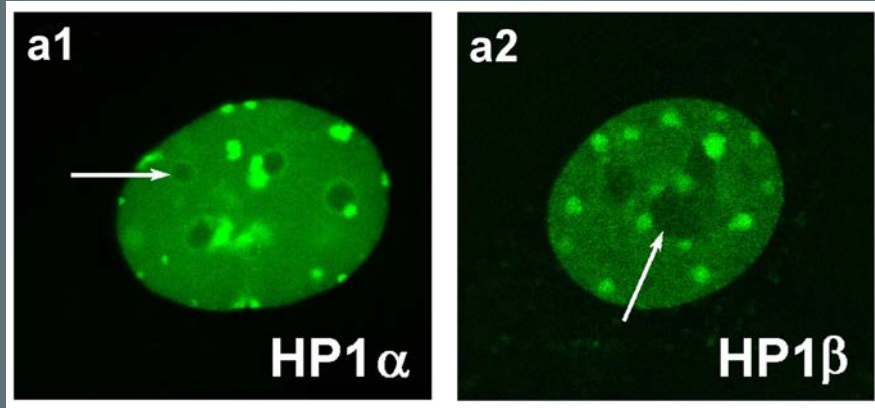
Kimura and Cook (2001)

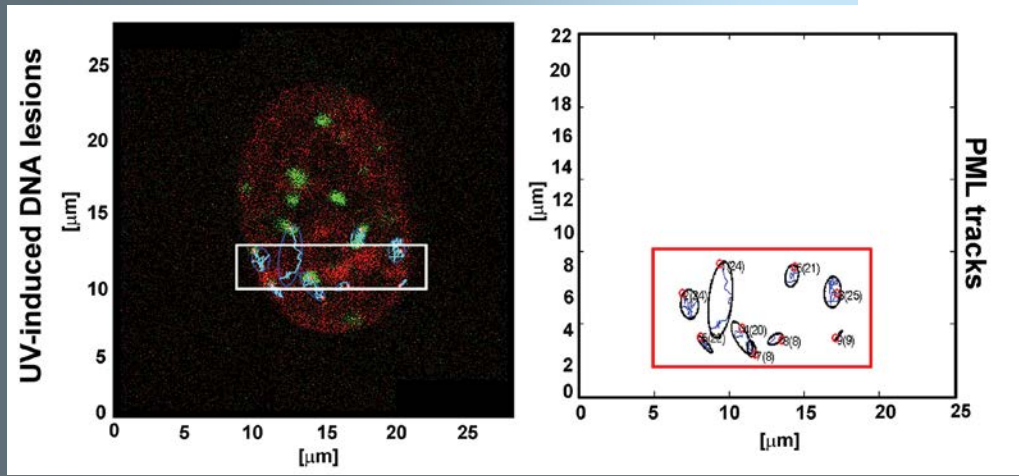
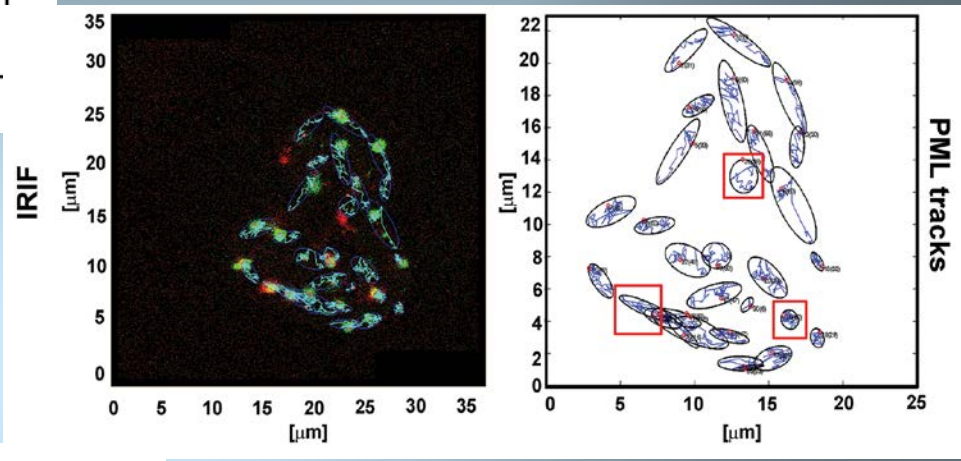
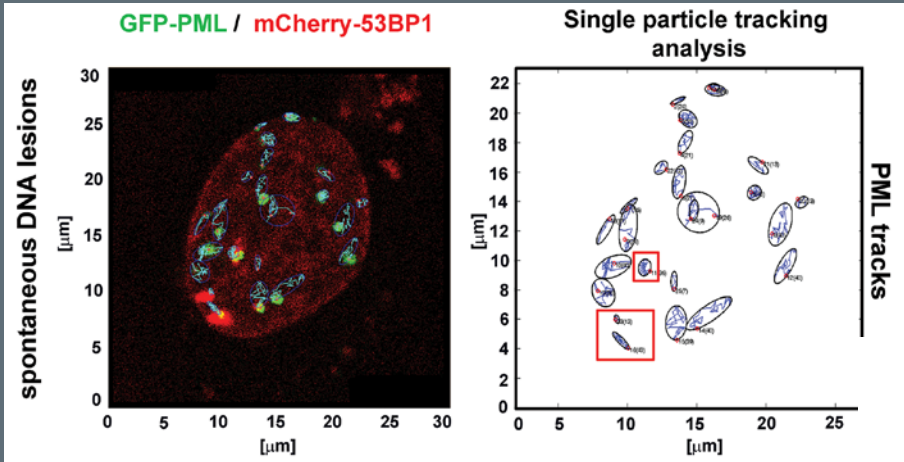


FRAP results on Jmjd2b-tagged by GFP



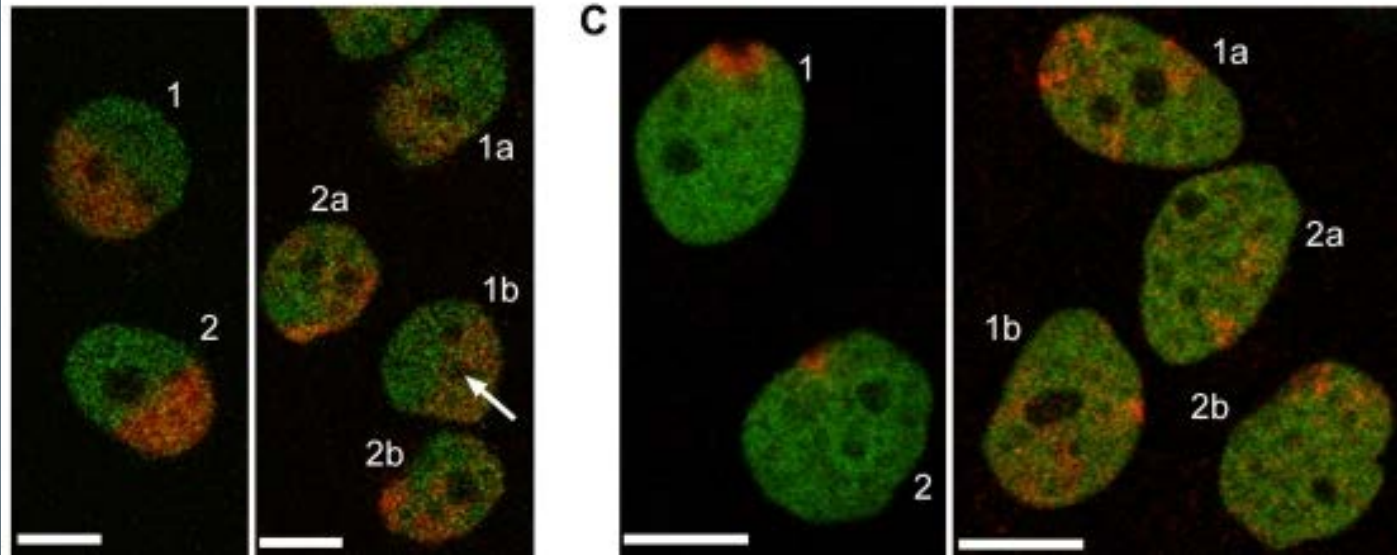
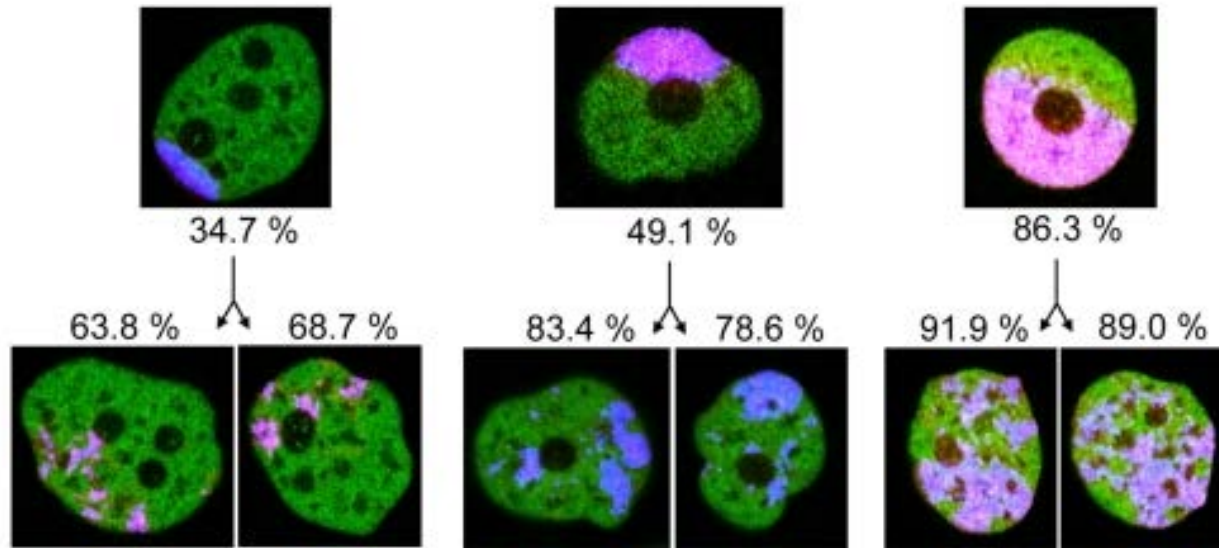
Single particle tracking analysis



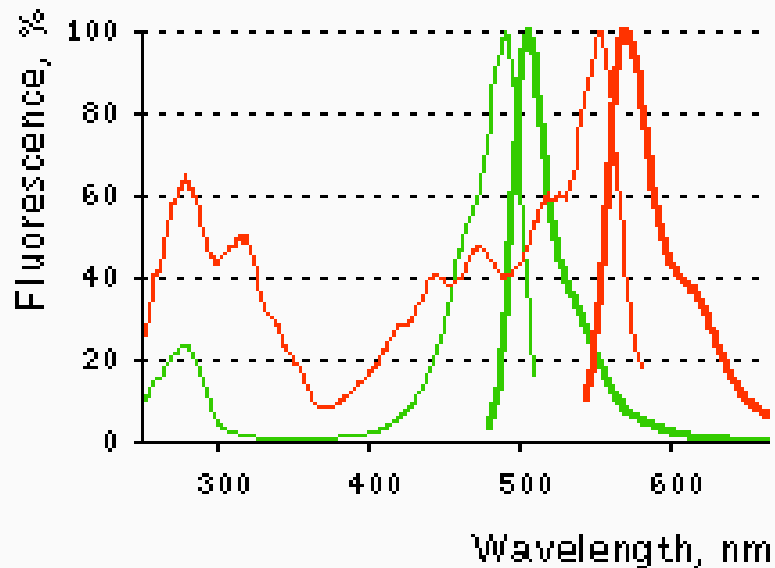


Experiments of Veronika Foltanková and Dmitry Sorokin

Dendra2 photo-conversion



Dendra2 is an improved version of a green-to-red photoswitchable fluorescent protein Dendra, derived from octocoral *Dendronephthya* sp. (Gurskaya *et al.*, 2006).

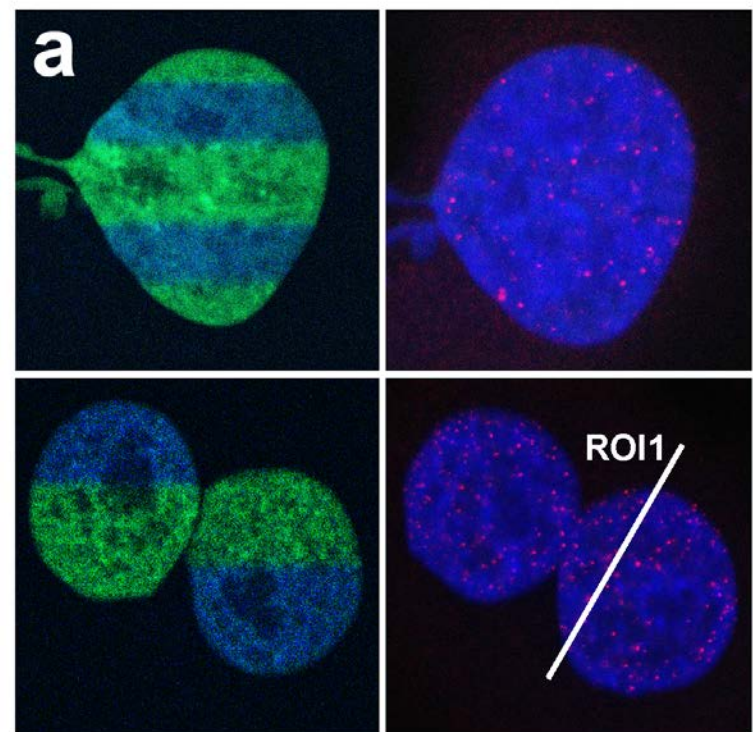


Normalized excitation (thin line) and emission (thick line) for non-activated (green) and activated (red) spectra.

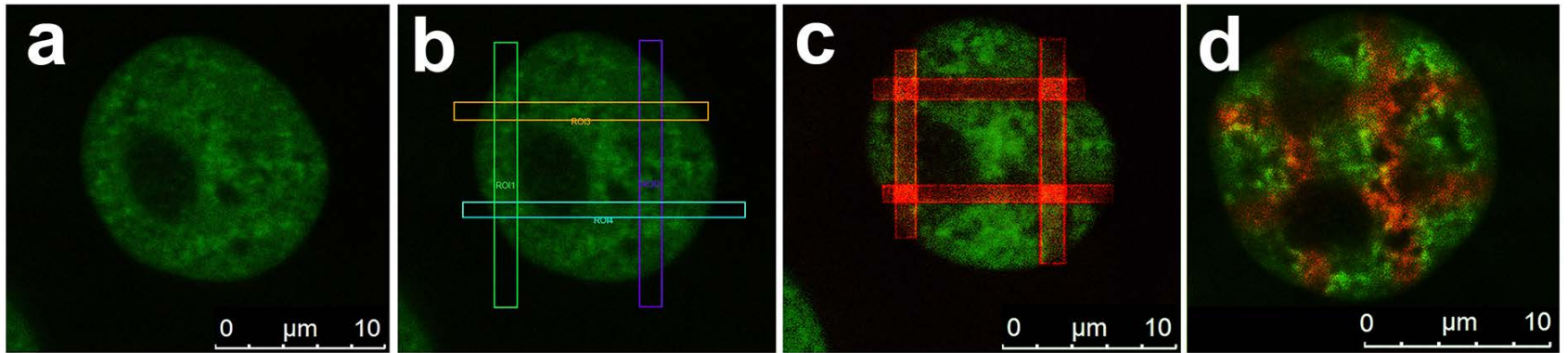
Photoconversion by UV laser

H4-Dendra2

CPDs / Nucleus



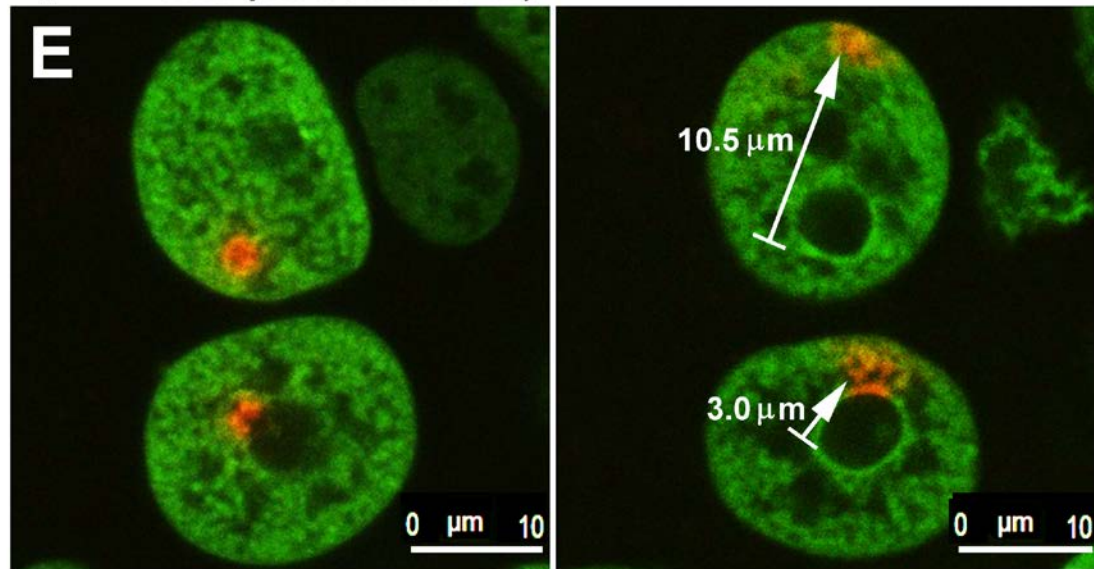
Dendra2-H4 photoconversion



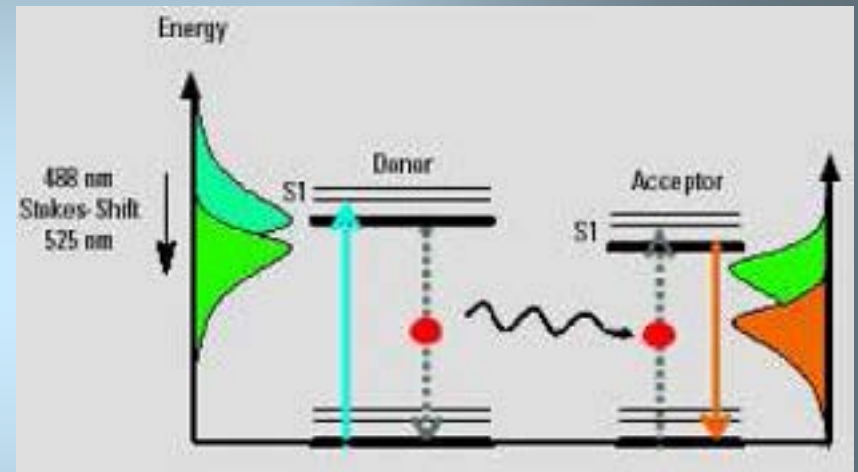
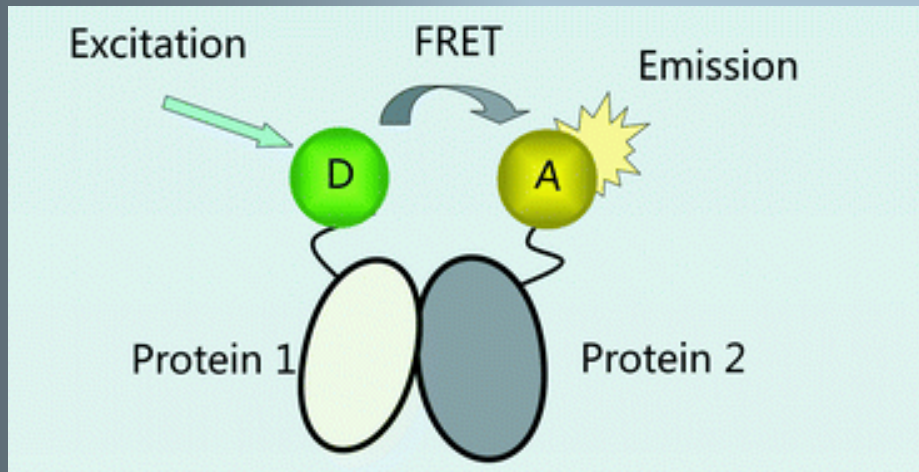
H4-Dendra2 / H4-Dendra2

Actinomycin-D
(0 min. after photoconversion)

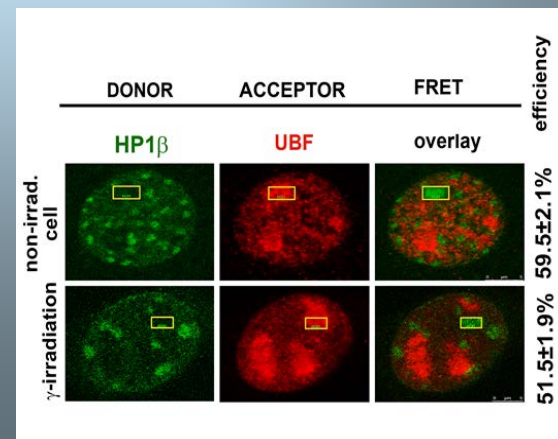
Actinomycin-D (90 min.)



FRET (Fluorescence Resonance Energy Transfer) is a technique for measuring interactions between two proteins *in vivo*. In this technique, two different fluorescent molecules (fluorophores) are genetically fused to the two proteins of interest.



<http://www.rsc.org/publishing/journals/>

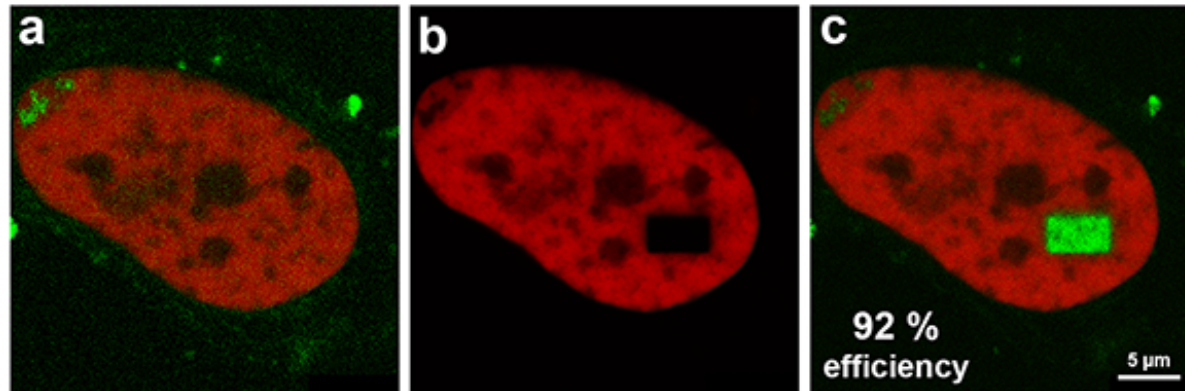
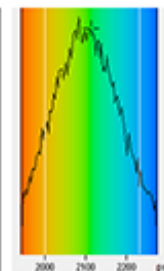
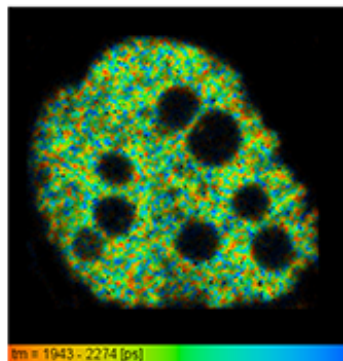
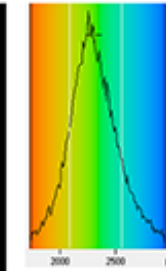
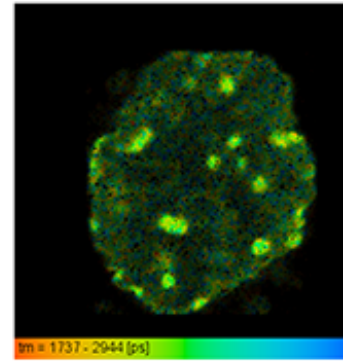


A**FRET AB analysis****p53 / 53BP1**

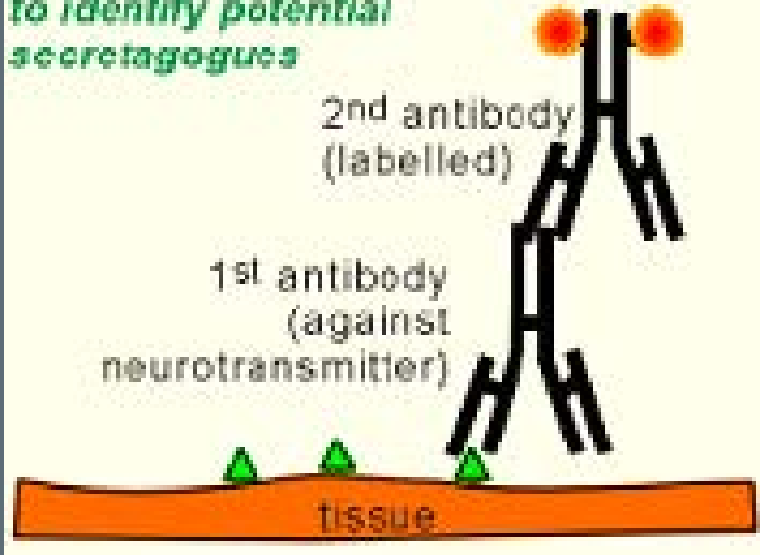
pre-bleach

bleaching

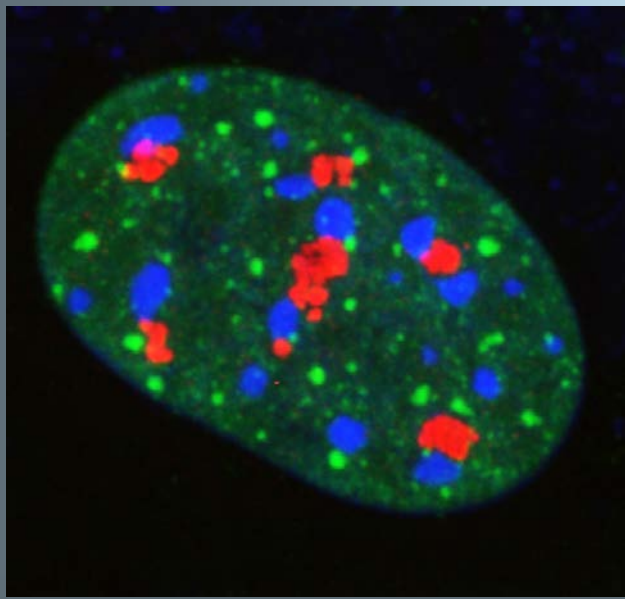
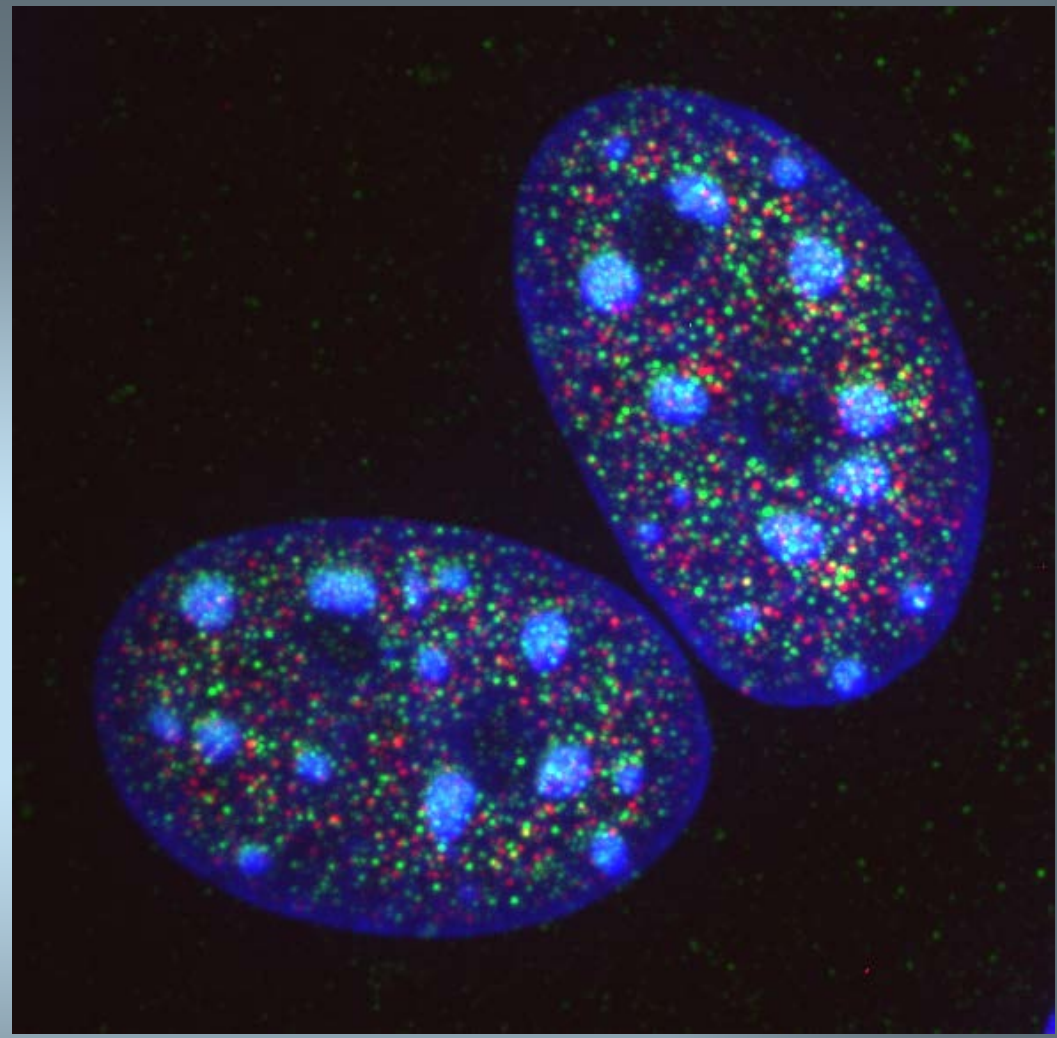
post-bleach

**B****FLIM-FRET analysis****a** p53 / 53BP1
(positive control)lifetime
histogram $T_0 = 2.40$ ns
 $T_{DA} = 2.09$ ns**b** HP1 β / 53BP1
(negative control)lifetime
histogram $T_0 = 2.40$ ns
 $T_{DA} = 2.35$ ns

Immunocytochemistry
to identify potential
secretagogues



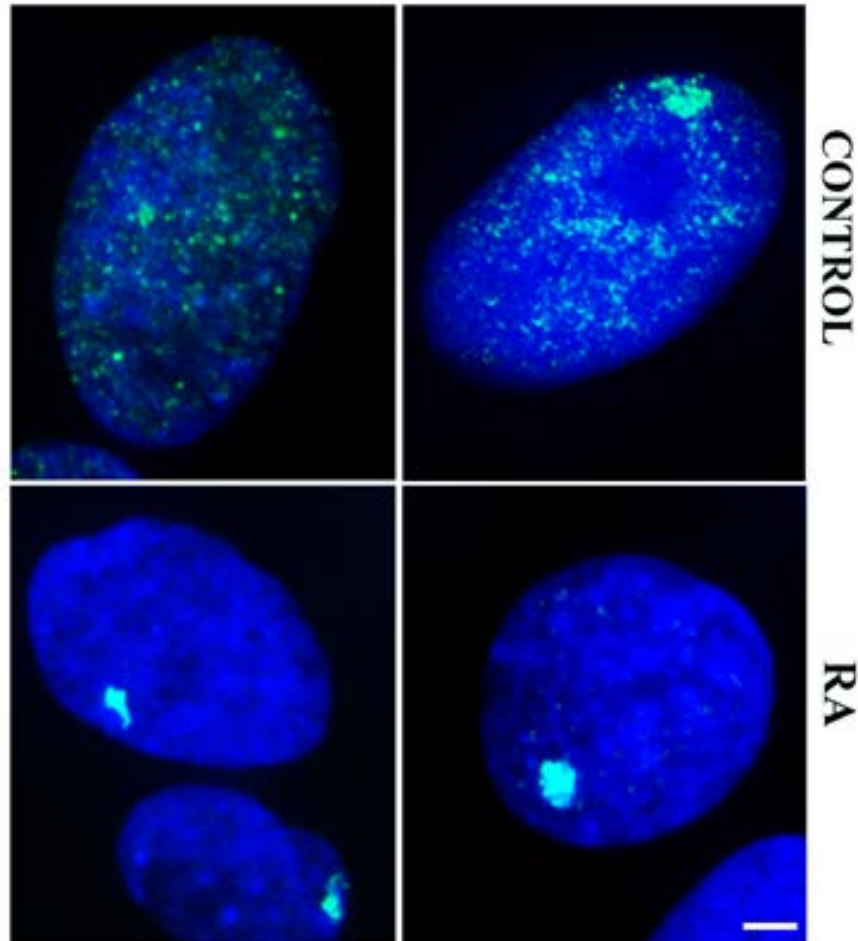
[http://www.celanphy.science.ru.nl/
Bruce%20web/construction.htm](http://www.celanphy.science.ru.nl/Bruce%20web/construction.htm)



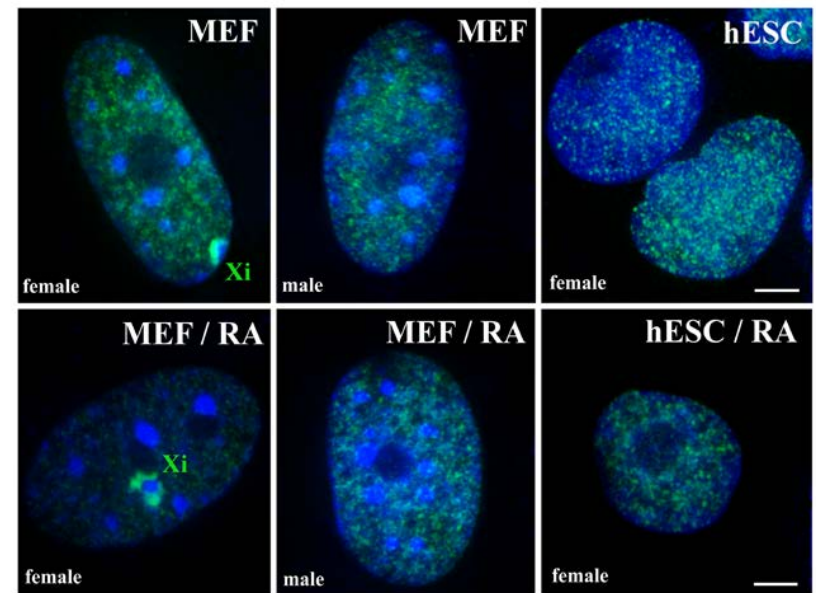
EB group, IBP, Brno

Inactivation of X chromosome in hESCs in comparison to MEFs

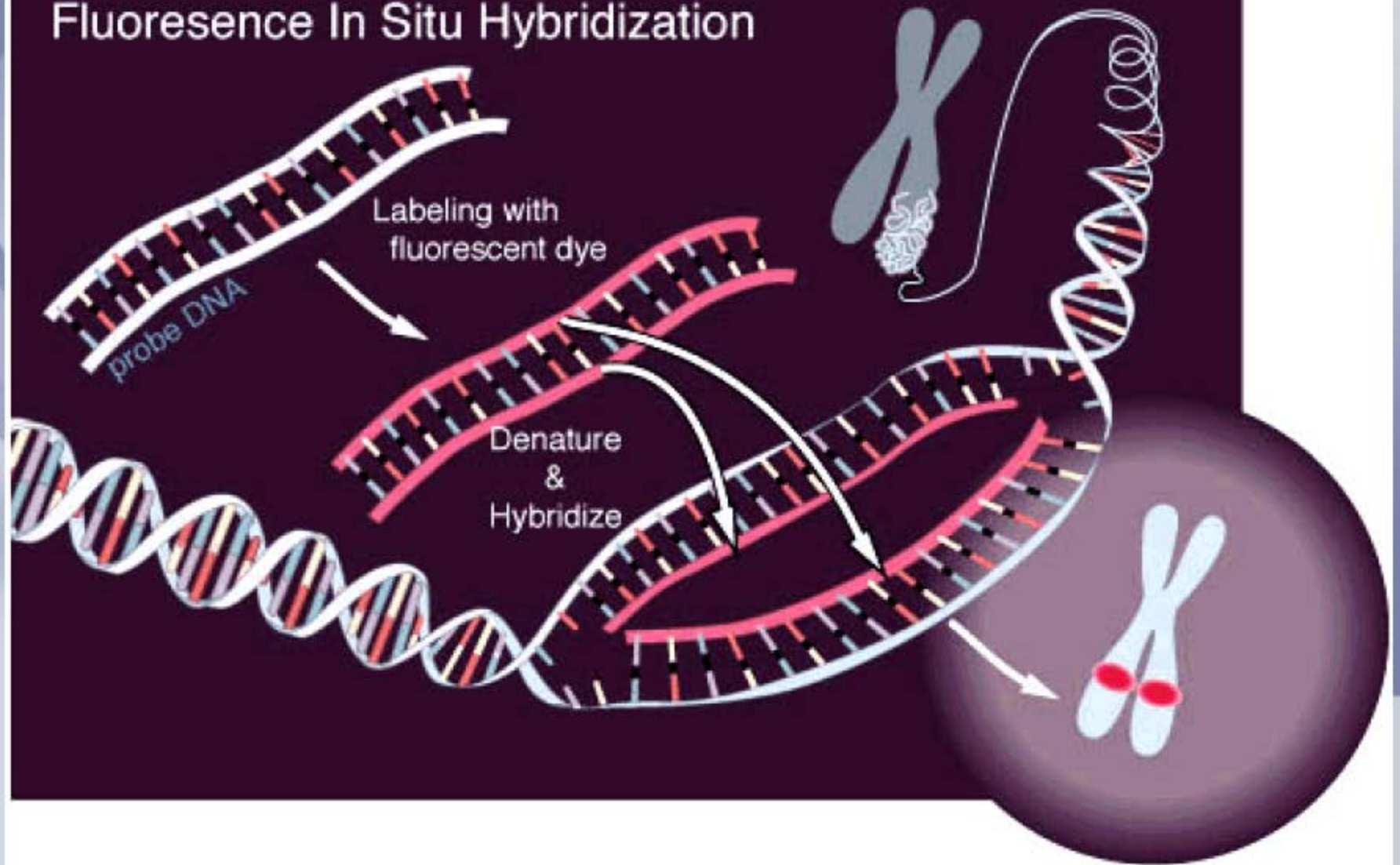
B H3K27me3 / DNA / HUES-1



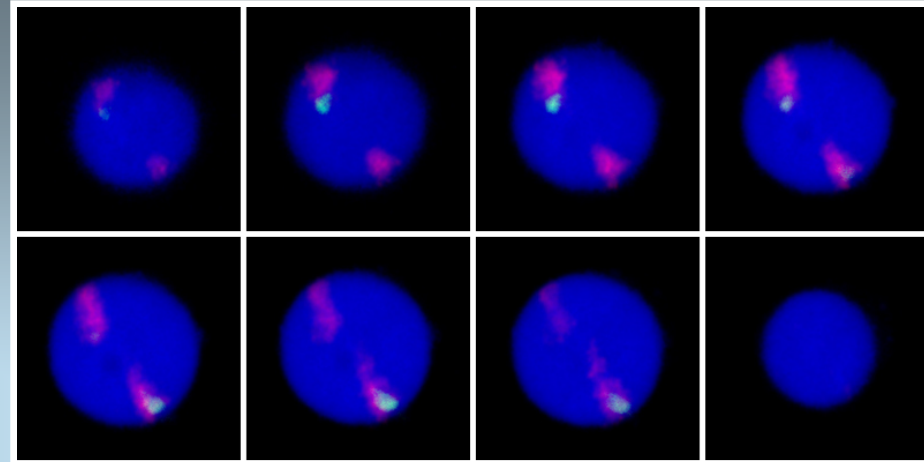
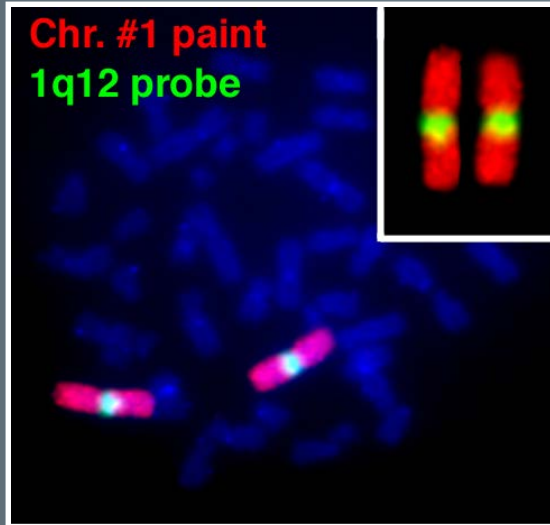
A H3K27me3 / DNA / HUES-9



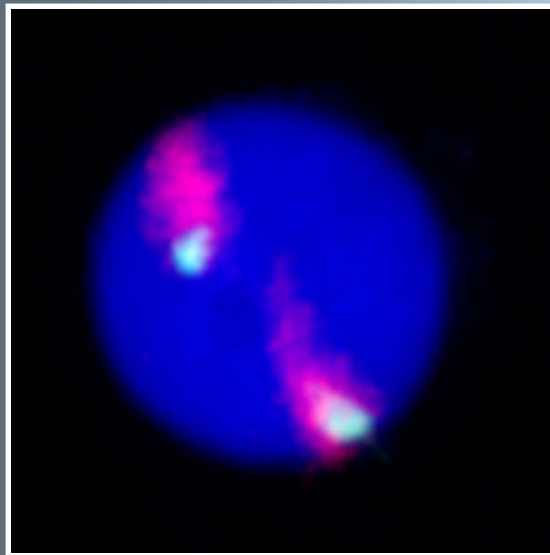
Fluorescence In Situ Hybridization



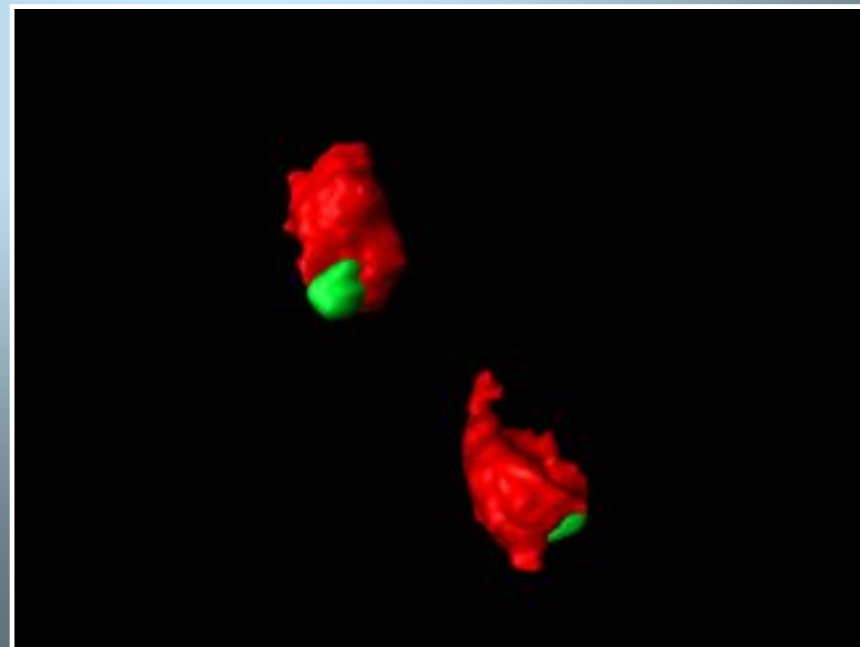
3D-FISH a konfokální mikroskopie



Galerie optických řezů

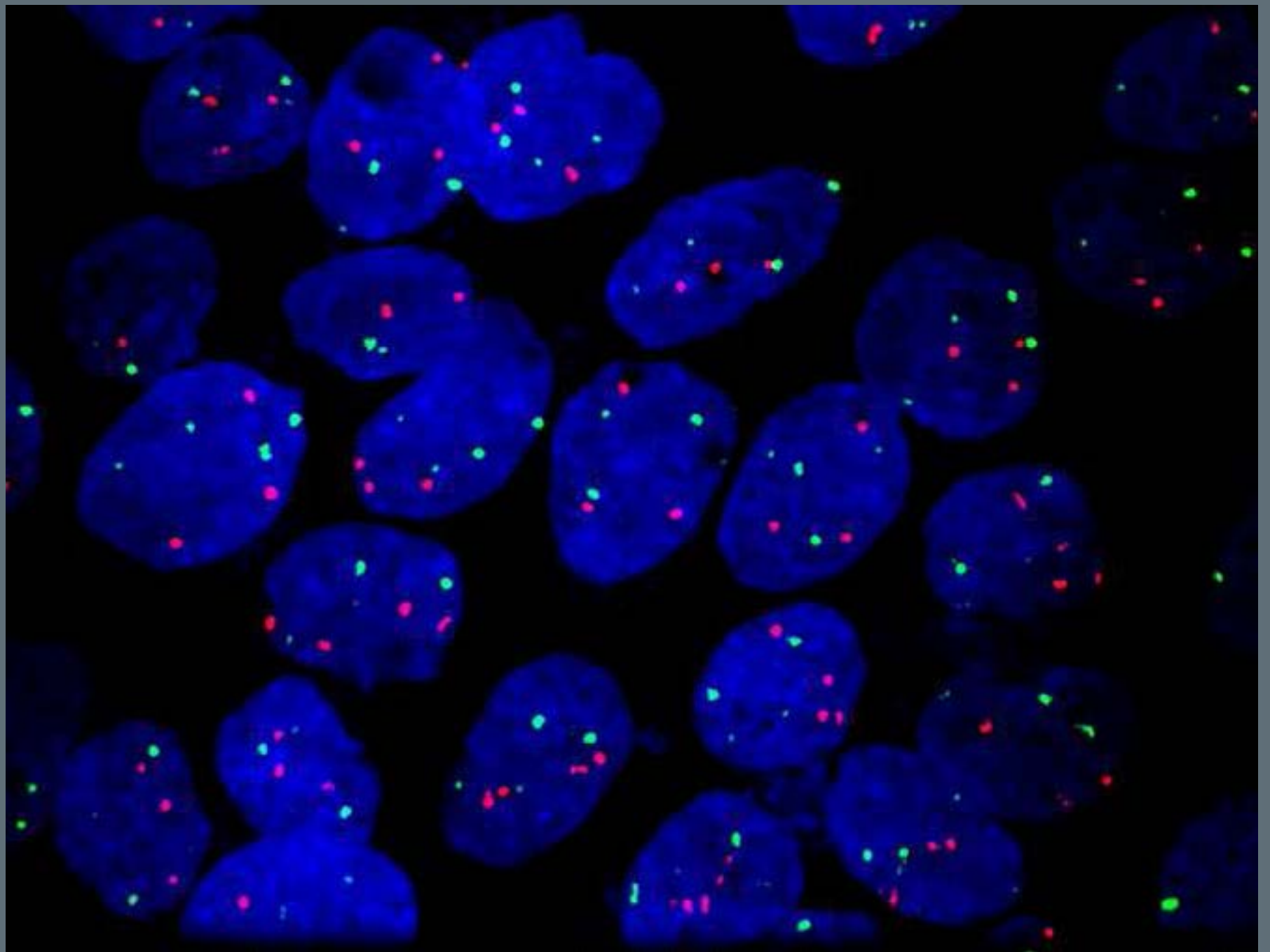


Maximální obraz
Všech řezů



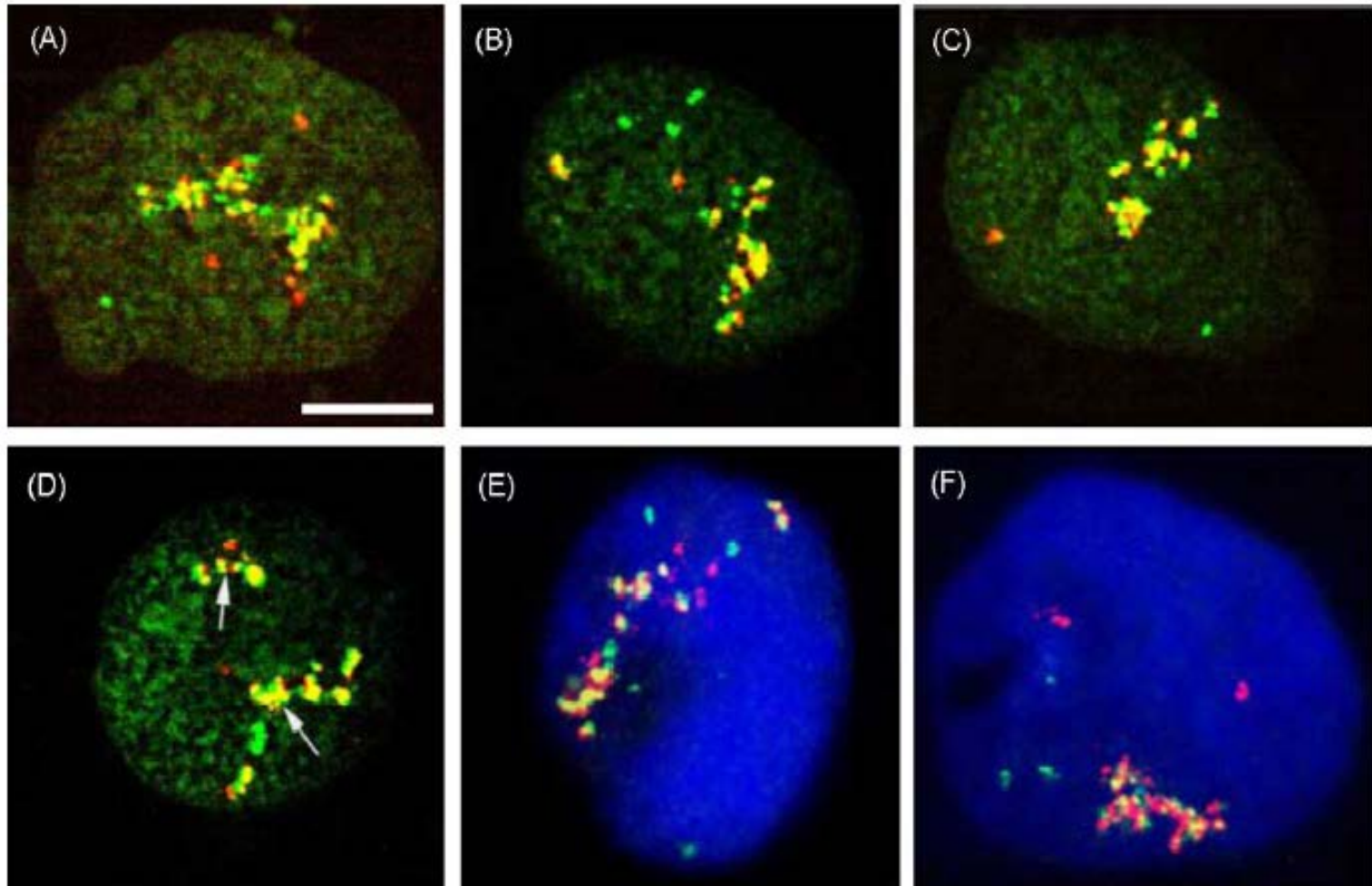
3D rekonstrukce CT

Weierich et al., (2003) in press



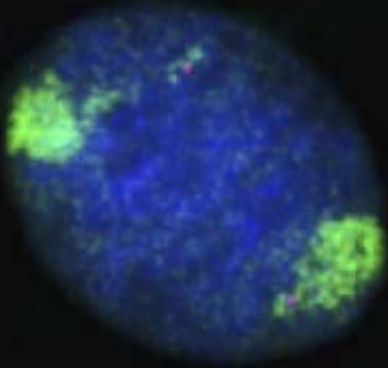
K562 cells t(9;22)

E. Bártová et al. / Leukemia Research 29 (2005) 901–913

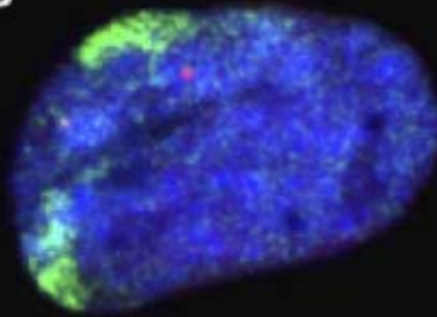


Oct4 / HSA 6 in hES cells

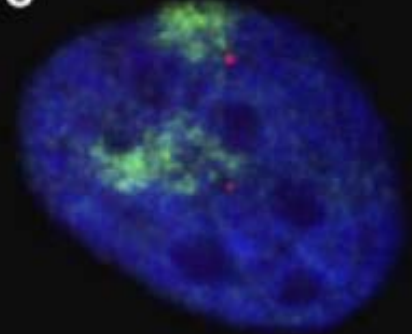
A



B

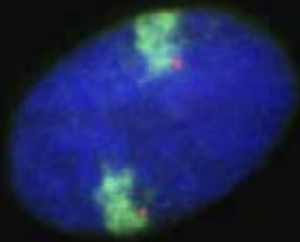


C

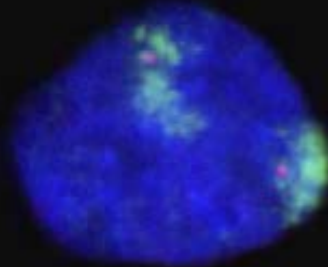


Oct4 / HSA 6 in hES cells - RA differentiated

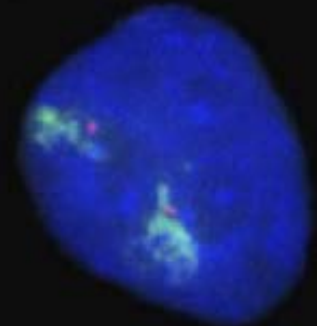
D



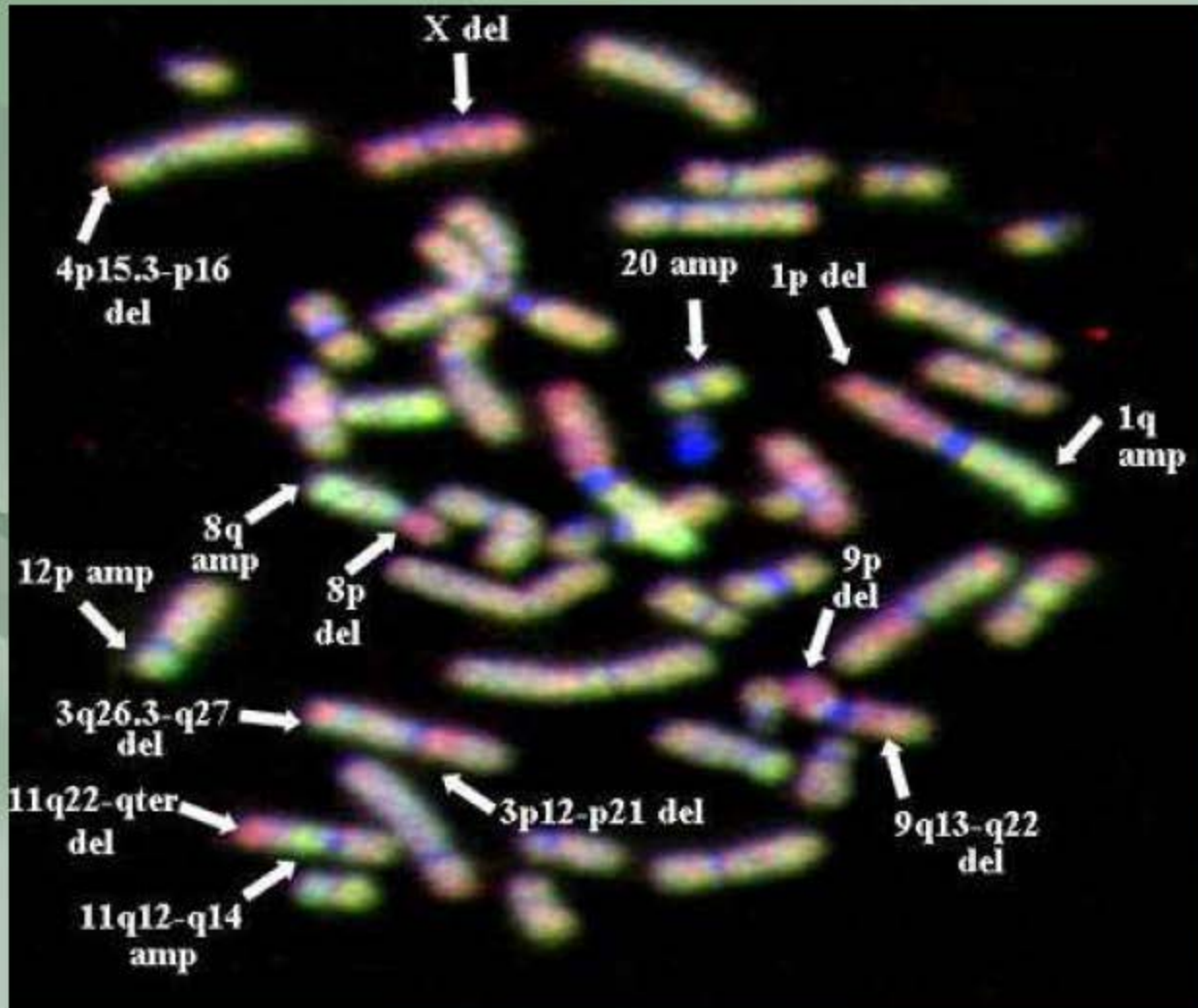
E



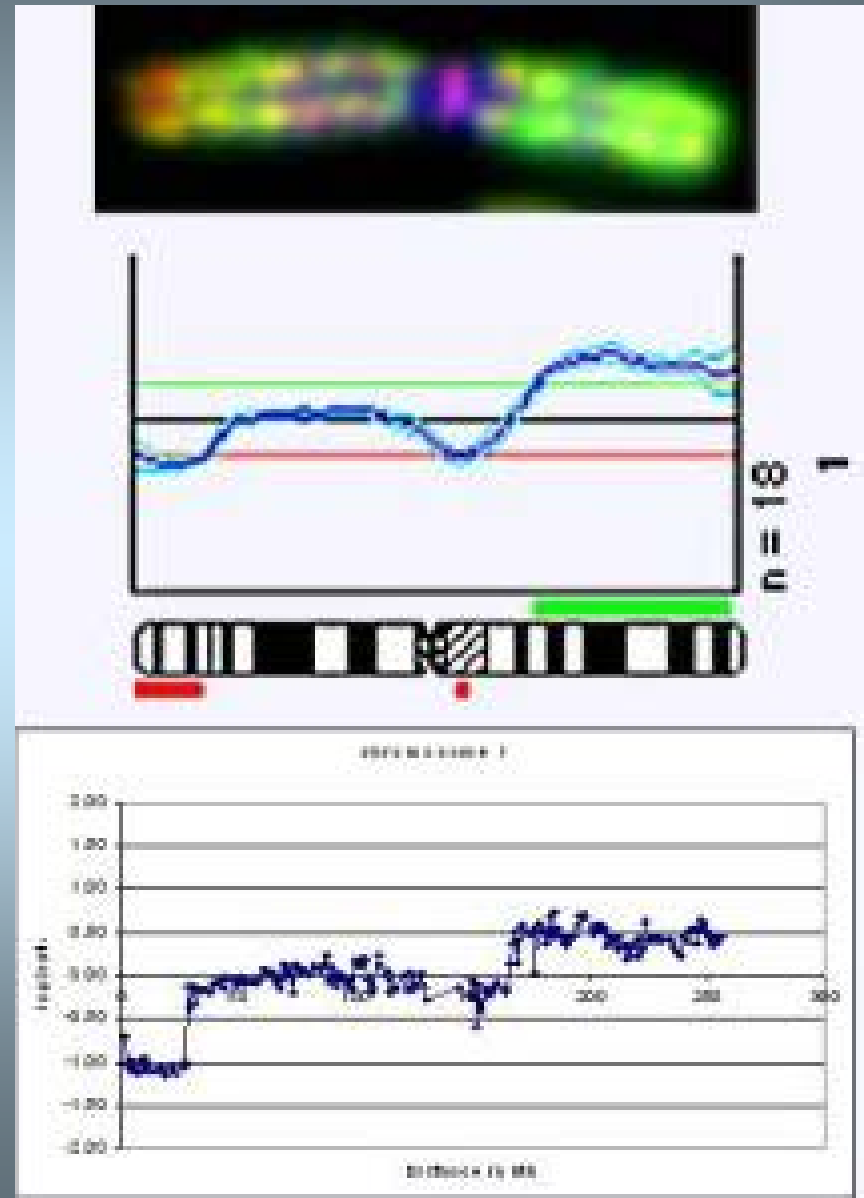
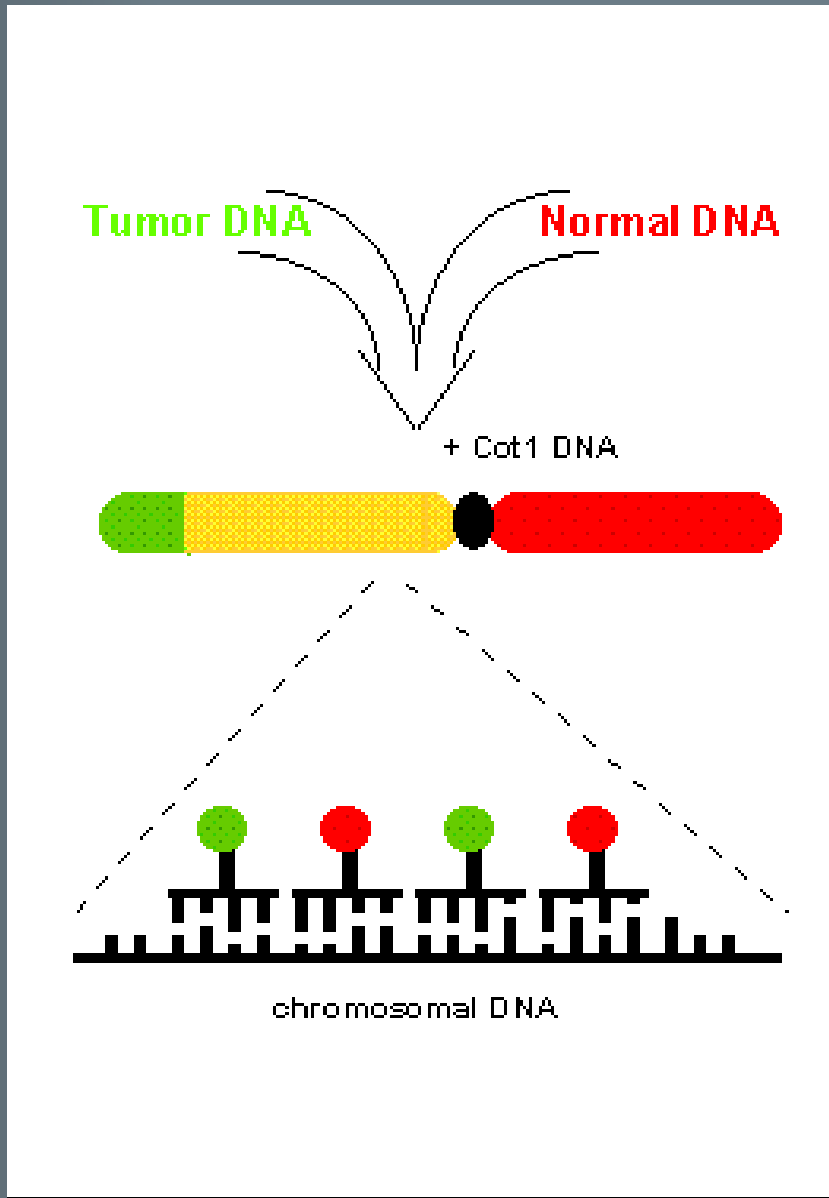
F



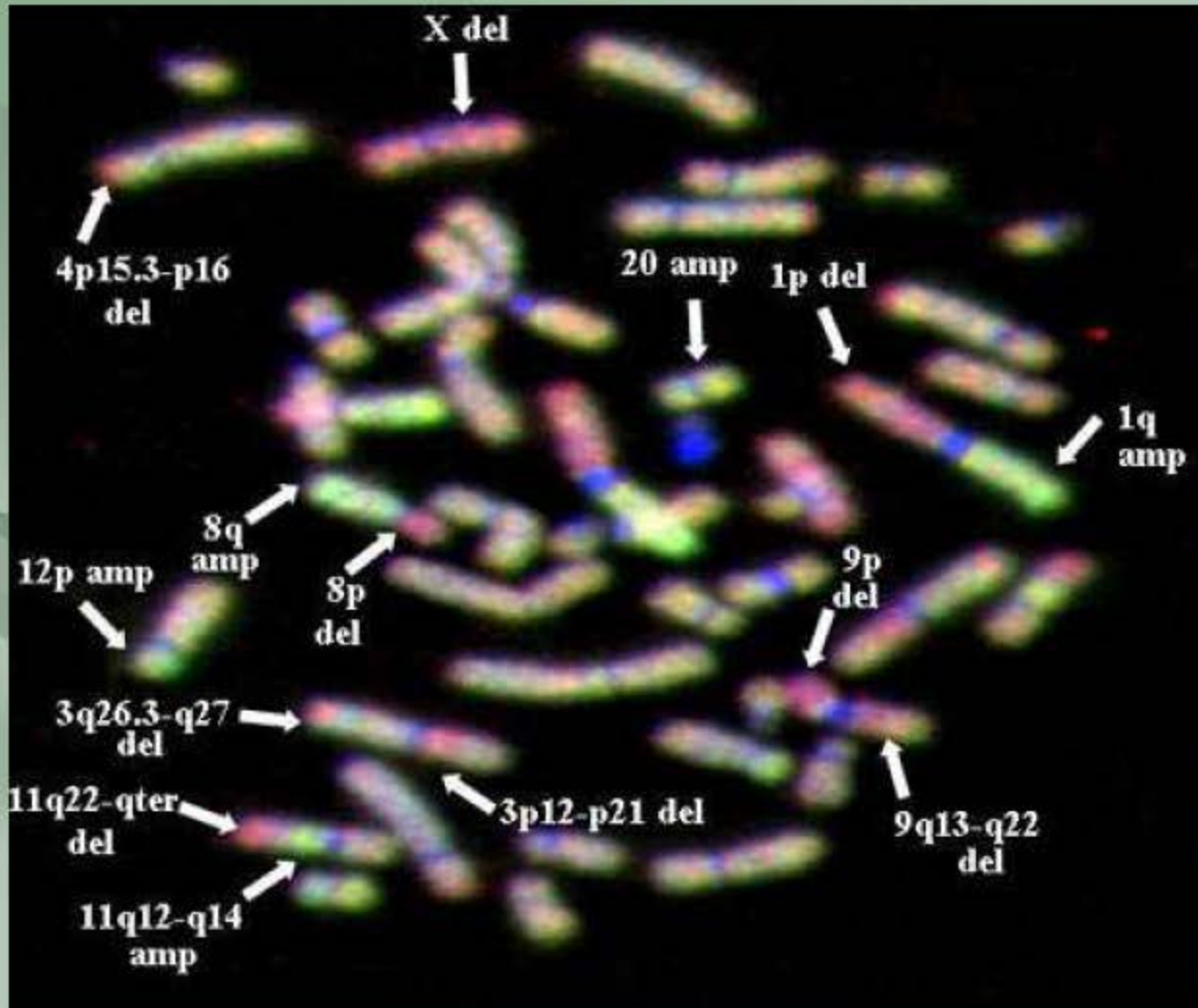
Comparative genome hybridization



CGH on metaphase spreads



Comparative genome hybridization



Advanced microscopic techniques

Electron Microscopes are: scientific instruments that use a beam of highly energetic electrons to examine objects on a very fine scale. This examination can yield the following information:

Topography

The surface features of an object or "how it looks", its texture; direct relation between these features and materials properties (hardness, reflectivity...etc.)

Morphology

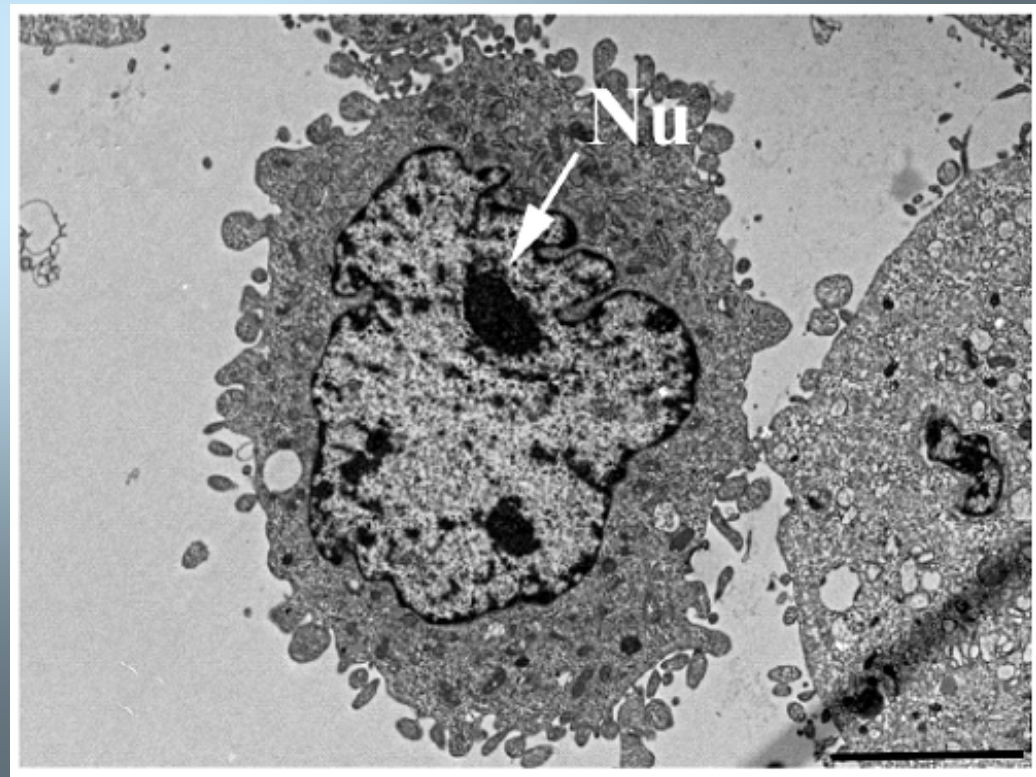
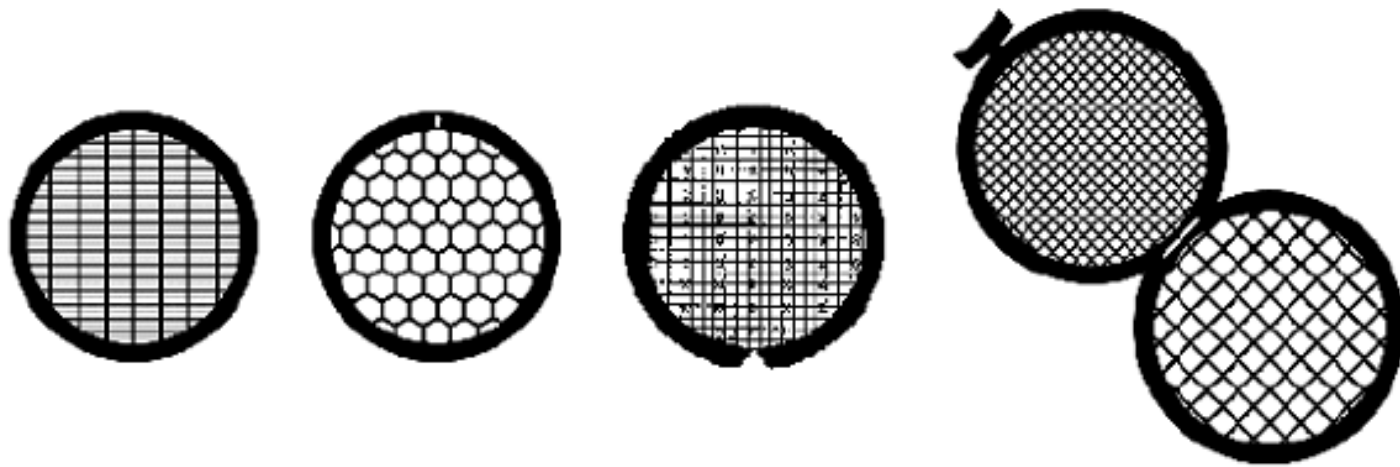
The shape and size of the particles making up the object; direct relation between these structures and materials properties (ductility, strength, reactivity...etc.)

Composition

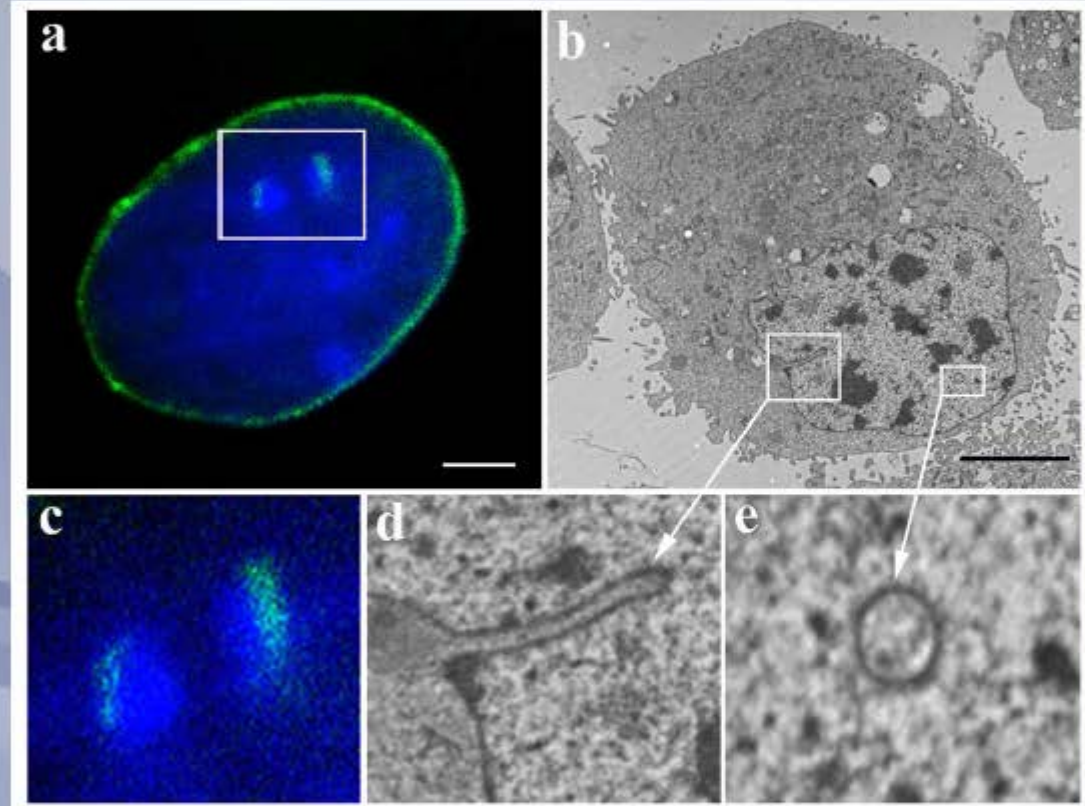
The elements and compounds that the object is composed of and the relative amounts of them; direct relationship between composition and materials properties (melting point, reactivity, hardness...etc.)

Crystallographic Information

How the atoms are arranged in the object; direct relation between these arrangements and materials properties (conductivity, electrical properties, strength, etc.)

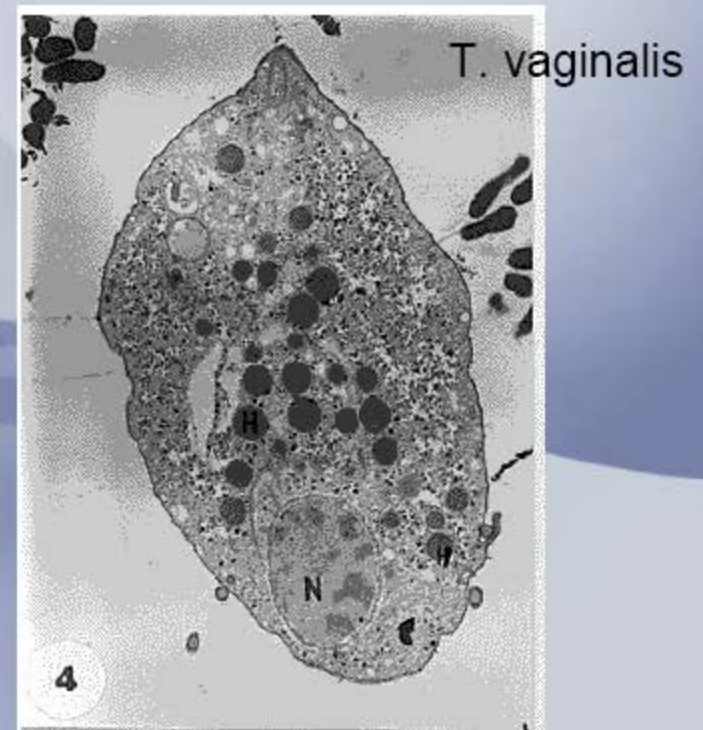
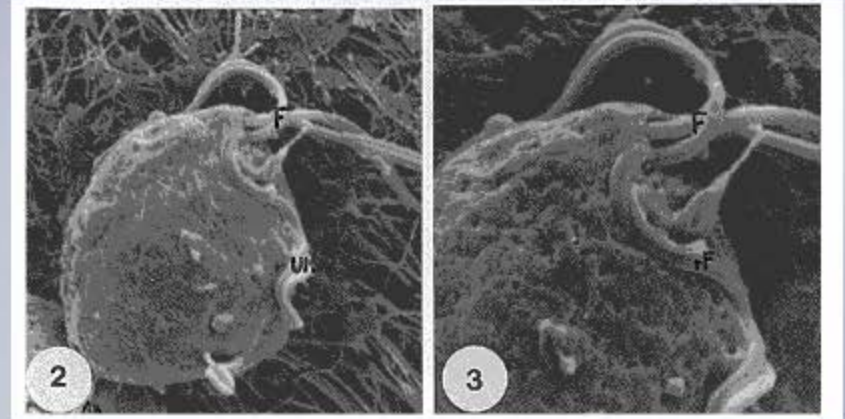


Transmission Electron Microscopes (TEM)



Galiová et al. EJCB (2008)

Scanning Electron Microscopes



X-RAY MICROSCOPY

Soft X-ray microscopes can be used to study hydrated cells up to 10 μm thick and produce images of 30 nm resolutions. X-ray microscopy, that has the more pronounced properties of laser scanning confocal microscopy (LSCM), has been a long-standing goal for experimental science (Seres et al., 2005). Since the cells are imaged in the X-ray transmissive "water window", where organic material absorbs approximately an order of magnitude more strongly than water, chemical contrast enhancement agents are not required to view the distribution of cellular structures (Meyer-Ilse et al., 2001). In such experiments, cells must be rapidly frozen to be studied on a cryostage, showing information which is closely similar to 4D-living cell observation by LSCM.

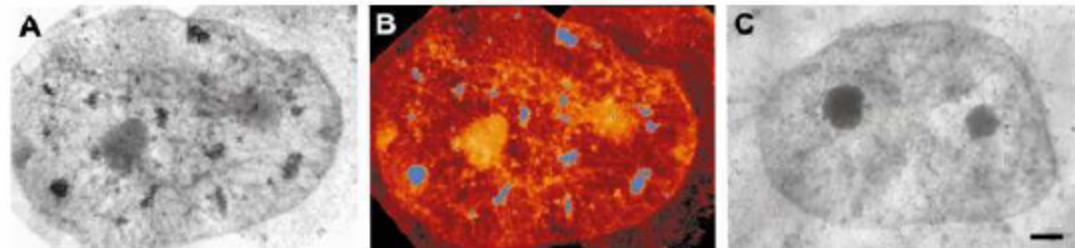
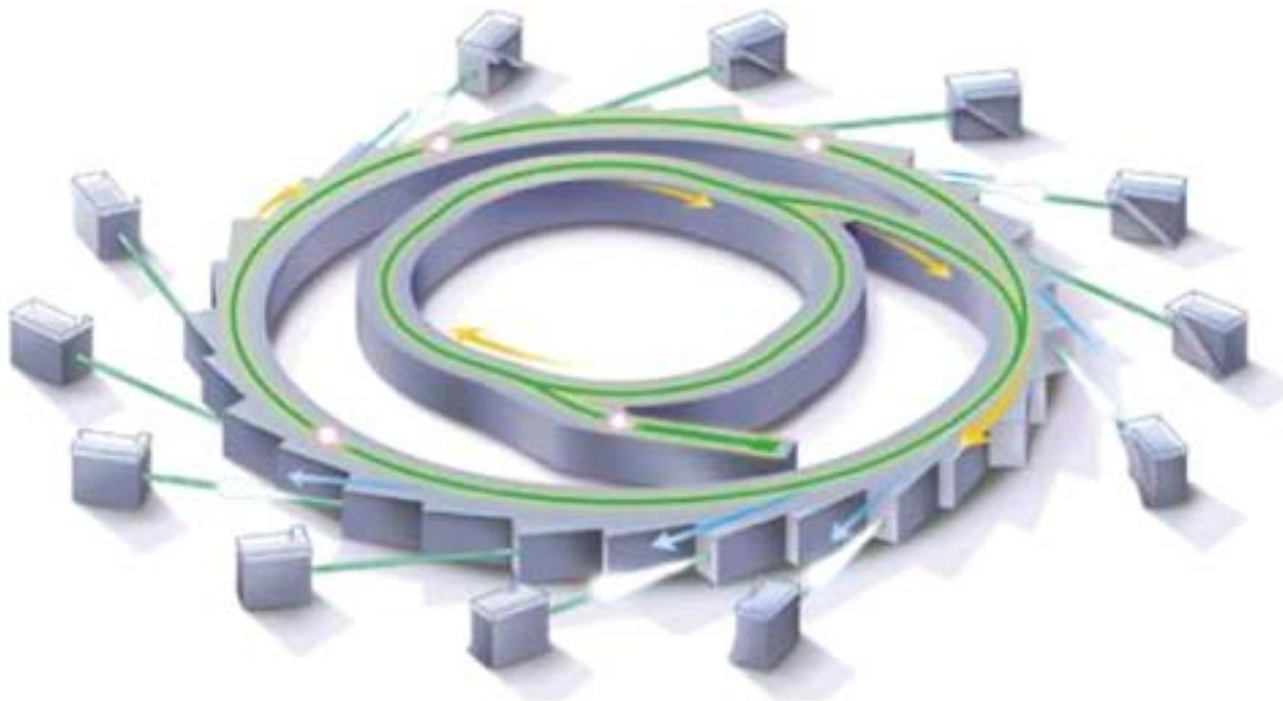


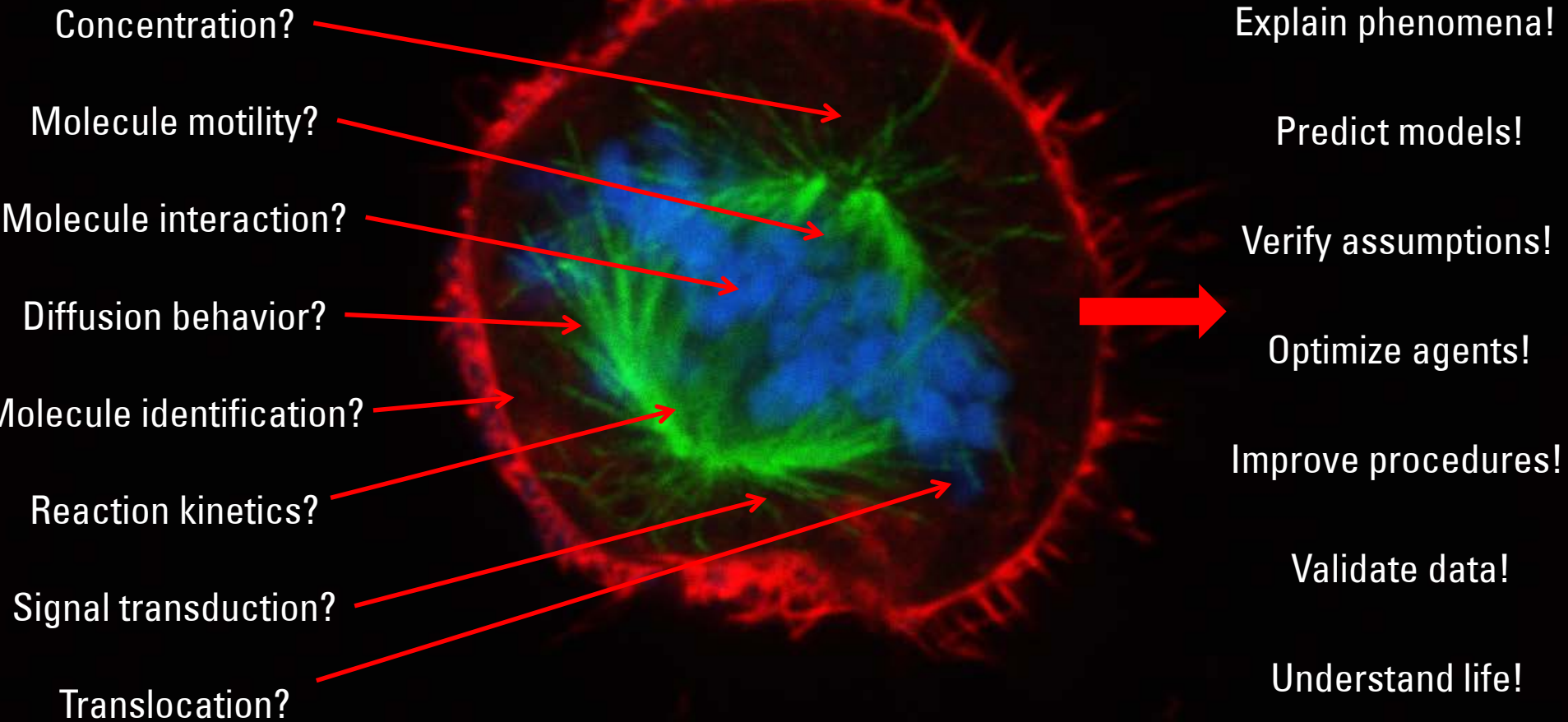
Fig. 4. Nuclei of human mammary epithelial cells (T4) labelled for RNA splicing factor (SRm300). (A) X-ray micrograph of a single nucleus after silver enhancement. This image is a montage compiled from two individual X-ray microscope images. (B) Same nucleus after colour coding to emphasize the label. (C) Control; single nucleus that was exposed to secondary antibodies and silver enhancement but not primary antibodies. This image is a montage compiled from two individual X-ray microscope images. Magnification = 2400 \times , 0.034 NA with 20 nm pixel size at 517 eV ($\lambda = 2.4 \text{ nm}$).

WHAT IS A SYNCHROTRON

A synchrotron is a device that accelerates electrons to almost the speed of light. As the electrons are deflected through magnetic fields they create extremely bright light. The light is channelled down beamlines to experimental workstations where it is used for research.



Quantify Life! – The Challenge





**Eva Bártová, Gabriela Šustáčková,
Lenka Stixová, Soňa Legartová, Darya Orlova, Veronika Foltánková, Pavel
Matula, Petra Sehnalová**
Institute of Biophysics, the Academy of Sciences of the Czech Republic, v.v.i., Brno

Projects: Ministry of Education Youth and Sports of the Czech Republic; COST-CZ project LC11020. Grant Agency of the Czech Republic by grants Nos. P302/10/1022 and P302/12/G157. European Union project COST TD09/05 and EU-Marie Curie project PIRSES-GA-2010-269156.